Aus dem Max von Pettenkofer-Institut
für Hygiene und Medizinische Mikrobiologie
der Ludwig-Maximilians-Universität München,
Lehrstuhl Virologie
Vorstand: Prof. Dr. med. Oliver T. Keppler

The Role of the Cytomegalovirus Glycoprotein Complex gHgLgO in Virus Entry

Dissertation
zum Erwerb des Doktorgrades der Naturwissenschaften
an der Medizinischen Fakultät der
Ludwig-Maximilians-Universität zu München

vorgelegt von
Yi-Quan Wu
aus
Chongqing, China
2016

Mit Genehmigung der Medizinischen Fakultät der Universität München

Erstgutachter: Priv. Doz. Dr. Barbara Adler

Zweitgutachter: Priv. Doz. Dr. Ursula Zimber-Strobl

Dekan: Prof. Dr. med. dent. Reinhard Hickel

Tag der mündlichen Prüfung: 22.02.2017

Eidesstattliche Versicherung

Wu, Yiquan

Ich erkläre hiermit an Eides statt, dass ich die vorliegende Dissertation mit dem Thema

The Role of the Cytomegalovirus Glycoprotein Complex gHgLgO in Virus Entry

selbstständig verfasst, mich außer der angegebenen keiner weiteren Hilfsmittel bedient und alle Erkenntnisse, die aus dem Schrifttum ganz oder annähernd übernommen sind, als solche kenntlich gemacht und nach ihrer Herkunft unter Bezeichnung der Fundstelleneinzeln nachgewiesen habe.

Ich erkläre des Weiteren, dass die hier vorgelegte Dissertation nicht in gleicher oder in ähnlicher Form bei einer anderen Stelle zur Erlangung eines akademischen Grades eingereicht wurde.

München, 23.02.2017 Wu, Yiquan

Table of Contents

Zusammenfassung

Infektionen mit dem humanen Cytomegalievirus (HCMV) können bei immungeschwächten Personen zu schweren Erkrankungen führen. Sie sind zudem die häufigste Ursache für Missbildungen nach intrauterinen Virusinfektionen. Der Zelltropismus von Herpesviren wird durch gH/gL Glykoproteinkomplexe in der Virushülle bestimmt. Diese gH/gL Komplexe vermitteln über Erkennung und Bindung zellulärer Rezeptoren und über Vermittlung der Fusion der Virushülle mit der Zellmembran den Eintritt des Virus in die Wirtszelle. HCMV kodiert für zwei alternative gH/gL Komplexe, gH/gL/gO und gH/gL/pUL(128,130,131a), welche beide den breiten Zelltropismus von HCMV definieren. Die entsprechenden Wirtszellrezeptoren wurden jedoch noch nicht identifiziert.

Ziel dieser Arbeit war es, den zellulären Rezeptor des HCMV gH/gL/gO Komplexes zu identifizieren. Während nach Infektionen mit Wildtyp-HCMV in Zellkultur reichlich infektiöse Viruspartikel in den Überstand abgeben werden, produzieren Mutanten, die keinen gH/gL/gO Komplex haben, kaum infektiöse Viren und breiten sich vorweigend zellassoziiert aus. In der vorliegenden Arbeit konnte über die Untersuchung der Bindung von HCMV Partikeln und rekombinantem gO-IgG Fc Fusionsprotein an Fibroblasten der "platelet-derived growth factor receptor-α" (PDGFRα) als Rezeptor des gH/gL/gO Komplexes von HCMV identifiziert werden. Ausschließlich gH/gL/gO-positive Viren infizieren Zellen PDGFRα-abhängig: i) Löslicher PDGFRα und dessen natürlicher Ligand PDGF-BB konnten eine Infektion mit Wildtypvirus hemmen, nicht aber Infektionen mit gO-Deletionsmutanten. ii) Eine Überexpression von PDGFRα in Zellen verstärkte die Infektion mit Wildtypvirus, nicht jedoch die Infektion mit einer gO-Deletionsmutante. Zusätzlich konnte gezeigt werden, dass vor allem die Infektion von PDGFRα-positiven Zellen mit freien Viruspartikeln, nicht aber die zellassoziierte Virusausbreitung, über die Interaktion von gH/gL/gO mit PDGFRα erfolgt. Die gH/gL/gO–PDGFRα Interaktion könnte damit in vivo hauptverantwortlich für die effiziente Infektion von ersten Zielzellen sein und stellt somit ein bedeutendes Angriffsziel für das Design von HCMV-Vakzinen oder neuen Therapeutika zur Behandlung von HCMV Primärinfektionen dar.

Die Infektion der Maus mit dem murinen Cytomegalievirus (MCMV) wird seit langem als Model für HCMV Infektionen genutzt. MCMV besitzt wie HCMV einen gH/gL/gO Komplex.

MCMV gO-Deletionsmutanten zeigen einen den HCMV gO-Deletionsmutanten vergleichbaren Phänotyp. Hier konnte gezeigt werden, dass die Deletion von gO bei MCMV und HCMV den Tropismus der Viren für verschiedene Zelltypen verschiebt. MCMV Partikel zeigten wie HCMV Partikel, die von unterschiedlichen Zelltypen produziert werden, einen unterschiedlichen Zelltropismus. Das könnte darauf zurückzuführen sein, dass in verschiedenen Zelltypen mehr oder weniger gH/gL/gO-Komplexe in die Viruspartikel eingebaut werden. Aufgrund der vergleichbaren Phänotypen von HCMV und MCMV gO-Mutanten in Zellkultur ist die Infektion der Maus ein geeignetes Tiermodell, die Rolle des gH/gL/gO Komplexes in vivo zu untersuchen.

Summary

Human cytomegalovirus (HCMV) infection is a major cause of morbidity and mortality in immunocompromised individuals and a leading cause of birth defects after congenital infection. Herpesvirus cell tropism is determined by gH/gL glycoprotein complexes in the viral envelope. The gH/gL complexes mediate virus entry into host cells through binding to host cell receptors and promote fusion of viral envelopes with cellular membranes. HCMV encodes two alternative gH/gL complexes, gH/gL/gO and gH/gL/pUL (128, 130, 131a) which both shape the broad cell tropism of HCMV. However, their respective host cell receptors have not been identified.

HCMV shows a broad cell tropism and readily produces infectious supernatant virus in cell culture. HCMV lacking the gH/gL/gO complex hardly produces infectious virus and spreads mainly cell-associated. By studying the binding of HCMV particles and recombinant gO-IgG Fc fusion proteins to fibroblasts, platelet-derived growth factor receptor-α (PDGFRα) could be identified as an HCMV entry receptor recognized by the gH/gL/gO complex. It could be shown that only gH/gL/gO-positive HCMV infects cells in a PDGFRα-dependent manner: i) Soluble PDGFRα receptor and the natural ligand PDGF-BB could inhibit infection with wildtype virus, but not infection with gO-knockout mutants. ii) Overexpression of PDGFRα enhanced infection with wildtype virus, but not infection with gO-knockout virus. It could also be shown that infection of PDGFRα-positive cells is up to 98% driven by the gH/gL/gO complex. This might indicate that, PDGFRα expression levels secure effective infection of first target cells. The PDGFRα - gH/gL/gO interaction may thus be an important target for the design of anti-HCMV vaccines or new anti-HCMV drugs to prevent primary infection.

Infection of mice with murine cytomegalovirus (MCMV) has been extensively used as a model to study HCMV infection in vivo. It has been shown before that MCMV also expresses a gH/gL/gO complex which, when knocked out, exhibits a phenotype in cell culture comparable to gO-knockout mutants of HCMV. Here, it could be shown that gO-knockout mutants of MCMV and HCMV show similar shifts in infection capacities for different cell types. MCMV progenies derived from different cell types differ like HCMV progenies derived from different cell types in their cell tropism. This is very likely due to cell

type-dependent incorporation of more or less gH/gL/gO complexes. This makes the MCMV infection of mice a good model to study the role of the gH/gL/gO complex *in vivo*.

1 Introduction

1.1 The family of herpesviridae

Herpesviruses are large, enveloped DNA viruses with double-stranded linear DNA genomes. The characteristic virion of a herpesvirus (Figure 1) is composed of an icosahedral capsid harboring the viral DNA, surrounded by a protein layer called tegument, and enclosed by an envelope consisting of a lipid bilayer containing different glycoproteins. After primary infection, all herpesviruses persist lifelong in their hosts by establishing a latent infection interrupted by recurrent reactivations. Based on the genomic organization, sequence homologies, and biological properties, the family of Herpesviridae is divided into three subfamilies; α-herpesviruses, β-herpesviruses and γ-herpesviruses. To date, more than 200 herpesviruses have been identified in vertebrates, including eight human herpesviruses: herpes simplex virus type 1 and 2 (HSV-1, -2) and varicella-zoster virus (VZV), which belong to the α-herpesvirus subfamily; human cytomegalovirus (HCMV), HHV-6 and HHV-7, which belong to the β-herpesvirus subfamily; and Epstein-Barr virus (EBV) and Kaposi's sarcoma-associated herpesvirus (KSHV), which belong to the γ-herpesvirus subfamily.

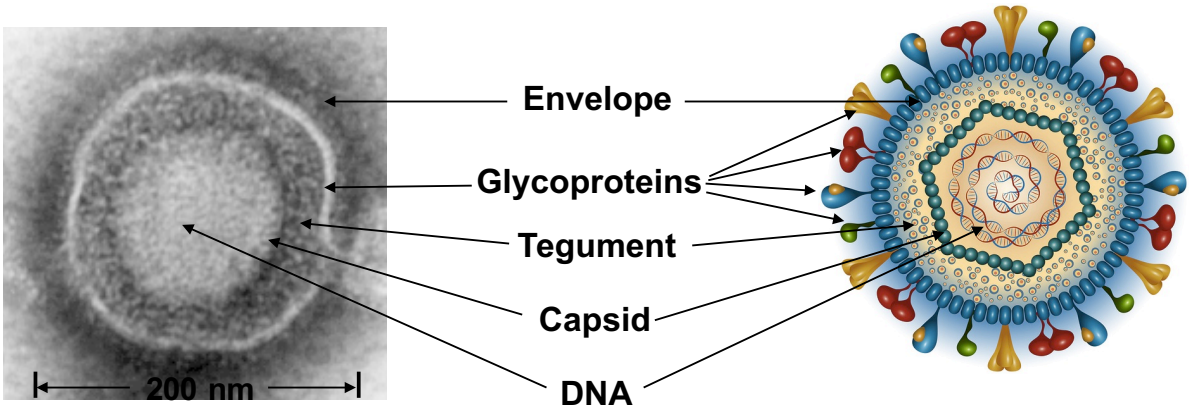

Electron microscope image of a negatively stained HSV-1 virion

Figure 1: Structure of an HCMV virion. (Adapted from http://people.virginia.edu/~jcb2g/background_hsv1_structure.html)
Shown are electron microscope image of a negatively stained HCMV virion (left) and a schematic representation of the virion structure (right).

1.2 Human Cytomegalovirus (HCMV)

HCMV, also referred to as human herpesvirus 5 (HHV-5) [1], is a human herpesvirus which is spread worldwide. It was first isolated and cultivated in 1956 [2, 3]. HCMV infection of cells leads to swelling and enlargement of the cells, a phenomenon named cytomegaly, which gave HCMV its name [4].

1.2.1 HCMV infection and diseases

HCMV seroprevalence ranges from 45 to 100%, depending on geographical locations and socioeconomic status [5]. Transmission of HCMV occurs through different routes, either horizontally via direct contact with infected individuals who excrete infectious virus in their bodily secretions including respiratory droplets, blood, urine and breast milk [6] or vertically from mother to infant. The majority of HCMV infections in normal immunocompetent individuals are asymptomatic. However, HCMV infection of immunocompromised individuals (for example, patients with acquired immunodeficiency syndrome (AIDS) or transplant patients) results in significant morbidity and mortality. These patients show HCMV-associated diseases like hepatitis, pneumonia, encephalitis, retinitis, gastrointestinal disease and transplant rejection [7, 8]. Primary HCMV infection of mothers during pregnancy can result in infection of the unborn child and lead to birth defects in 0.2% to 2.5% of all births [9]. Typical symptoms of a congenital infection are cerebral injuries resulting in severe developmental defects and hearing loss [9]. Associations of HCMV infection with the development of glioblastoma [10] and atherosclerosis [11] are also discussed. However, it is unknown whether HCMV is the cause of those diseases or whether cells in glioblastoma or atherosclerotic lesions are preferred targets for HCMV.

1.2.2 HCMV therapy and HCMV vaccines

Despite decades of the research dedicated to prevent HCMV infection, there is currently no authorized vaccine against HCMV.

There are five antiviral drugs licensed by the FDA and the European Medicines Agency (EMA) to treat HCMV diseases in immunocompromised patients: Ganciclovir, Foscarnet, Cidofovir, Valganciclovir, and Fomivirsen. The former four drugs target the viral DNA polymerase to exert their antiviral action while Fomivirsen blocks an immediate early gene of HCMV [12]. All of these antiviral drugs have been shown to reduce HCMV infection and control related diseases in immunocompromised patients [13]. However, they have

limitations such as significant side effects [14] and development of resistance [15]. Moreover, due to teratogenicity, they cannot be used to treat congenital infections. Thus, there is a strong need for developing new drugs which target other steps in viral replication, such as attachment and entry [12].

The neurodevelopmental disabilities of children caused by congenital HCMV infection cause high economic costs in many countries. To eliminate congenital HCMV infection and eradicate HCMV from the human population, vaccination would be a priority. During the last decades, researchers have attempted different strategies to develop vaccines against HCMV, such as live attenuated vaccines (e.g. laboratory-adapted HCMV strains AD169 and Towne), recombinant chimeric vaccines (e.g. Towne/Toledo chimeric vaccines) and subunit vaccines (e.g. glycoprotein B and tegument protein pp65 vaccines) [16]. However, none exhibited effective protection, thus, to date, there is no licensed HCMV vaccine available. The lack of specific and effective treatments for HCMV infection and disease highlights the need for a thorough understanding of HCMV-host cell interactions, including HCMV entry into host cells and host immune responses against HCMV.

1.2.3 HCMV genome

The HCMV genome is the largest herpesvirus genome with a size of approximately 235 kbp comprising up to 250 opening reading frames (ORFs) [17]. It can be divided into two segments, named unique long (UL) and unique short (US) regions which are flanked by terminal repeats (TR) and internal repeats (IR) (Figure 2) [18]. ORFs located in the UL region and US region are named according to their positions.

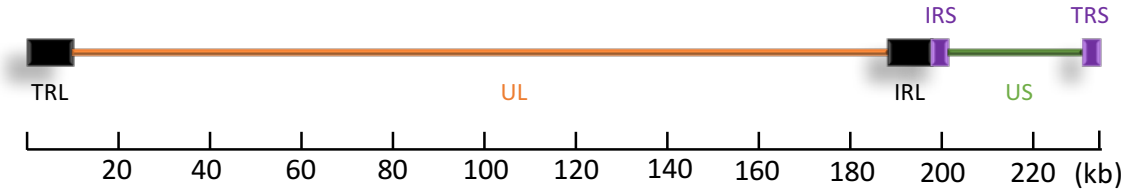

Figure 2: Schematic map of the HCMV genome.
The HCMV genome contains a unique long (UL) and a unique short (US) region which are flanked by inverted repeats: 1) terminal repeat long (TRL) and internal repeat long (IRL); 2) terminal repeat short (TRS) and internal repeat short (IRS).

To date, over 70 viral proteins have been identified in purified virions [19]. Only ~50 proteins are thought to be essential for viral replication, and the vast majority of HCMV proteins interfere with cellular signals resulting in host immunomodulation [17].

1.2.4 Replication cycle of HCMV

HCMV showes the typical replication cycle of herpesviruses (Figure 3). To infect a cell, the virus first penetrates the host cell membrane either through direct fusion at the plasma-membrane or in endocytic vesicles [20-22]. Following fusion, the viral nucleocapsid together with the tegument is released into the cytoplasm and transported to the nucleus via microtubules [23, 24]. The viral genome is released into the nucleus where the viral gene expression starts in a temporal cascade comprising three main phases: immediate early (IE), early (E), and late (L) phase [25]. IE-proteins, (i.e. IE-1 and IE-2) are the first viral genes transcribed. Their transcription does not require replication of viral DNA or de novo viral protein synthesis. They mainly function as transcriptional activators to promote the expression of viral and cellular genes, including viral early genes. Expression of early genes requires prior synthesis of IE proteins. Early proteins promote viral DNA replication, which starts around 24 h post infection (p.i.). Following replication of the viral genome, late genes which code for capsid components, tegument proteins, and envelope glycoproteins are expressed and then assembled into progeny virions. The detailed mechanism of virion assembly and egress is not well-defined. In the nucleus, viral genomes are packaged into the capsids. These nucleocapsids undergo a primary tegumentation and an initial envelopment step by budding through the inner nuclear membrane into perinuclear cisternae, followed by a de-envelopment by fusion with the outer nuclear membrane, resulting in the release of the nucleocapsids into the cytoplasm [26]. Tegumentation and secondary envelopment occur within a cytoplasmic compartment termed the trans-Golgi network possessing mature forms of viral glycoproteins [27, 28]. Assembled mature virions, as well as other non-infectious particles (e.g. dense bodies [29]) are transported by virus secretory vesicles to the plasma membrane and released into the extracellular space of the infected cells.

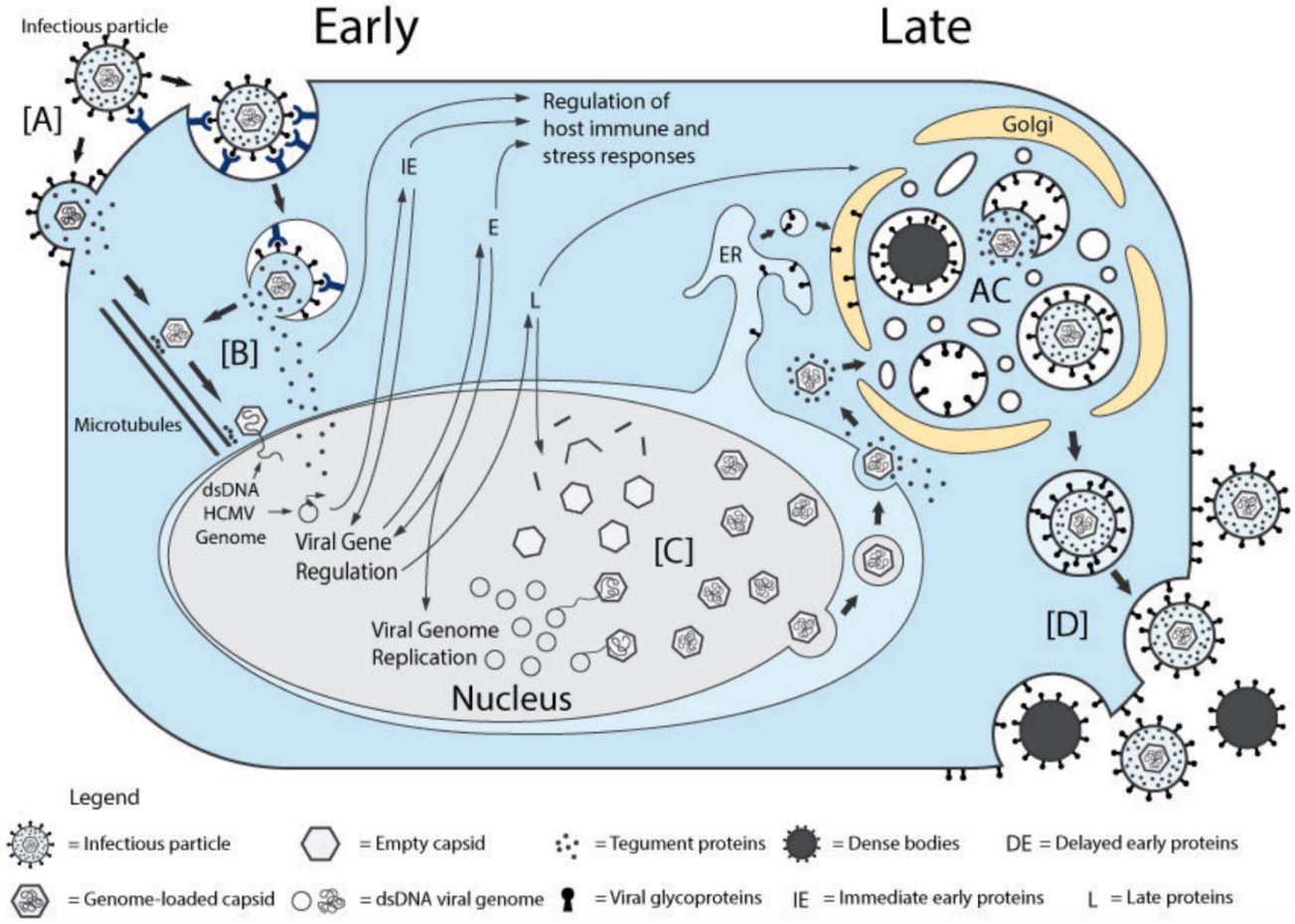

Jean Beltran PM and Cristea IM, 2014

Figure 3: Overview of the HCMV life cycle in a human cell. (Repinted from [30])
(A) Virus enters the host cell through interaction with cell surface receptors. Capsid and tegument proteins are transferred to the cytoplasm. (B) Capsids are delivered to the nuclear pore, where the DNA is penetrated and circularized. Tegument proteins initiate the expression of viral immediate early (IE) genes which then induce the expression of early (E) genes. Early proteins promote viral genome replication and late gene expression. (C) Late protein initiates virion assembly, including assembling of nucleocapsid in the nucleus and tegumentation and envelopment in the viral assembly complex (AC) (D) Infectious virus and non-infectious dense bodies are released from cytoplasma.

1.3 HCMV cell tropism

HCMV infects a broad range of cell types in many different organs [31], including neuronal cells in the brain and retina [32], fibroblasts, epithelial and endothelial cells (EC) in lung and gastrointestinal tract [33], hepatocytes in the liver [34] and peripheral blood mononuclear lymphocytes (PBML) [35]. Several cell types are considered to be responsible for HCMV dissemination. Circulating infected monocytes may release infectious virus within target organs upon differentiation into tissue macrophages [36]. Productive infection in EC of the blood vessels may lead to detachment of these cells, thus initiating hematogenous dissemination [37, 38]. In contrast, fibroblasts likely provide the loci for efficient production

of HCMV, presumably contributing to the establishment of primary infection. HCMV is also capable of infecting different cell types in vitro. However, there are variations of virus productivity among the various cell types. Fibroblasts, smooth muscle cells, endothelial cells and epithelial cells are permissive for productive infection of HCMV [31], while poorly differentiated cells such as progenitor cells of the myeloid lineage restrict the replication of the virus [39]. Fibroblasts are the most commonly used cells for the laboratory passage of HCMV since virus yields are highest in this cell type [13]. Specifically, HCMV binds to fibroblasts with a capacity of 2500 - 3000 particles per cell [40, 41].

1.4 Entry of HCMV into different host cells

The complex HCMV entry process consists of serial steps (Figure 4a), which involves multiple sequential interactions between viral envelope glycoproteins and corresponding proteins on the host cell surface [21, 22]. Initial attachment of HCMV virions to the surface of host cells is essential, but not sufficient for HCMV entry into cells. It is mediated by low-affinity binding of the glycoprotein complex gM/gN and/or gB to cellular heparan sulfate proteoglycans (HSPGs) [42-44]. The docking likely enables a more stable interaction of other glycoproteins, for instance, gH/gL complexes, with specific cellular receptors, subsequently activating a direct fusion with plasma membrane or endocytosis followed by fusion with the endosomes (Figure 4b).

Previous studies revealed that HCMV entry into fibroblasts involved direct fusion at the plasma membrane and is pH-independent [21]. However, a recent report showed that HCMV entry into fibroblasts can follow a macropinocytosis pathway [46]. HCMV entry into epithelial and endothelial cells has been described to follow a pH-dependent endocytosis pathway [22, 47]. Virus particles have been located in intracellular vesicles post-entry [47, 48]. Based on the size of the endosomes, the endocytic pathway in these two cell types was suggested to be macropinocytosis [20, 47-50]. For HCMV entry into dendritic cells (DC), macropinocytosis was also identified as the entry pathway [51]. In contrast to HCMV entry into endothelial and epithelial cells, this process was shown to be pH-independent [51].

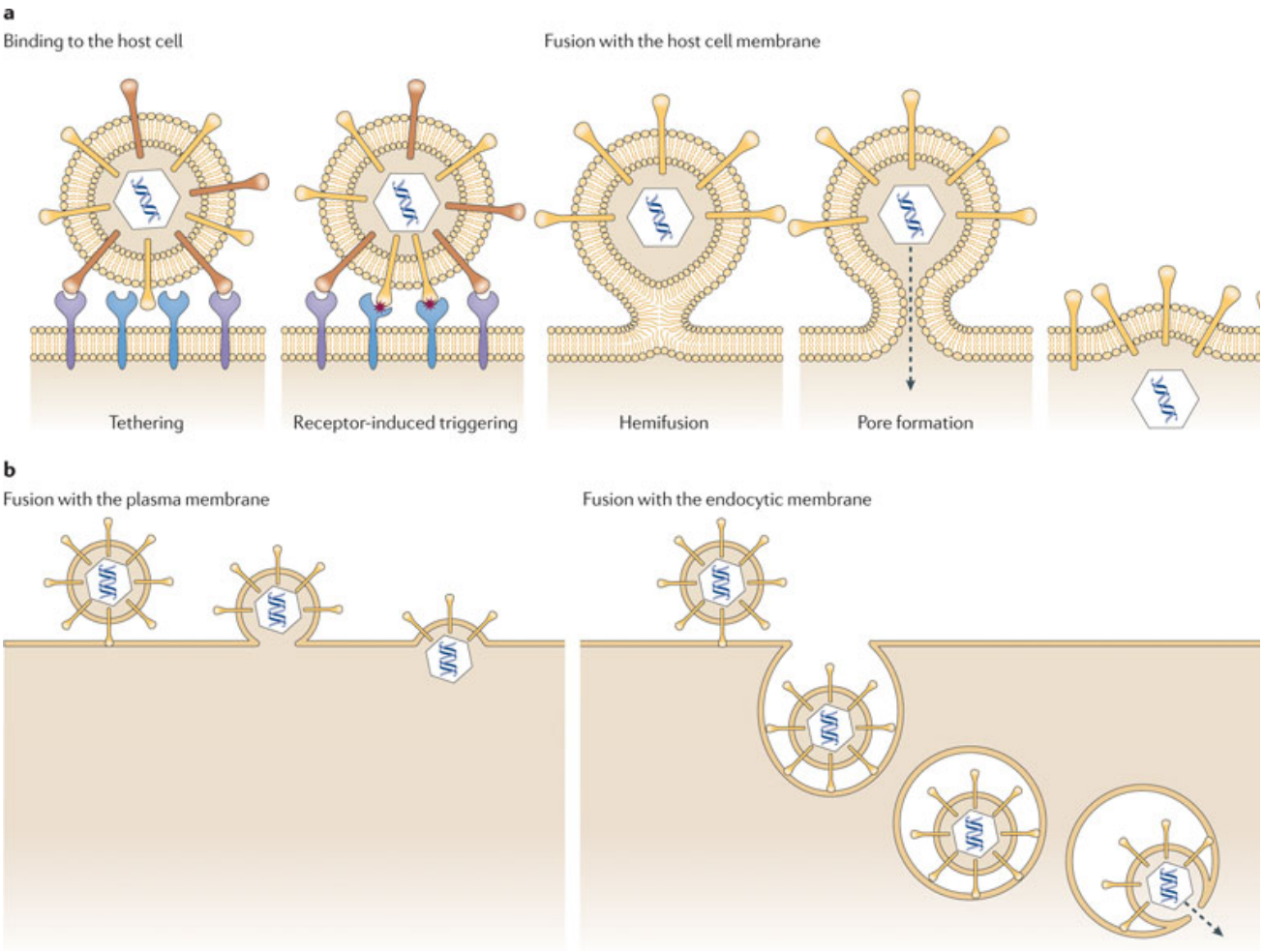

Figure 4: Schematic of HCMV entry into host cells. (Reprinted from [45])
a. Two steps of HCMV entry: binding to the host cell and fusion with the cell membrane.
b. Two entry pathways. HCMV enters cells by fusion at the plasma membrane or fusion with an endocytic membrane after endocytosis.

1.5 HCMV envelope glycoproteins involved in HCMV entry

Multiple envelope glycoproteins are implicated in the viral entry process of herpesviruses. For example, gB, gC, gD, gH and gL are involved in HSV entry into host cells [52]. gp350/220, gp42, gB, gH, and gL mediate EBV entry process [53]. For HCMV, so far 4 envelope-embedded viral glycoproteins: gB, gH, gM and gN, and 5 envelope-associated glycoproteins: gL, gO, pUL128, pUL130 and pUL131a, have been described to contribute to HCMV entry (Figure 5).

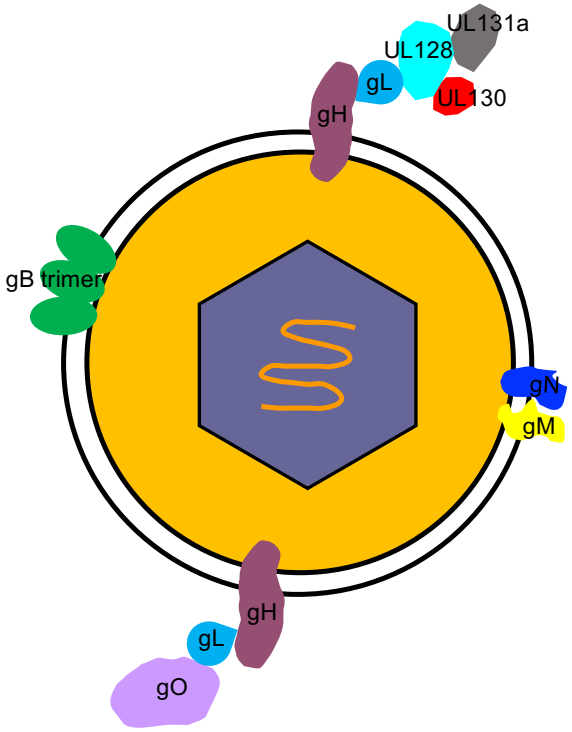

Figure 5: Schematic presentation of HCMV envelope glycoproteins involved in entry.

1.5.1 Glycoprotein B

HCMV gB, encoded by the open reading frame UL55, is a type I membrane protein which consists of 906 amino acids [54]. It is highly N- and O-glycosylated. It possesses a large ectodomain, a transmembrane domain, and an intracellular domain. gB carries an ER-signal sequence (amino acids 1 to 29), which is cleaved in the ER. The 160 kDa protein contains a furin cleavage site between residues 460 and 461. In HCMV infected cells, it is cleaved, resulting in an N-terminal product of about 116 kDa and a C-terminal product of about 58 kDa [55-61]. The two subunits are linked by a disulfide bond, and embedded in the envelope of HCMV virions in a form of trimer.[62, 63]. A recent report showed the crystal structure of HCMV gB exposed on the virion surface [64], which revealed that a large area of the protein was covered by a thick glycan layer, providing an explanation that only rarely neutralizing anti-gB antibodies are observed [65].

HCMV gB is the most abundant viral glycoprotein in the virion envelope [19], and it is essential for HCMV entry into all cell types. It is currently considered to be involved in the initial attachment step and subsequent fusion step [66].

gB mediates initial adsorption of HCMV to cell surfaces through heparan sulfate glycosaminoglycans [43, 44]. This process very likely serves a cell surface concentration of HCMV and promotes interactions with entry receptors. In addition, several studies reveal that gB is involved in fusion of the virion with the plasma membrane. For instance, co-expression of gB and gH/gL is indispensable for cell-cell fusion of fibroblasts, epithelial cells and endothelial cells [67, 68]. gB has also been shown to interact with cell-surface proteins, like integrins [69, 70], epidermal growth factor receptor (EGFR) [71] and platelet-derived growth factor receptor-α (PDGFRα) [72]. However, both EGFR and PDGFRα could not be confirmed as entry receptors for HCMV [73, 74]. A gB deletion has been shown to be unable to enter host cells but entered cells expressing recombinant gB, indicating that gB functions as a viral fusion protein rather than a receptor binding protein [75].

1.5.2 Glycoproteins gM/gN

The gM and gN proteins are conserved among all members of the herpesvirus family. HCMV gM (UL100) is a 42- to 45-kDa type III membrane protein containing 7 potential transmembrane domains [76]. It is a highly hydrophobic protein and is minimally glycosylated [76]. In contrast, gN (UL73) is a typical type I glycoprotein with low levels of glycosylation [77]. It has a 18-kDa polypeptide backbone and is extensively modified both by N-linked and O-linked carbohydrates in the presence of gM, resulting in a mature protein with a molecular mass of over 40 kDa in SDS-PAGE gels [77]. gN exhibits significant amino acid sequence variability among different HCMV strains [78]. Both gM and gN are essential for in vitro replication of HCMV since deletion of the C-terminal cytoplasmic tail of gM or the carboxy-terminal domain of gN both resulted in replication-deficient viruses [79, 80]. Together, gM and gN form a heterodimeric complex through disulfide bonds between cysteine 44 of gM and cysteine 90 in gN [77, 81]. The gM/gN complex is an abundant protein component of the HCMV envelope [19]. Like gB, gM/gN also binds to cell surface heparan sulfate glycosaminoglycans, and thus, is involved in the initial attachment of virions to the target cells [82]. Collectively, the HCMV gM/gN complex is an essential viral component which interacts with heparin sulfate glycosaminoglycans to mediate the initial attachment of virions to the cell surface [44, 82].

1.5.3 gH/gL glycoprotein complexes

The gH/gL complex of herpesvirus plays a core role in mediating virus entry through interactions with cellular receptors and the fusion protein gB. HCMV gH (UL75), an N-

glycosylated 86 kDa type 1 transmembrane protein, is linked to the 34 kDa gL (UL115) via a disulfide bond to form a stable heterodimeric complex which is indispensable for HCMV entry. Both gH and gL null mutants are defective for entry [83-89]. The gH/gL heterodimer possesses prominent structural plasticity, suggesting that gH/gL may trigger entry signals via interacting with various molecules on the cell surface and activate the highly conserved fusion protein gB [90]. It has been shown that viral particles lacking gH/gL cannot enter cells expressing gH/gL [75], indicating that the gH/gL complexes function as binding partners of entry receptor rather than simply being fusion triggers. gO and UL128 mutually exclusively bind the same site on gL via a disulfide bond and form two alternative gH/gL complexes: gH/gL/gO [91, 92] and gH/gL/pUL(128, 130, 131a) [93, 94] , which are suggested to play key roles in recognizing cellular receptors of HCMV and determine the HCMV cell tropism [48, 65, 93-95] (Figure 6). The relative amounts of the two gH/gL complexes in virion envelopes are highly relevant to viral entry [50]. To date, it is largely unknown how gH/gL interacts with receptor-binding glycoproteins or molecules on the cell surface and how it activates gB.

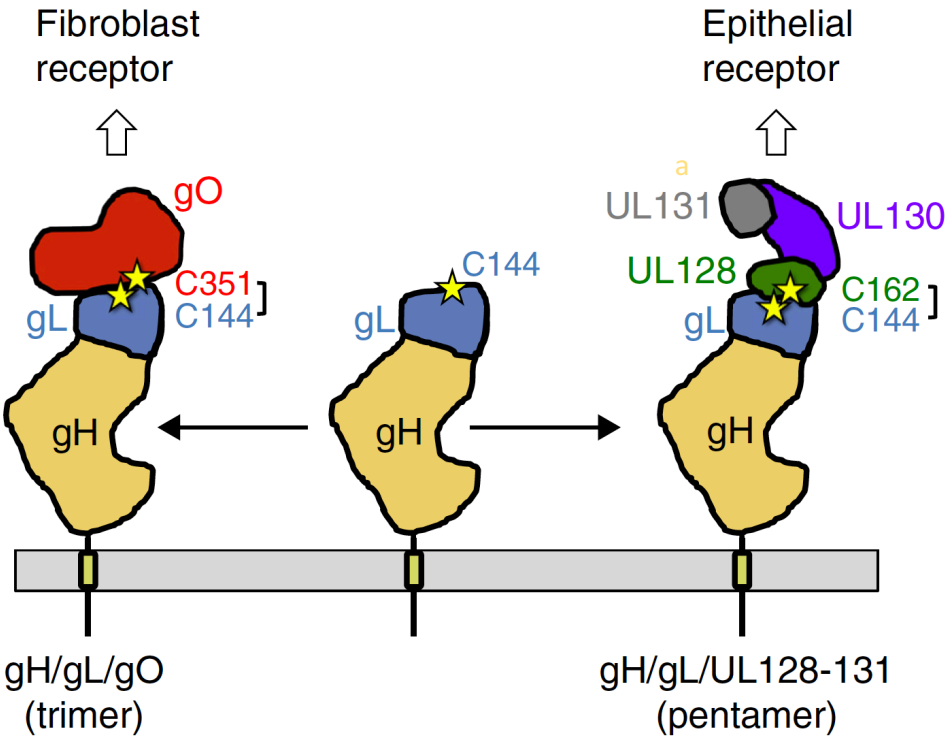

Figure 6: Schematic presentation of HCMV's mutually exclusive gH/gL complexes. (Reprinted from [98]) This illustration of CMV gH/gL complexes is based on their structures [99]. Cysteines are shown as stars and labeled. Approximate locations and shapes of gH, gL, gO, UL128, UL130 and UL131 are shown. Membrane and transmembrane anchors are shown schematically.

1.5.3.1 gH/gL/gO

HCMV glycoprotein O (UL74) is unique for β-herpesviruses [92]. gO possesses several conserved cysteines and 18 potential N-glycosylation sites and the mature form runs at around 125 kDa in polyacrylamide gels [92, 100]. In HCMV-infected human foreskin fibroblasts (HFF), gO covalently binds to gH/gL in the ER [89, 92], and is subsequently processed in the Golgi apparatus [89, 101]. The mature gH/gL/gO complex is about 240 kDa, and has been proven to be incorporated into the virion envelopes in all tested HCMV strains [89, 102]. There are more than eight isoforms of HCMV gO with an identity of amino acids ranging from 70% to 90% [102]. Different gO isoforms have distinct affinities to bind gH/gL [102]. gO is not essential for HCMV replication [103], but the gH/gL/gO complex plays key roles in mediating virus entry into host cells. HCMV mutants lacking gO, or mutants with low amounts of gH/gL/gO in their envelopes, have been shown to be compromised in entry into all tested cell types, including fibroblasts, epithelial cells, EC and macrophages [104]. Virus particles of gO deletion mutants released from infected cells have much lower infections titers (<1000) than the wildtype virus. Infections with gO-deletion mutants exhibit a cell-associated spread pattern in cell cultures [103, 105-108]. Of note, the supernatant-driven spread of the gO-null mutants has been shown to be severely impaired in fibroblasts, whereas the focal growth was not affected [106]. In particular, it has been shown that HCMV mutants lacking gH/gL/gO were impaired at the fusion step of entry into host cells, despite containing relatively more gH/gL/pUL(128, 130, 131a) [107]. Antisera to gO neutralized HCMV entry into fibroblasts, suggesting that gO plays a direct role in HCMV entry (Patent US7147861 B2, 2001). The recombinant gH/gL/gO complex interferes with HCMV entry into fibroblasts but not entry into other cell types, suggesting that the trimer may bind to a fibroblast-specific receptor [68]. What role the HCMV gH/gL/gO complex plays in vivo is not clear, however, a recent in vivo study of mouse CMV gH/gL complexes revealed that gH/gL/m74 (a functional homologous of HCMV gH/gL/gO), is essential for entering the first target cells including epithelial cells, EC and macrophages in primary infection [109]. Intriguingly, there are abundant neutralizing antibodies to gH detected in HCMV-serum positive individuals [110], but only one neutralizing antiserum to gO has been reported [92].

1.5.3.2 gH/gL/pUL(128, 130, 131a)

It has been shown that the gene products of UL128, UL130 and UL131a bind gH/gL to form the alternative pentameric gH/gL complex, gH/gL/pUL(128, 130, 131a) [93]. pUL130 is a

35-kDa glycoprotein, and both pUL128 and pUL131a have a size of approximately 15- to 18-kDa. The more closely characterized pUL128 has four conserved cysteine residues near the N-terminus which are a structural characteristic of β- (or CC-) chemokines [111]. HCMV strains lacking the UL128, UL130 and UL131 gene locus have lost their tropism for epithelial and endothelial cells [93, 112-114]. The intact pentameric complex is essential for mediating HCMV infection of epithelial and endothelial cells and monocyte-macrophages [94, 97, 115-117]. Recent studies found that recombinant gH/gL/pUL(128, 130, 131a), but not the gH/gL dimer, inhibited HCMV entry into epithelial cells and pUL(128, 130, 131a) are necessary for the interaction with cell surface receptors [118-120]. These findings suggest that pUL(128-131a) is essential for binding of epithelial-specific receptors.

1.5.3.3 gH/gL/gO and gH/gL/pUL(128, 130, 131a) complexes shape the HCMV tropism

gO and pUL(128, 130, 131a) form mutually exclusive complexes with gH/gL which are incorporated into the virions. HCMV mutants lacking gH/gL/pUL(128, 130, 131a) can efficiently infect fibroblasts, whereas mutants lacking gH/gL/gO are severely impaired for infecting all cell types [103, 107], leading to the conclusion that gH/gL/gO and gH/gL/pUL(128, 130, 131a) bind different cellular receptors, however, only gH/gL/gO maintains the general gH/gL entry functions in all cell types, such as activating gB [104].

Current studies support a model in which gH/gL/gO mediates virus entry into fibroblasts, while gH/gL/pUL(128, 130, 131a) mediates virus entry into epithelial cells and EC. The relative abundance of the trimer and pentamer may shape HCMV tropism by influencing the efficiencies of virus entry into different cell types. Viruses with relatively higher amounts of pentamer preferentially infect epithelial cells and EC whereas viruses with relatively higher amounts of trimer tend to enter fibroblasts [50].

Among different HCMV strains, gO varies a lot [102] while UL128, UL130 and UL131a genes are highly conserved [121]; therefore, the diversity of gO might affect the ratio of gH/gL/gO to pentamer incorporated into the virions. In accordance with this, a study found that gO isoforms from different HCMV strains have distinct affinities to bind gH/gL, and may affect the relative ratios of gH/gL/gO and gH/gL/pUL(128, 130, 131a) incorporated, thus contributing to their distinct cell tropism [102].

HCMV progenies produced from both fibroblasts and EC cultures show a distinct cell tropism due to the incorporation of different amounts of gH/gL/gO and gH/gL/pUL(128, 130, 131a) complexes in their virions [122]. Fibroblast-derived virus contains both the trimer and pentamer, and is thus capable of infecting both fibroblasts and EC [122]. In contrast, EC-specifically retain EC-tropic virus with high amount of gH/gL/pUL(128, 130, 131a) complex. EC-released virus has relative low amount of the pentameic complex, and therefore can readily infect fibroblasts, but scarcely infects EC [122]. The spread-pattern of HCMV in fibroblast cultures is supernatant-driven whereas spread in EC cultures is cell-associated.

It is commonly known that gH/gL complexes mediate entry of HCMV into host cells The mechanism of the cell-type dependent switch of HCMV cell tropism remains largely unknown, however it has been shown that the relative ratio of the alternative gH/gL complexes shape the cell tropism. Recent work has identified the a viral glycoprotein pUL148 acts as a regulator of the relative amounts of the gH/gL/gO and gH/gL/pUL(128, 130, 131a) complexes in virions. pUL148 is capable to bind gL, thus interferes with incorporation of pUL128 or gO into the gH/gL dimer [123].

1.6 Cellular receptors involved in HCMV entry

HCMV's broad cell tropism suggests that HCMV either utilizes multiple cell type-specific receptors or a broadly expressed receptor or a combination of both for entry. Over the past two decades, many receptor candidates have been put forward. However, none of these molecules have been verified to be indispensable entry receptors for HCMV [50].

The first candidate shown to bind HCMV virions was β_2-microglobulin [124, 125]. However, it has later been shown that there is no correlation between β_2-microglobulin expression and in vitro entry or in vivo spread of HCMV [126, 127].

Annexin II expression has also been shown to promote HCMV infection by interacting with HCMV gB [128-132]. However, cells lacking annexin II are still fully permissive for HCMV entry and initiation of infection [133].

Human aminopeptidase (CD13) has also been implicated as an HCMV receptor. Only CD13-positive human peripheral blood mononuclear cells (PBMCs) supported productive HCMV infection [134-136]. Both CD13-specific antibodies and chemical inhibitors of CD13

activity inhibited HCMV binding and entry [134]. However, later reports negated CD13 as a receptor for HCMV based on the observations that CD13 antibodies could bind and neutralize virus before contact with cells and HCMV could enter CD13-depleted cells [137].

THY-1 (CD90), has recently been suggested to play a role during HCMV entry based on the observation of a positive correlation between HCMV infectivity and THY-1 expression levels, and an interaction between THY-1 and HCMV gH and gB [138]. Both HCMV gH and cell surface THY-1 were reported to interact with αvβ3 integrin to trigger cellular signaling, thus, the observed interaction between gH and THY-1 might be promoted by αvβ3 integrin during HCMV entry.

EGFR was initially described as a ligand for gB. Upon HCMV infection, EGFR is activated and triggers EGFR-dependent signaling in fibroblasts, breast cancer cells and monocytes [71, 139, 140]. However, EGFR-negative cells, such as hematopoietic cells, can nevertheless be infected by HCMV. Inhibition of EGFR with antibodies or inhibitors or siRNAs had no effect on HCMV entry [73, 134].

Cellular integrins, α2β1 and α6β1, were reported to bind to a disintegrin-like domain of HCMV gB [69, 70]. Integrin signaling and HCMV entry could be inhibited by disintegrin domain peptides and anti-integrin antibodies [69, 70]. In addition, αvβ3 has been shown to interact with gH and associate with EGFR in lipid rafts to facilitate HCMV infection of fibroblasts [139]. Anti-integrin antibodies had no effect on HCMV attachment but specifically inhibited the transport of pp65 (pUL83), a virion tegument protein, suggesting that integrins function at a post-attachment entry step. Interestingly, EGFR can be phosphorylated by activation of β1, β3 and αv integrins [141, 142].

PDGFRα has initially been identified as a ligand for recombinant gB. HCMV binding to fibroblasts and EC has been shown to result in PDGFRα phosphorylation and activation of downstream molecules [72]. Based on the observation that recombinant gB can interact with PDGFRα and that HCMV infection can be inhibited by knockdown of PDGFRα, by the PDGFRα ligand PDGF-AA, by the tyrosine-kinase inhibitor Imatinib mesylate and by a PDGFRα-neutralizing antibody, it has been claimed that PDGFRα functions as an entry receptor for HCMV [72]. In contrast, a later study contested the previous claim that PDGFRα acts as a receptor for HCMV gB [74]. Although overexpression of PDGFRα

strongly enhanced HCMV infection of epithelial and endothelial cells for both wildtype HCMV and gH/gL/pUL(128, 130, 131a) deficient mutants, virus entry was neither affected by a panel of PDGFRα antibodies or PDGFRα ligand in fibroblasts, epithelial, or endothelial cells nor by knockdown of PDGFRα in epithelial cells [74].

In summary, currently HCMV entry receptors are still not well defined.

1.7 MCMV as a model to study HCMV

Due to the strict species specificity of HCMV, strategies designed to test anti-HCMV vaccines or therapies have to use appropriate animal models using closely related viruses [143]. Rhesus CMV infection of rhesus monkeys serves as a good model to study HCMV infection [144]; however, it is time-consuming, scale limited and expensive. Murine CMV (MCMV) is by far the most commonly used model to study CMV infection in vivo with the following advantages: i) HCMV and MCMV share 80 conserved ORFs [145, 146] and some of them can even be exchanged [147, 148]. ii) the pathology and host immune response to MCMV infection are similar with those of HCMV infection [149]. For instance, MCMV is also able to establish latent infection in immunocompetent mice [150], whereas it is lethal for immunosuppressed mice [151, 152]. Moreover, activation from latent infection [152-156] and transmission during transplantation and blood transfusion were also observed for MCMV [154, 157]. The MCMV model has also been used to evaluate potential antiviral drugs and the identification of host resistance genes. It permits the study of MCMV mutants in vivo [158].

1.7.1 MCMV gH/gL glycoprotein complexes

The structure of the MCMV genome is equivalent to that of HCMV. Multiple MCMV proteins have homologs in HCMV [159], including a number of essential proteins such as the IE-1 protein [160, 161], the DNA polymerase [162] and some glycoproteins like gH, gL, and gB [163, 164].

m74 of MCMV, the positional homolog of HCMV UL74 (Figure 7), codes for a glycosylated protein which is found to be incorporated into the gH/gL (m75/m115) complex and packaged into MCMV virions [159, 165]. m74 deletion mutants of MCMV exhibit similar entry and spread defects as HCMV lacking gO. Virus spread shifts from supernatant-driven to cell-associated spread. Entry into fibroblasts shifts from energy independent and pH-

insensitive to an energy-dependent and pH-sensitive pathway for m74 deficient mutants. This suggests that the MCMV m74 protein and HCMV gO possess similar functions in CMV entry and spread [165]. When studied in vivo, it was found that gH/gL/m74 was found to be critical for infection of first target cells by mediating virus entry into diverse cell types such as endothelial cells, liver macrophages, and hepatocytes, whereas it was dispensable for intra-tissue spread [109].

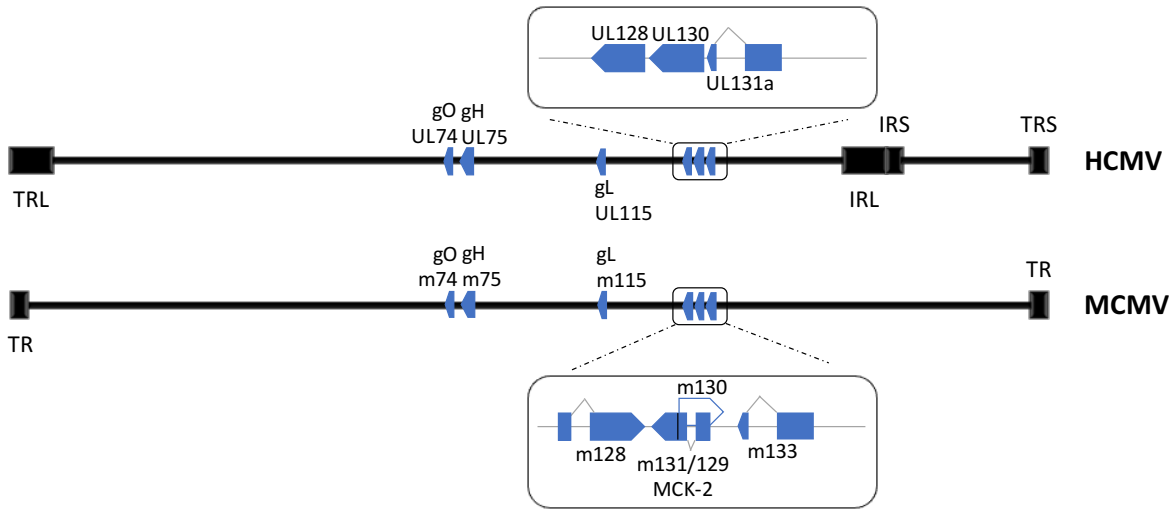

Figure 7: Schematic presentation of gene loci of the constitutions of the HCMV and MCMV gH/gL complexes.
The positions of genes encoding gH, gL, gO for both viruses are indicated. The upper insert shows the loci of UL128, UL130 and UL131A of HCMV. The lower insert indicates the locus of m128-m133 of MCMV. Terminal long (TRL) and short repeats (TRS), inner long (IRL) and short (IRS) repeats are also shown for HCMV. Terminal repeats at both ends of the MCMV genome are indicated.

For MCMV, the m131/129 (Figure 7) protein products was found to encode a protein which forms an alternative MCMV gH/gL complex [166]. The gene product of m131/129 is the MCMV MCK-2 chemokine [167, 168]. Notably, similar to the HCMV pUL128, MCMV MCK-2 has four conserved cysteine residues near the N-terminus, which is characteristic for a CC chemokine. Both MCK-2 and pUL128 have been shown to be active chemokines [117, 169, 170]. Deletion of MCK-2 reduced MCMV infection of macrophages both in cell culture and in vivo [109, 166, 171].

MCMV mutants lacking both m74 and MCK-2 are not able to produce infectious virus, a character shared by double-deficient mutants of HCMV. Accumulatively, current data support the concept that MCMV expresses functional homologues of gH/gL/gO and

gH/gL/pUL(128, 130, 131a), which also determine the entry pathways, cell tropism, and spread pattern.

1.7.2 Cell tropism of MCMV

Similarly to HCMV, MCMV has the capacity to infect a broad spectrum of cell types and tissues in vivo [172]. MCMV DNA was detected in different organs of infected mice, such as salivary glands, liver, kidney and lung [173, 174]. MCMV is also able to be propagated in vitro in many different cell types, including fibroblasts, epithelial cells, EC and macrophages [175, 176]. Of note, fibroblasts are the most productive cell culture system for both HCMV and MCMV [175, 176].

1.8 Objectives

For most human herpesviruses, one or more cellular receptors have been identified, but not for HCMV. Numerous studies on HCMV entry have identified the alternative HCMV gH/gL glycoprotein complexes, gH/gL/gO and gH/gL/pUL(128, 130, 131a), as the envelope glycoprotein complexes recognizing cell type-specific receptors, however, their respective host cell receptors are still undiscovered.

Objectives of this thesis were:

1) identification and characterization of the cellular receptor of HCMV gH/gL/gO complex by using either recombinant gO protein or virions expressing only the gH/gL/gO complex;
2) evaluation of the role of the receptor to HCMV cell tropism in cell culture;
3) comparison of the role of HCMV and MCMV gH/gL/gO in cell tropism in vitro.

Identification of cellular receptors will not only facilitate to understand the complex cell tropism of HCMV but also aid the development of antiviral strategies and vaccines.

2 Materials and Methods

2.1 Materials

2.1.1 Devices

Device	Company
Centrifuges:	
Eppendorf Centrifuge 5417R	Eppendorf, Hamburg, DE
Multifuge 3 S-R	Heraeus Instruments, Gera, DE
Biofuge stratos	Thermo Fisher Scientifc, Osterode, DE
Ultracentrifuge L8-55 M	Beckmann Coulter GmbH, Krefeld, DE
Gel electrophoresis:	
Power Pac 200	Bio-Rad, Hercules, DE
Mini-PROTEAN 3 Cell	Bio-Rad, Hercules, DE
Mini-PROTEAN Tetra System	Bio-Rad, Hercules, US
Incubators:	
HERA cell 150 (eukaryotic cell culture)	Heraeus Instruments, Gera, DE
HERA cell 150i (eukaryotic cell culture)	Heraeus Instruments, Gera, DE
CERTOMAT BS-1 (bacterial shaker)	Sartorius AG, Göttingen, DE
Microscopes:	
Axiovert 40C (light microscope)	Carl Zeiss MicroImaging GmbH, Jena, DE
Leica DMI4000 B (fluoresence microscope)	Leica, Wetzlar, DE
Pipettes:	
PIPETBOY acu pipet	INTEGRA Biosciences AG, Zizers, CH
Eppendorf® Multipette® Plus pipette	Eppendorf, Wesseling, DE
PIPETMAN Classic™: P20, P100, P200, P1000	Gilson S.A.S., VILLIERS LE BEL, FR
Miscellaneous:	
BD FACSCanto™ II (FACS machine)	BD Biosciences, San Jose, US
Bio-Photometer	Eppendorf, Hamburg, DE
Cell culture laminar flow hood	BDK, Sonnenbühl-Genkingen, DE
CLARIOstar microplate reader (luciferase assay)	BMG LABTECH GmbH, Ortenberg, DE
Developing machine FPM-100A	Fuji Photo Film Co., LTD, Tokyo, JP
Gel-Doc™ 200 (imaging of blots)	Bio-Rad, Hercules, DE
Gel Doc™ EZ Gel Documentation System	Bio-Rad, Hercules, DE
Gene Pulser Xcell™ Electroporation Systems	Bio-Rad, München, DE

Device	Company
Hypercassette™	Amersham life science, Buckinghamshire, UK
MS1 Minishaker (votexing)	IKA, Wllmington, NC
NanoDrop 1000	Thermo Fisher Scientifc, Osterode, DE
Neubauer Chamber (cell counting)	Celeromics, Grenoble, FR
Overhead shaker REAX 2	Heidolph, Schwabach, DE
PH meter 430	Corning, NY, US
Roller mixer SRT1	Stuart, Staffordshire, UK
Sonifier 450	Branson, UK
Thermomixer 5436	Eppendorf, Hamburg, DE
Water Bath GFL	Gesellschaft für Labortechnik GmbH, Burgwedel, DE
Weighing machine KERN 470-36	KERN & Sohn GmbH, Balingen, DE
VACUSAFE (aspiration of liquids)	INTEGRA Biosciences AG, Zizers, CH
VERSAmax microplate reader (ELISA)	Molecular Devices, Sunnyvale, US

2.1.2 Consumables

Name	Company
Amicon® Ultra-15 Centrifugal Filters	Merck Millipore, Darmstadt, DE
Cell culture dishes (10 cm and 15 cm)	Becton Dickinson, Heidelberg, DE
Cell culture plates (6-, 12-, 24-, 48-, 96-well)	Becton Dickinson, Heidelberg, DE
Combitips plus (5 ml, 10 ml)	Eppendorf, Hamburg, DE
CryoTube™ Vial	Nunc, Langenselbold, DE
Electroporation cuvettes	Bio-Rad, München, DE
Falcon conical tubes (15 ml, 50 ml)	Becton Dickinson, Heidelberg, DE
Falcon Tubes for FACS	Becton Dickinson, Heidelberg, DE
Hybond™-N+ Nylon membrane	GE Healthcare, Freiburg, DE
Hyperfilm™ ECL™ detection film	GE Healthcare, Freiburg, DE
PCR Tubes	Biozym, Hessisches Oldendorf, DE
Pipettes (2 ml, 5 ml, 10 ml, 25 ml)	Sarstedt, Nümbrecht, DE
Pierce™ NeutrAvidin™ Coated Clear Strip Plates	Thermo Fisher Scientific, Rockford, US
Photometer cuvettes	Brand, Wertheim, DE
Safe lock tubes (0.5 ml, 1.5 ml, 2 ml)	Eppendorf, Hamburg, DE
Screw cup tubes 1.5 ml	Biozym, Hessisches Oldendorf, DE
Ultracentrifugation tubes	Beckman Coulter GmbH, Krefeld, DE
Whatman blotting paper (0.7 mm)	Macherey-Nagel, Düren, DE

2.1.3 Reagents

Name	Company
Acrylamid/Bis-acrylamide 30% Solution	Merck, Darmstadt, DE
Agarose	Invitrogen, Karlsruhe, DE
APS	Sigma-Aldrich, Steinheim, DE
Bacto™ Agar	Becton Dickinson, Heidelberg, D
Bacto™ Tryptone	Becton Dickinson, Heidelberg, D
Bacto™ Yeast Extract	Becton Dickinson, Heidelberg, D
BenchMark prestained protein ladder	Invitrogen, Karlsruhe, DE
Beta-Mercaptoethanol	Sigma-Aldrich, Steinheim, DE
Coomassie Blue G-250	Sigma-Aldrich, Steinheim, DE
BSA	Sigma-Aldrich, Steinheim, DE
cOmplete™ Protease Inhibitor Cocktail	Roche, Mannheim, DE
DMSO	Merck, Darmstadt, DE
DNA 100bp ladder and 1 kb ladder	NEB, Frankfurt am Main, DE
DTSSP (3,3'-Dithiobis (sulfosuccinimidylpropionate))	Thermo Fisher Scientific, Bonn, DE
DTT (dithiothreitol)	Roth, Karlsruhe, DE
EDTA (ethylenediaminetetraacetic acid)	Sigma-Aldrich, Steinheim, DE
Ethisiumbromide 1%	Roth, Karlsruhe, DE
EZ-Link Sulfo-NHS-LC-Biotin	Thermo Fisher Scientific, Bonn, DE
Glycerin	Roth, Karlsruhe, DE
Glycin	Roth, Karlsruhe, DE
imatinib mesylate	Sigma-Aldrich, Steinheim, DE
Isopropanol	Sigma-Aldrich, Steinheim, DE
Kanamycin	Sigma-Aldrich, Steinheim, DE
Methanol	Sigma-Aldrich, Steinheim, DE
Mouse IgG Fc-PDGFRα fusion protein	R&D Systems, Minneapolis, US
Mouse IgG Fc-PDGFRβ fusion protein	R&D Systems, Minneapolis, US
NaCl (natrium chloride)	Merck, Darmstadt, DE
Ampicillin	Invitrogen, Karlsruhe, DE
PFA (Paraformaldehyde)	Merck, Darmstadt, DE
Polyethylenimine	Sigma-Aldrich, Steinheim, DE
Ponceau S solution	Sigma-Aldrich, Steinheim, DE
Protein A IgG Binding and Elution Buffers	Thermo Fisher Scientific, Bonn, DE

Name	Company
Protein A sepharose beads	GE Healthcare, Freiburg, DE
Restore™ Western blot Stripping Buffer	Thermo Fisher Scientific, Bonn, DE
SDS	Merck, Darmstadt, DE
Skimmed milk powder	Merck, Darmstadt, DE
TEMED	Roth, Karlsruhe, DE
Tris-Base	Sigma-Aldrich, Steinheim, DE
Triton X-100	Sigma-Aldrich, Steinheim, DE
Trypan blue 0,5% (w/v)	Biochrom KG, Berlin, DE
Tween 20	Sigma-Aldrich, Steinheim, DE
Versene Solution	Thermo Fisher Scientific, Bonn, DE
Zeocin™	Thermo Fisher Scientific, Bonn, DE
crystal violet	Sigma-Aldrich, Steinheim, DE

2.1.4 Commercial kits

Name	Company
Expand High Fidelity PCR system	Roche, Mannheim, DE
EZ-Link™Sulfo-NHS-Biotinylation Kit	Thermo Fisher Scientific, Bonn, DE
FireSilver Staining Kit	Proteome factory, Berlin, DE
FuGENE HD Transfection Reagent	Roche, Mannheim, DE
illustra™ plsamidPrep Mini Spin Kit	GE Healthcare, Freiburg, DE
Luciferase Reporter Assay Kit I (Firefly)	PromoKine, Heidelberg, DE
Nucleobond® PC100 Kit	Macherey-Nagel, Düren, DE
Pierce™ ECL Plus Western blotting Substrate	Thermo Fisher Scientific, Rockford, US
QIAquick® Gel Extraction-Kit	Qiagen, Hilden, DE

2.1.5 Enzymes

All restriction endonucleases and enzymes for DNA analysis were purchased from NEB, Frankfurt am Main, DE and and applied according to the manufacturers' instructions.

2.1.6 Primers

Primers were synthesized by Metabion (Martinsried, DE).

Primers for cloning HCMV gO

Name	Sequence (5' to 3')	Restriction site
forward	ATAACCATGGGTAAGGTCGTTAGACCACCGG	*Nco* I
reverse	CAGAAGATCTCTGCAACCACCACCAAAGGC	*Bgl* II

Primers for sequencing cloned gO

Name	Sequence (5' to 3')
forward	TCTGTTCTGCGCCGTTACAG
reverse	AGGAGCTGGGCATTTGTGAC

2.1.7 Plasmids

pFUSE_mIgG2B_Fc2 (Cat. No. pfuse-mg2bfc2, InvivoGen): An eukaryotic expression vector for cloning and expressing of Fc-fusion proteins. The vector expresses the hinge region and the Fc region of the murine IgG2b heavy chain. The flexible hinge region allows each part of the fusion protein to function independently. It also expresses the IL-2 signal sequence for secretion of the Fc-fusion proteins.

pCMV-PDGFRα (Cat. No. HG10556-UT, Sino Biological Inc.): The pCMV3 vector (6223bp) expresses the full length (3270bp) cDNA of human platelet-derived growth factor receptor alpha polypeptide (NCBI RefSeq: NM_006206.4).

pEGFP-c1 (Clontech): An eukaryotic expression vector for fusing enhanced green fluorescent protein to the C-terminus of a partner protein. Here it was used as an indicator of transfection efficiency.

2.1.8 Antibodies

Antibody	Source
Primary antibodies and antiserum:	
mouse anti-HCMV IE1	PerkinElmer, Waltham, US
mouse anti-HCMV gB (IP), (SM5-1)	kindly provided by M. Mach (University Erlangen-Nürnberg, DE)
mouse anti-HCMV gB (WB), (2F12)	Biozol, Echingen, DE

Antibody	Source
mouse anti-HCMV gH (IP), (14-4b)	kindly provided by W. Britt (University of Alabama, Birmingham, US)
mouse anti-HCMV gH (WB), (SA4)	kindly provided by M. Mach (University Erlangen-Nürnberg, DE)
mouse anti-HCMV gO, (gO.02)	kindly provided by Stipan Jonjic (University of Rijeka, Croatia)
mouse anti-MCMV ie1, (Croma 101)	
mouse anti-PDGFRα (C-9)	SANTA CRUZ
rabbit anti-HCMV pUL131A, (3058)	[94]
Secondary antibodies:	
goat anti-mouse IgG (Fc Specific)-peroxidase	A0168, Sigma-Aldrich, Steinheim, DE
sheep anti-mouse-peroxidase	515-035-062, Dianova, Hamburg, DE
goat anti-mouse light chain (κ)-peroxidase	115-035-174, Dianova, Hamburg, DE
goat anti-rabbit-peroxidase	111-035-003, Dianova, Hamburg, DE
Alexa Fluor 488-goat-anti mouse	A-11001, Invitrogen, Karlsruhe, DE
mouse anti-human β Actin)-peroxidase	AC-74, Sigma-Aldrich, Steinheim, DE
anti-mouse IgG (Fc specific)−biotin	B9904, Sigma-Aldrich, Steinheim, DE
streptavidin-peroxidase polymer	S2438, Sigma-Aldrich, Steinheim, DE

2.1.9 Cells and media

2.1.9.1 Prokaryotic cells

E.coli	Features	Remarks
DH10 B	F- mcrA Δ(*mrr-hsdRMS-mcrBC*) Φ80d*lac*ZΔM15 Δ*lac*X74 *end*A1 *recA*1 *deo*R Δ(*ara, leu*) 7697 *ara*D139 *gal*U *gal*K *nup*G *rpsL* λ [177]	Invitrogen, Karlsruhe, DE

2.1.9.2 Eukaryotic cells

Cells	Description	Remarks
293	Human kidney epithelia cells	ATCC, CRL-11268™
ANA-1	Murine bone marrow-derived macrophage-like cells	[178]
ARPE-19	Human retinal pigmented epithelial cells	ATCC® CRL2302™
HFF	Human foreskin fibroblasts	from PromoCell

Cells	Description	Remarks
HUVEC	Human umbilical vein endothelial cells	From Lonza
MEF	Murine embryonic fibroblasts	Own prepared from BALB/c mice
MHEC-5T	Murine heart endothelial cells	[179]
MRC-5	Human lung fibroblasts	ATCC® CCL-171™
NIH3T3	Murine embryo fibroblasts	ATCC® CRL-1658™
TCMK-1	Murine kidney epithelial cells	ATCC® CCL-139™
TIME	Human telomerase-immortalized microvascular endothelial cells	[180]

2.1.10 Viruses

Cloning of herpesvirus genomes as bacterial artificial chromosomes (BACs), allows the maintenance and rapid engineering of viral genomes within E. coli. Virus can be reconstituted by transfection of the BAC plasmid in permissive eukaryotic cells. Human cytomegalovirus strain TB40/E was originally isolated from a bone marrow transplant recipient [34] and then cloned as a bacterial artificial chromosome (BAC) [181]. It is an endotheliotropic HCMV strain which is widely used around the world. All viruses used were derived from a wildtype BAC clone of TB40/E, TB40-BAC4 [181].

TB40-BAC4: A BAC clone containing the complete sequence of HCMV strain TB40/E. Virus reconstituted from TB40-BAC4 shows wildtype-like growth properties.

TB40-UL131stop: A TB40-BAC4 mutant generated by introducing a G to A exchange at position 20 in ORF UL131, resulting in a stop mutant.

TB40-ΔgO: A TB40-BAC4 mutant generated by deleting the first 533 nucleotides of ORF UL74 from TB40-BAC4.

TB40-Luc: ORFs UL5 to UL9 were deleted from the TB40-BAC4 genome, and then a luciferase report gene inserted into TB40-BAC4△UL5-UL9 genome. TB40-Luc shows wildtype-like growth properties in cell culture.

TB40-UL131stop-Luc: A TB40-Luc mutant generated by introducing a G to A exchange at position 20 in ORF UL131, resulting in a stop mutant.

TB40-ΔgO-Luc: A TB40-Luc mutant generated by deleting the first 533 nucleotides of the ORF UL74.

Mouse cytomegalovirus strain Smith was originally isolated from salivary glands of infected laboratory mice [182]. It was cloned as a bacterial artificial chromosome (BAC) named

pSM3fr [183, 184]. A frameshift mutation within the open reading frame (ORF) of MCK-2 was repaired later and named pSM3fr-MCK-2fl [185]. MCMV BACs used here were all derived from pSM3fr-MCK-2fl [185].

2.1.11 Software

Software	Company
Microsoft Office (Excel, Powerpoint, Word)	Microsoft
FACSDiva	BD Biosciences
GraphPad Prism 5	GraphPad Software
Vector NTI	Thermo Fisher Scientific
Image J	Developed by NIH for public
Image Lab	Bio-Rad

2.2 Methods

2.2.1 Cultivation of bacteria

DH10B were grown at 37°C either in suspension (LB-medium) or on agar-plates (LB-agar). The respective antibiotics were added for plasmid selection (see below). Cell density was determined by measuring the optical density of a bacterial suspension at 600 nm (OD_{600}). OD_{600} of 1 corresponds to approximately 1×10^8 cells/ml.

Medium	Composition
LB-medium	10 g Bacto™ Trypton, 5 g Bacto™ Yeast Extract, 5 g NaCl, in 1 L H_2O
LB-Agar	15 g Bacto™ Agar, in 1 L LB-medium

Antibiotics

ampicillin	50 µg/ml
zeocin	30 µg/ml

2.2.1.1 Glycerol stocks

To maintain plasmid-carrying bacteria, glycerol stocks were prepared by adding 500 µl 50% glycerol to 500 µl dense bacterial culture. Stocks were stored at -80°C.

2.2.1.2 Preparation of electrocompetent bacteria

To prepare competent cells which are susceptible to introduction of foreign DNA by electroporation, 150 ml LB-medium was inoculated with 1.5 ml overnight DH10B culture and grown at 37°C to reach an OD_{600} of about 0.4. All following steps were conducted at low temperatures at 4°C. Briefly, bacteria were cooled on ice for 15 min and then pelleted by centrifugation at 5,500×g for 10 min and subsequently washed for 3 times with 100 ml 10% glycerol. The bacterial pellet was finally resuspended in 1 ml 15% glycerol and snap frozen in liquid nitrogen as 70 µl aliquots and stored at –80°C.

2.2.1.3 Transformation of bacteria

Plasmid DNA was introduced into bacterial cells by electroporation. Briefly, 70 µl competent cells were thawed on ice for 10 min and mixed with 10 µl ligation product (100 - 200 ng) or 1 - 10 ng plasmid DNA. The mixture was transferred to a pre-cooled electroporation cuvette (Biorad; 0.2 mm in diameter) and electroporated (4.5 ms, 2,5 kV, 200 Ohm and 25 mFD). 1

ml antibiotic free LB-medium was immediately added to the mixture before incubation at 37°C for 1 h. Then, 200 µl were plated on LB agar plates and incubated at 37˚C over night.

2.2.2 Molecular biology

2.2.2.1 Polymerase chain reaction (PCR)

To amplify DNA fragments, PCR was performed using Expand High Fidelity Polymerase (Roche). The reaction was done in a total volume of 100 µl. The PCR reaction mixture and program are shown below:

PCR reaction mixture

Component	Volume	Final concentration
10×Expand High Fidelity buffer	10 µl	1×
10 mM dNTPs	2 µl	200 µM
Forward primer (25 µM)	1 µl	500 nM
Reverse primer (25 µM)	1 µl	500 nM
Template DNA	2 µl	10 ng
Expand High Fidelity enzyme mix	1 µl	3.5 U/reaction
ddH_2O	added up tp 100 µl	

PCR program

Step	Temperature	Time	Cycles
Initial Denaturation	94°C	5 min	1×
Denaturation	94°C	30 s	
Annealing	52°C	30 s	30×
Elongation	72°C	70 s	
Final Elongation	72°C	5 min	1×
End	4°C	hold	

The PCR products were purified using the QIAquick® Gel Extraction-Kit (Qiagen) according to the manufacturer's instruction.

2.2.2.2 Preparation and purification of plasmid DNA

Plasmids were extracted from 3 ml or 200 ml overnight bacterial cultures using the illustra plasmidPrep Mini Spin Kit (GE Healthcare) for minipreparation and the Nucleobond® PC100 Kit (Macherey-Nagel) for maxipreparation respectively. The isolated plasmid DNA was eluted in TE buffer (50 µl for minipreparation and 200 µl for maxipreparation) and analyzed by restriction enzyme digestion.

TE buffer (pH 7.5)

10 mM Tris/HCl

1 mM EDTA

2.2.2.3 Determination of DNA concentration

The concentration of isolated plasmid DNA was assessed by measuring the absorbance at 260 nm using NanoDrop 1000 (Thermo Fisher Scientific). An OD_{260} of 1 = 50 µg/ml double-stranded DNA.

2.2.2.4 Restriction enzyme digestion

1 µg (analytic digestion) or 5 µg (preparative digestion) DNA were digested with 1 U or 5 U of restriction enzyme, respectively. Digestions were performed in the appropriate buffer for 1 - 3 h at the temperature recommended by the manufacturer.

2.2.2.5 Agarose gel electrophoresis

To analyze DNA after digestion with restriction enzymes, DNA samples were mixed with 10×DNA loading buffer and then separated by gel electrophoresis in 0.8 - 1.5% agarose/TAE gels containing 1 µg/ml ethidium bromide. Gels were run for 30 to 60 min at 120 V. DNA was visualized by UV light using the Gel Doc™ EZ Gel Documentation System.

50×TAE buffer (pH 7.3)	10×DNA loading buffer
2 M Tris/HCl	50 mM Tris pH7.6
250 mM Na-acetate	60% glycerol
50 mM EDTA	2.5 mg/ml orange G

2.2.2.6 Isolation of DNA fragments from agarose gels

DNA fragments were cut from the gel and purified using the QIAquick Gel Extraction Kit (QIAGEN) according to the manufacturer's instruction. Purified DNA was eluted in 30 µl TE.

2.2.2.7 Dephosphorylation of DNA fragments

To prevent recircularization of linearized plasmids, the 5' phosphate group was removed using Antarctic Phosphatase (AP). 1 unit of AP per µg DNA was added to the DNA in a final volume of 20 µl. The mixture was incubated at 37°C for 30 min followed by inactivation of AP at 65°C for 10 min. Dephosphorylated DNA was purified with using QIAquick Gel Extraction Kit according to the manufacturer's instruction.

2.2.2.8 Ligation of DNA fragments

DNA fragments were mixed with 100 ng linearized vector at a molecular ratio of 1 : 3 to 1 : 8, 1 unit of T4 DNA ligase added and then incubated at 16°C overnight.

2.2.2.9 DNA sequencing

Plasmids were sent to Sequiserve (Vaterstetten, DE) for sequencing. The sequencing results were analyzed using Vector NTI Advance software.

2.2.3 Analysis of proteins

2.2.3.1 Purification of IgG Fc-fusion proteins

Supernatants from cells transfected (2.2.4.3) with vectors expressing IgG Fc fusion proteins were concentrated to roughly 5 ml using filters with pore diameters of 10 or 50 kDa (Millipore). These concentrated supernatants were mixed with the same volume of Protein A IgG Binding buffer, pH 8.0 (Thermo Fisher Scientific) and 100 µl protein A sepharose beads (GE Healthcare) followed by an overnight incubation at 4℃ on a overhead shaker The next day, beads were pelleted by centrifugation in a precooled centrifuge and bound proteins were eluted using protein A IgG elution buffer, pH 2.8 (Thermo Fisher Scientific) and neutralized with Tris/HCl buffer (1M, pH8.0). Eluted proteins were frozen in aliquots and stored at －80℃. Amounts of Fc proteins were determined by a capture ELISA (see 2.2.3.2)

2.2.3.2 Precipitation of proteins in supernatant with ethanol

To precipitate proteins in the supernatants, 1 ml supernatant of each sample was collected and mixed with 25 µl 5 M NaCl and 1 ml ethanol, followed by a 15 min centrifuge at 4 ℃.

Supernatants were then removed and the pellets were resuspended with 50 µl 2×sample buffer.

2×sample buffer

10% SDS	6 ml
0.5 M Tris pH6.8	2.5 ml
1-Thioglycerol	1 ml
Glycerol	1 ml
Bromphenol Blue	sprinkling

2.2.3.3 Enzyme-linked immunosorbent assay (ELISA)

A capture-ELISA was used to quantify the levels of mouse IgG Fc proteins. All dilutions and washes were done with ELISA buffer and all incubations were performed at room temperature. Specifically, Pierce™ NeutrAvidin™ coated plates (Thermo Fisher Scientific) were washed for 3 times before wells were coated with the capture antibody (anti-mouse IgG-Biotin, Sigma) at 1 µg/ml for 1 h. Samples were diluted and standards were prepared using mouse IgG (Sigma) at concentrations of 800, 400, 200, 100, 50, 25, 12.5 and 0 ng/ml. After washing the antibody-coated plates for 3 times, samples and standards were applied to the wells (100 µl/well) and incubated for 30 min. Subsequently, wells were washed for 3 times and then incubated with detection antibody (1:10000; anti-mouse IgG peroxidase, Sigma) for 30min, followed by another 3 washes. For colorimetric quantification, 100 µl TMB substrate reagent (BD Biosciences) was added to each well and reactions were stopped with 100 µl 10% phosphoric acid. Absorbance at 450 nm was measured with an ELISA plate reader. Standard curves were generated by plotting the absorbance (y axis) against the protein concentration (x axis). Concentrations of samples were determined using the standard curves.

ELISA buffer (pH7.2)

Tris/HCl	25 mM
NaCl	150 mM
BSA	0.1%
Tween-20	0.05%

2.2.3.4 Biotinylation of cell surface proteins

To label cell surface proteins, a biotin reagent which does not enter cells was used. Cell monolayers were biotinylated in 0.5 mg/ml EZ-Link Sulfo-NHS-LC-LC-Biotin (Thermo Scientific) in PBS for 30 min at RT and the reaction was stopped by washing the cells 3 times with 100 mM glycine in PBS.

2.2.3.5 Cell lysates

To prepare total cell lysates, cell monolayers were directly lysed with 2×sample buffer and ultrasonicated. To extract cytosolic proteins, cells were lysed with cold standard lysis buffer containing proteinase inhibitor cocktail (Roche) for 1 h at 4°C on a roller mixer. Cell nuclei were pelleted at 13,000 rpm for 10 minutes at 4°C and the supernatants were harvested and stored at -80°C. For lysis of virions, virus stocks were directly mixed with the standard lysis buffer and extracted as above.

Standard lysis buffer (50 ml)

1 M Tris pH8.0	0.8 ml
NaCl	0.4 g
Triton X-100	0.5 ml
H_2O	to 50 ml

2×sample buffer

10% SDS	6 ml
0.5 M Tris pH6.8	2.5 ml
1-Thioglycerol	1 ml
Glycerol	1 ml
Bromphenol Blue	sprinkling

2.2.3.6 Sodium dodecyl sulfate polyacrylamide gel electrophoresis (SDS-PAGE)

Protein mobility depends on its size and mass-to-charge ratio. To separate proteins with different sizes, SDS-PAGE was used. Due to incorporation of SDS into lysed proteins, separation of proteins solely depends on size. Specifically, cells, virus lysates, or purified proteins were mixed with 2×sample, and heated for 5 min at 95°C prior loading. Proteins were separated by polyacrylamide gel electrophoresis (PAGE) for about 55 min at 170 V in running buffer. A prestained protein marker (Thermo Fisher Scientific) was loaded in parallel to allow determination of molecular weights. After electrophoresis, separated proteins were further analyzed by Western blot analysis.

Preparation of gels

Component	Stacking gel	Separating gel	
	5%	10%	15%
ddH_20	2.81 ml	4 ml	2.33 ml
Tris/HCl	1.25 ml (0.5 M, pH6.8)	2.5 ml (1.5 M, pH8.8)	2.5 ml (1.5 M, pH8.8)
10% SDS	50 µl	100 µl	100 µl
Acrylamid/Bis-acrylamide 30%	840 µl	3.3 ml	5 ml
10% APS	50 µl	100 µl	100 µl
TEMED	3 µl	5 µl	5 µl

10×Running buffer (1 L)	
Tris-Base	30 g
Glycin	144 g
10% SDS	100 ml
H_2O	to 1 L

2.2.3.7 Coomassie blue staining

To directly visualize proteins in SDS gels, gels were rinsed 3 times for 10 minutes with ultrapure H_2O and then incubated with coomassie staining solution for 3 h. After rinsing two times with ultrapure H_2O, gels were treated with destaining solution for 10 – 60 minutes.

Staining solution	Destaining solution
0.02% Coomassie Blue G-250	10% Ethanol
5% Aluminiumsulfat-(14-18)-Hydrat	2% orthophosphoric acid
10% Ethanol	
2% orthophosphoric acid	

2.2.3.8 Silver staining

A mass spectrometry compatible silver staining kit (FireSilver Staining Kit, Proteome Factory) was used to stain protein bands in SDS-PAGE gels according to the manufacturer's instruction. Specifically, all steps were performed in a clean environment with clean devices and reagents to avoid contaminations from operators (e.g. keratin) or from reagents (e.g. trypsin) which would interfere with efficient data acquisition and analysis of target proteins. Excised gel slices were transferred to a clean tray and fixed with fix solution for 2 h. Gels were then washed with 20% ethanol for 10 min followed by a sensitization with sensitizer solution for 1 min. Gels were subsequently washed twice with ultra pure water for 1 min and then equilibrated with silver solution for 30 min. After another wash with ultra pure water for 30 s, gels were developed first with pre-developer solution for 1 min and then with developer solution for 1-15 min. Thereafter, reaction was stopped with stop solution for 20 min. Gels were stored in ultra pure water.

2.2.3.9 Western blot analysis

To detect specific proteins, Western blot analysis was used. Proteins separated on SDS-PAGEs were transferred to a Hybond-ECL nitrocellulose membrane (Amersham) using a Mini-PROTEAN Tetra System (Bio-Rad), at 100 V for 1 h at room temperature (RT). Before

transfer, membranes and gels were incubated in blotting buffer for 2 minutes. Afterwards, membranes were blocked in blocking buffer for 1 h, and then incubated with a primary antibody diluted in blocking buffer. Incubations with primary antibodies were performed overnight at 4°C on a roller mixer. Membranes were washed five times (5×5 min) with TBST and then incubated with corresponding peroxidase-conjugated secondary antibodies in blocking buffer for 2 h at RT. After another five washes with TBST, specific bands were detected by chemiluminescence using the Pierce™ ECL Plus Western Blotting Substrate (Thermo Fisher Scientific) according to the manufacturer's instructions. Blots were exposed to Hyperfilm™ ECL™ detection film (GE Healthcare) and the images were developed by using the developing machine FPM-100A. If necessary, initial antibodies could be stripped with Restore™ Western blot Stripping Buffer (Thermo Fisher Scientific) for 8 to 15 minutes at room temperature. The nitrocellulose membrane was then washed with TBST, reblocked with 5% milk in TBST and reprobed with other primary antibodies

Buffers used for Western blot

Blotting buffer	TBST	Blocking buffer 1	Blocking buffer 2
25 mM Tris	150mM NaCl	TBST	PBS, pH 7.4
192 mM glycine	10 mM Tris/HCl, pH 8.0	5% skimmed milk powder	0.05% TWEEN 20
20% methanol	0.1% Tween 20		1% BSA

2.2.3.10 Ponceau S staining for Western blots

To visualize transfer of proteins, the membranes were soaked in Ponceau S solution (Sigma) for 1 min following Western blotting. The membrane was then rinsed with distilled water.

2.2.3.11 Mass spectrometry

Proteins in gel slices from silver stained gels were identified with high resolution nanoHPLC-ESI-MSMS chromatography (Protein Factory, Berlin, Germany) and blasted against human cellular protein databases.

2.2.3.12 Co-immunoprecipitation (Co-IP)

Cells or viruses were lysed in 1 ml standard lysis buffer containing proteinase inhibitor cocktail (PIC, Roche) for 1 h on a roller at 4 °C. Afterwards, lysates were centrifuged at 20,000x g at 4 °C for 10 min. Supernatants were transferred to new Epps and precleared

with 25 µl of 50 %protein A sepharose beads (GE Healthcare) for 1 h on a roller at 4 °C. This is followed by a 2 min centrifugation at 13,000x g to remove proteins unspecifically bound to beads. Supernatants were co-incubated with antibodies or Fc fusion proteins at 4°C overnight. Protein-antibody complexes were precipitated with 50 µl of 50% protein protein A sepharose beads. The precipitates were dissociated in protein sample buffer and subjected to SDS-polyacrylamide gel electrophoresis (SDS-PAGE), followed by either silver stain or Western blot.

2.2.3.13 Crosslinking of proteins bound to cell surfaces

Cells were seeded in 10 cm dishes one day before crosslink. Cell monolayers were washed for 5 times with PBS and then detached with 4 ml Versene (Thermo Fisher Scientific) per dish. Subsequently, cells were pelleted, washed once with PBS and incubated with Fc proteins on ice for 90 min. Thereafter, cells were washed once with PBS and resuspended with the crosslinker 2 mM 3,3′-dithiobis(sulfosuccinimidyl propionate) (DTSSP, Thermo Fisher Scientific) dissolved in PBS. After another 90 min incubation on ice, crosslink reaction was stopped by adding Glycine buffer to a final concentration of 10 mM. Then, cells were pelleted and subjected to further analysis.

2.2.3.14 Indirect immunofluorescence

To detect specific cellular proteins or protein-protein interactions on cell surfaces, indirect immunofluorescence which relys on the specific interaction between fluorescent dye-labeled antibodies and their antigen, was applied.

1) Staining of fixed adherent cells. Cells in the 96-well plates were fixed with 50 µl fix buffer per well for 10 min at RT and then washed with PBS for 3 times followed by an incubation with antibodies (diluted in staining buffer) directed against cellular proteins or viral proteins if virus-infected cells were used for 45 min at 37℃. After washing for 3 times, infected cells were visualized by staining using a Fluor 488-coupled anti-mouse antibody (1:1000 diluted in staining buffer). For counterstaining of cell nuclei, cells were incubated in PBS containing 2 µg/ml Hoechst 333258 (Invitrogen) for 1 min followed by washing 3 times with PBS. Staining of cells was analysed by fluorescence microscopy. Total cell nuclei and infected cells were counted by using the software ImageJ (National Institutes of Health).

fix buffer		staining buffer	
acetone	50% (v/v)	FCS	2% (v/v)
methanol	50% (v/v)	PBS	98% (v/v)

2) Cell surface staining for FACS analysis. Flow cytometry analysis was used to assess the binding of Fc fusion proteins to cell surfaces. Cells were seeded to 10 cm dishes one day day ahead of the flow cytometry experiment. Cells were washed for 3 times with PBS and then detached with 4 ml/dish Versene (Thermo Fisher Scientific). Thereafter, all steps were carried out using precooled devices and reagents and all dilutions of antibodies and washings were done with staining buffer. Cells were pelleted and resuspended with mouse IgG Fc proteins for 90 min on ice. After washing once, cells were incubated with anti-mouse Fluor 488-coupled antibody for 30 min on ice in the dark. After 3 more wash steps, cells were resupended in PBS and analysed using a BD FACS Canto II cytometer. Data were analyzed by using BD FACS Diva software (BD Biosciences).

staining buffer	
FCS	5% (v/v)
PBS	95% (v/v)

3) Intracellular staining for FACS analysis. For intracellular staining of viral ie protein in CMV infected cells, cells were harvested and fixed with fix buffer for 10 min at RT. After washing once with wash buffer, cells were incubated with mouse anti-ie antibody (croma 101) diluted in staining buffer at 4℃ for 30 min on a roller mixer. After another washing, cells were stained with anti-mouse Fluor 488-coupled antibody at 4℃ for 30 min on a roller mixer. Thereafter, cells were pelleted and resuspended with fix buffer. Samples were then subjected to flow cytometry analysis

fix buffer		wash buffer		staining buffer	
formaldehyde	1% (m/v)	saponin	0.03% (v/v)	saponin	0.3% (v/v)
PBS		PBS	99.97% (v/v)	PBS	99.7% (v/v)
				BSA	1% (m/v)

2.2.4 Cultivation of mammalian cells

Mammalian cells were cultivated at 37℃, 8% CO_2, in a humidified cell culture incubator, and regularly sub-cultured. For sub-culturing, medium was removed. Adherent cells were rinsed once with PBS and detached with 1.0 ml (for 10 cm culture dish) or 3 ml (for 15 cm culture dish) 0.25% Trypsin-EDTA solution for 1 to 5 min at 37℃. Reaction was stopped by

adding the corresponding medium and then reseeded into new dishes containing fresh medium and incubated at 37°C.

2.2.4.1 Cultivation of primary cells

HFF (passage 7-23) and MEF (passage 1-3) were cultured in DMEM supplemented with 10% FBS, 0.3 mg/ml L-glutamine (only for HFF) and 100 U/ml penicillin + 100 U/ml streptomycin. HFF were split 1:3 once a week and MEF were split 1:2 once a week.

HUVEC, passage 1-6, were cultured in Lonza EGM™-2MV medium, and split 1:3 twice a week.

2.2.4.2 Cultivation of cell lines

293, MHEC-5T, NIH3T3 and TCMK-1 cells were cultured in DMEM supplemented with 10% FBS (5% for NIH3T3 and MHEC-5T) and 100 U/ml penicillin +100 U/ml streptomycin. 293 were split 1:10 twice a week, NIH3T3 and TCMK-1 1:4 twice a week, and MHEC-5T 1:6 once a week.

ANA-1 and ARPE-19 cells were cultured in RPMI 1640 medium supplemented with 10% FBS and 100 U/ml penicillin + 100 U/ml streptomycin. ANA-1 were split 1:6 twice a week and ARPE-19 1:4 twice a week.

TIME cells were cultured in EGM-2 MV SingleQuot Kit Suppl. & Growth Factors, split 1:3 twice a week, and fed once in between.

2.2.4.3 Freezing of cells

Cells were harvested at 90% confluence and then pelleted at 300×g for 5 min at RT. Cell pellets were resuspended in freezing medium at a density of 1×10^6 cells/ml and 1 ml aliquots dispensed into cryo tubes (Nunc), which were then placed in an isopropanol isolated cryo-box and transferred to -80°C. Forty-eight hours later, cells were transferred to a nitrogen tank for long-term storage. For recovery of frozen cells, frozen cells were quickly thawed at 37 ºC in a water bath, then resuspended in 10 ml fresh cell-type specific medium and seeded into appropriate dishes.

Freezing medium

70% cell-type specific medium

20% FBS

10% DMSO

2.2.4.4 Transfection of cells

Two methods of transfection were used in this study. 293 cells were seeded into 10 cm dishes or 6-well plates one day before the experiment to reach an 80% confluence at the time of transfection. Cells were either transfected with vector expressing Fc fusion protein using polyethylenimine (PEI) or with FuGENE HD (Promega). A plasmid expressing EGFP (pEGFP-C1, Clontech) was transfected in parallel to evaluate the transfection efficiency. For transfection, the following mixture was prepared for each dish in a 1.5 ml Epp. tube, and standing for 30 min at RT. The original medium was exchanged with Opti-MEM serum-free medium (Gibco, Invitrogen) three hours after transfection.

Transfection with PEI (for 10 cm dishes)		Transfection with FuGENE HD (for 6-well plates)	
Opti-MEM	400 µl	Opti-MEM	100 µl
Plasmid	12 µg	Plasmid	6 µg
PEI	60 µl	FuGENE HD	15 µl

2.2.6 Virological methods

2.2.6.1 Virus infection of cells

Cells were seeded one day before infection to achieve 80% - 90% confluence. To infect cells, virus inocula were diluted in medium and applied to cells for 1.5 h at 37°C. To remove the inocula, cells were washed three times, supplied with fresh medium and incubated at 37°C. In infection experiments using TB40-ΔgO virus, all virus infections were subjected to a centrifugation step (2.000 g at RT, 30 min), followed by incubation at 37°C for 60 min.

2.2.6.2 *In vitro a*mplification and purification of CMV particles

To prepare virus inocula, three different methods were used.

1) Supernatant virus. Supernatants of infected cells with complete cytopathic effects were centrifuged at 5.500 g for 15 min to remove cellular debris, aliquoted and frozen at -80°C.

2) Virus stocks. For the preparation of virus stocks, eight to twelve 15 cm dishes of NIH3T3

(MCMV) or HFF (HCMV) were infected at a multiplicity of infection (MOI) of 0.1 to 1. Supernatants of infected cells showing a complete cytopathic effect were precleared at 5.500 g for 15 min. All following steps were performed at 4℃ or on ice. Virus particles were pelleted at 26.000 g for 3 h for MCMV or at 21.000 rpm for 70 min for HCMV (Beckmann, SW32Ti). Virus pellets were resuspended in DMEM containing 5% FBS (1/200 - 1/500 of the starting volume) and stored in small aliquots at -80°C.

3) For the preparation of sucrose-cushion-purified MCMV, virus pellets as described under 2). Pellets were then resuspended and dounced in 3 ml VSB buffer. Then, ten ml VSB buffer containing 15% were overlaid with the virus suspension. Viruses were subsequently pelleted through the sucrose cushion by ultracentrifugation at 21.000 rpm for 70 min (Beckmann, SW32Ti). After washing once with VSB buffer, virus pellets were resuspended in 1.5 ml VSB buffer, aliquoted and stored at -80℃.

VSB buffer (pH 7.8)

Tris/HCl	0.05 M
KCl	0.012 M
EDTA (Na2 salt)	0.005 M

2.2.6.3 Determination of viral titers of CMV preparations

Virus titers were determined with a TCID50 assay performed on MEF (MCMV) or HFF (HCMV) in 96-well plates. Specifically, cells were seeded on 96-well plates in a volume of 100/well one day before infection. Virus was 10-fold serially diluted in DMEM containing 5% FBS from 10^{-1} to 10^{-8}. 100 µl/well diluted virus were added in quadruplicates onto corresponding cells, followed by incubation at 37°C for 3-4 days (MCMV) or 7-9 days (HCMV). To identify plaque positive wells, medium was removed and cells were stained with 1×crystal violet for 10 min at RT. After 3 times of washing with water, both plaque positive and plaque negative wells were counted under the microscope and virus titers were calculated according to the Reed and Muench method [186].

10×crystal violet (in PBS)

formaldehyde	10 %
crystal violet	1 % (w/v)
EDTA (Na_2 salt)	0.005 M

2.2.6.4 Luciferase assay

A luciferase assay was used to evaluate infection capacities of HCMV expressing the firefly luciferase in different cell types. Briefly, HFF or 293 cells were grown in 96 well plates (20,000 cells/well) and infected in triplicates for 1.5 h at 37°C. Thereafter, inocula were replaced with 100 µl fresh medium supplemented with 300 µg/ml phosphono acetic acid (PAA) to block viral replication. 48 hours post infection, supernatants were removed and cells were directly lysed on the plate in 50 µl 1×lysis buffer (Luciferase Reporter Assay Kit I, PromoKine) for 10 min at RT on a shaker. Subsequently, 20 µl of the lysates were transferred to a light-proof 96-well plate, mixed with 40 µl/well firefly substrate (Luciferase Reporter Assay Kit I, PromoKine) and the luciferase activity was measured using the CLARIOstar microplate reader (BMG LABTECH GmbH).

2.2.7 Statistical analysis

All statistics and calculations were conducted with Prism 6.0 software (GraphPad, CA). The statistical significance between two groups was determined by unpaired student's two-tailed t-test and Mann-Whitney Rank Sum test. All significance tests were denoted as: n.s. means $p>0.05$; * means $0.01 < p < 0.05$; ** means $0.001 < p < 0.01$; *** means $p < 0.001$.

3 Results

3.1 The role of the HCMV envelope glycoprotein gO in infection

Envelopes of all herpesviruses contain gH/gL glycoprotein complexes which promote virus entry. The glycoprotein O (gO) of HCMV binds to gH/gL to form a gH/gL/gO complex. gO, with a size of 464 amino acids (aa), is the protein product of the UL74 open reading frame (ORF). It contains an N-terminal signal sequence which is cleaved during processing. It is highly glycosylated and runs in an SDS-polyacrylamide gel at a size of about 125 kDa [91, 92, 187].

HCMV mutants lacking gO (ΔgO) release particles which are hardly infectious and show a focal, cell-associated spread pattern in cell culture [106, 107]. This focal spread is dependent on the alternative gH/gL/pUL(128,130,131a) complex [122]. To study ΔgO virus, large numbers of virus particles are needed to achieve infection levels which allow studies on the role of the gH/gL/gO complex.

3.1.1 The role of gO in HCMV infection of different cell types

All HCMV mutants used here are derived from TB40-BAC4, a bacterial artificial chromosome (BAC) clone of the HCMV strain TB40/E [181]. To compare the tropism of TB40-BAC4 (wildtype) with TB40-BAC4-ΔgO virus for different cell types, BACs expressing firefly luciferase (TB40-Luc and TB40-ΔgO-Luc) [122] were used to quantitatively analyze infection of cells. Infection of human foreskin fibroblasts (HFF), human lung fibroblasts (MRC-5), embryonic kidney epithelial cells (293), retinal pigmented epithelial cells (ARPE-19) and human umbilical vein endothelial cells (HUVEC) was compared. The TB40-Luc and TB40-ΔgO-Luc preparations used for infection of different cell types were adapted to give a comparable infection on HFF. The upper panel in Figure 8 shows the luciferase signal from infected cells. The lower panel shows relative infection capacities. Here, the signals were normalized to infection of HFF which was arbitrarily set to 100%. TB40-Luc showed a higher capacity to infect fibroblasts when compared to infection of epithelial cells and endothelial cells (EC). In contrast, TB40-BAC4-ΔgO-Luc exhibited a relatively higher infection capacity for epithelial cells and EC when compared to infection of fibroblasts with TB40-Luc. Thus, the loss of gO and with it, the capability to form a gH/gL/gO complex is associated with a shift of relative infection capacities for certain cell types, which suggests

that infection of fibroblasts but not infection epithelial cells and EC is predominantly driven by the gH/gL/gO complex. If gH/gL/gO is missing, infection is driven by the gH/gL/pUL(128,130,131a) complex. This also implies that fibroblasts have more receptors for the gH/gL/gO complex than for gH/gL/pUL(128,130,131a) complex.

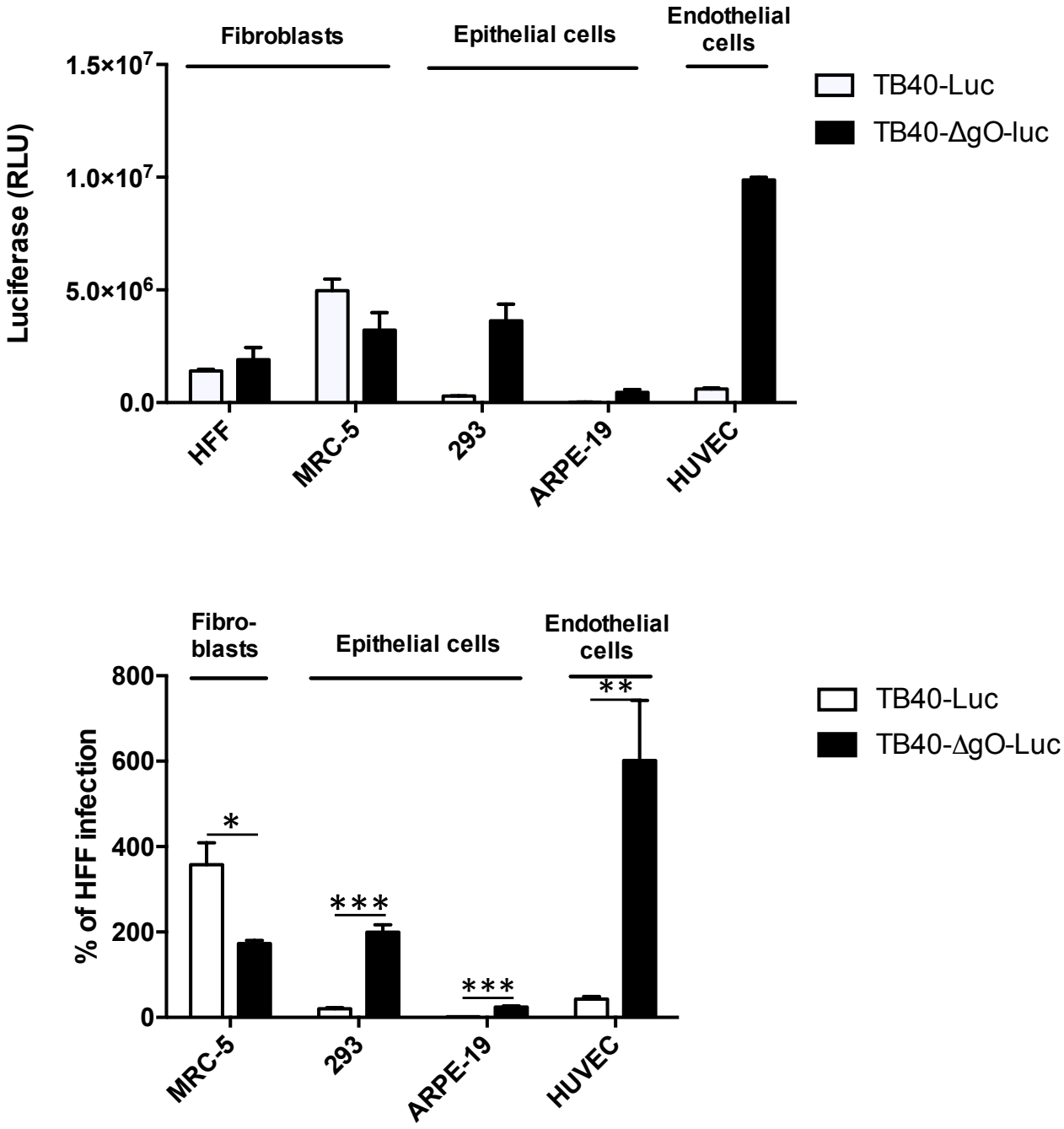

Figure 8: Comparison of the infection capacities of wildtype TB40-Luc and TB40-ΔgO-Luc for different cell types in culture.

Fibroblasts (HFF and MRC-5), epithelial cells (293 and ARPE-19) and EC (HUVEC) were infected with TB40-Luc or TB40-ΔgO-Luc. Infection capacities were determined 24h p.i. by a luciferase assay. The upper panel shows the luciferase signal measured in infected cells. The lower panel shows infection capacities relative to the infection capacity for HFF which is set to 100%. Shown are means +/- SD of 3 independent experiments done in triplicates. Unpaired student's t-test was performed for statistical analysis. (* means $0.01 < p < 0.05$; ** means $0.001 < p < 0.01$; *** means $p < 0.001$)

3.1.2 Cloning of a gO-Fc fusion protein to study the role of HCMV gO in infection of host cells

3.1.2.1 Cloning and expression of a gO-Fc fusion protein

It has been suggested that HCMV gO mediates HCMV entry into fibroblasts via interaction with a fibroblast-specific cell surface protein [68]. To create a tool to study the interaction of gO and potential cellular receptors, a gO-IgG Fc fusion protein was cloned. Secreted IgG Fc fusion proteins can be purified from supernatants of transfected cells using protein A sepharose beads. In addition, they are good tools for coimmunoprecipitation of binding partners. There have been several studies using IgG Fc-fused viral glycoproteins to identify the corresponding cellular receptors. For example, HLA class II was identified as a binding partner for gp42 which is a component of the Epstein-Barr virus gH/gL/gp42 glycoprotein complex [188]. Another group successfully precipitated EphrinB2 as an entry receptor for Nipah virus [189].

The TB40-BAC4 gO ORF without the N-terminal signal sequence (aa1 - aa 20) [190] was cloned into the eukaryotic expression vector pFUSE-mIgG2b-Fc2 (InvivoGen) which expresses the mouse IgG2b Fc. It also expresses an IL-2 secretion signal (IL-2ss) for release of the recombinant protein (Figure 6a, adapted from InvivoGen). The DNA sequence of gO (bp 86 to bp 1392), was amplified from a pSG5 vector expressing the complete gO sequence (see Materials and Methods) and inserted into the vector pFUSE-mIgG2b-Fc2 between the N-terminal secretion signal IL-2ss and the mouse IgG2b Fc using an *Nco* Ⅰ site and a *Bgl* Ⅱ site in the multiple cloning site (Figure 9a and 9b). This expressing vector was called pgO-Fc and was subsequently used for the production of gO-Fc protein in transfected cells.

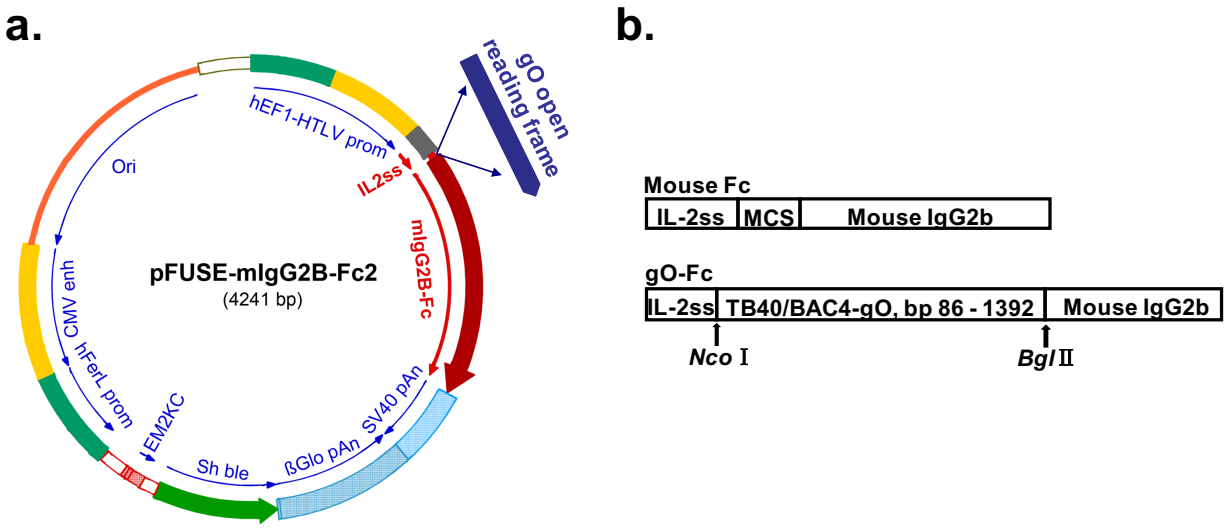

Figure 9: Schematic presentation of pFUSE-gO-mIgG2B-Fc.
The gO ORF lacking the signal peptide was amplified and cloned into the plasmid pFUSE-mIgG2B-Fc2. Shown are a) the map of the vector and the corresponding insertion site (adapted from InvivoGen) and b) a schematic presentation of the structure of the fused gO-Fc.

For expression of gO-Fc, 293 cells were transfected with pFUSE-gO-mIgG2B-Fc or the empty vector as a control. Supernatants were collected 24h after transfection and proteins were precipitated with ethanol. Expression of gO-Fc was then tested by Western blot analysis (Figure 10). The molecular weight of the mouse IgG Fc protein is about 35kDa. The recombinant gO-Fc showed a molecular weight of around 150 kDa.

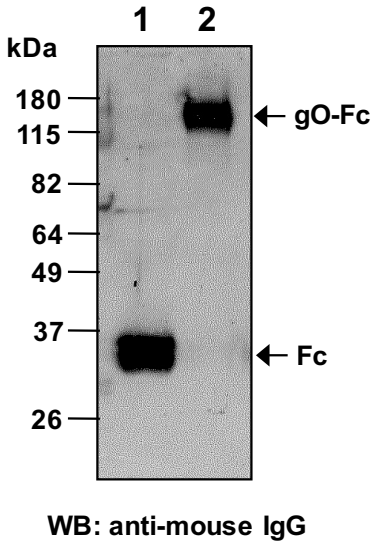

Figure 10: Secretion of Fc and gO-Fc into supernatants of transfected 293 cells.
293 cells were transfected with pFUSE-mIgG2B-Fc (1) or pFUSE-gO-mIgG2B-Fc (2). The cell culture supernatants of the transfected cells were harvested after 24h, precipitated with ethanol, and analyzed by Western blot. Secreted Fc and gO-Fc were detected using a peroxidase-conjugated anti-mouse Fc antibody. The positions of the molecular weights of the marker are indicated on the left.

A capture ELISA detecting mouse IgG Fc (see Methods) was used to evaluate the amount of IgG Fc and gO-Fc. Measurements revealed that gO-Fc was produced in much lower amounts than IgG Fc. This may be due to the large size and the abundant glycosylation of the gO-Fc fusion protein. To express and purify large amounts of gO-Fc, different experimental conditions were tested to achieve an optimal yield. Briefly, 293 cells were transfected with pFUSE-gO-mIgG2B-Fc. Supernatants were collected and concentrated using filters with a cutoff of 50 kDa, followed by purification with protein A sepharose beads. For transfection, three commercially available reagents (FuGENE HD (Roche), PEI (Sigma) and SuperFect (Qiagen)) and different ratios of DNA versus transfection reagents for vector transfection were compared. In addition, operability and productivity of 6-well plates and 10 cm dishes were also compared. For the time point of harvest, 96 h after transfection was superior to the time points 24h and 48h after transfection. Additionally, binding of gO-Fc to protein A sepharose was strongly reduced when the supernatant was concentrated too much. A comparison of protein A sepharose beads in suspension to commercial protein A columns (NAb^{TM} Protein A plus Spin Column, Cat. No. 89956, Thermo Scientific) gave a better yield for the beads in suspension. To achieve a high elution efficiency, different elution buffers with different pH were compared. In the end, the optimized protocol was to transfect ten 10 cm dishes, harvest at 96 hours after transfection, concentrate to about 5ml, purify with protein A sepharose beads and elute with a pH 2.8 buffer. This protocol produced gO-Fc protein yields of around 3 - 16 µg/ml (Figure 11).

a.

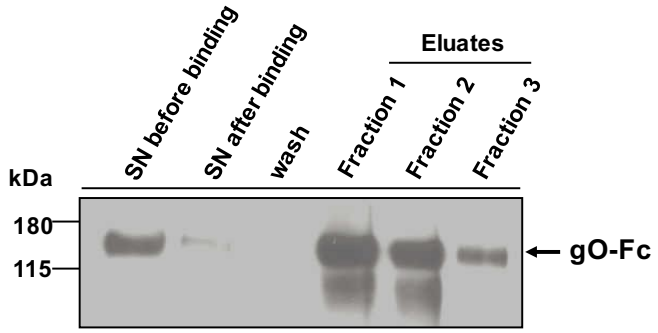

b.

ELISA	SN Before Binding	SN after Binding	Fraction 1	Fraction 2	Fraction 3
C (µg/mL)	2.9	0.4	15.8	11.2	3.8

Figure 11: Production and purification of gO-Fc.
10 x 10cm dishes of 293 cells were transfected with pFUSE-gO-mIgG2B-Fc. The cell culture supernatants of these cells were harvested after 96h, concentrated to 5ml (before binding), bound to protein A sepharose beads (supernatant after binding was denoted “after binding”), washed 3 times with binding buffer (collected washing buffer was named “wash”) and eluted 3 times with elution buffer (pH 2.8) (Fraction 1, Fraction 2 and Fraction 3). The eluates were immediately neutralized with 1M Tris-HCl (pH 8.5) and analyzed by Western blot (a) and ELISA (b). C: concentration.

3.1.2.2 Binding properties of gO-Fc

To find out whether the gO-Fc fusion protein binds to the surface of HCMV host cells, gO-Fc was coincubated with fibroblasts (HFF) and EC (HUVEC) and the cells analyzed by flow cytometry. gO-Fc only bound to HFF, but not to HUVEC, while the control Fc protein bound to neither cell type (Figure 12). This binding pattern of gO-Fc correlates with the infection capacity of HCMV mutants expressing only the gH/gL/gO complex which can infect fibroblasts, but fail to infect EC [94].

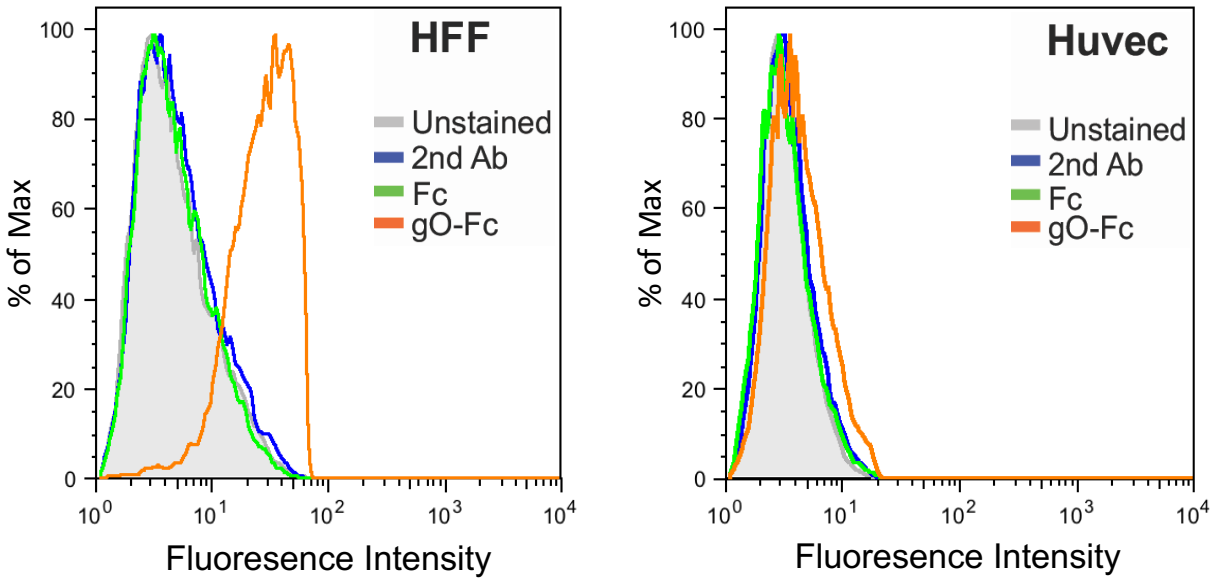

Figure 12 : **gO specifically binds to fibroblasts.**
IgG Fc protein (green line) or gO-Fc protein (orange line) or buffer (brown line and filled histogram) were coincubated with HFF (left panel) or Huvec (right panel). Cell-surface binding was detected using an Alexa Fluor® 488 conjugated anti-mouse IgG secondary antibody.

To clarify whether gO-Fc binding to fibroblasts is dose dependent, binding of serially diluted gO-Fc protein was analyzed. A dose-dependent binding pattern could be observed (Figure 13).

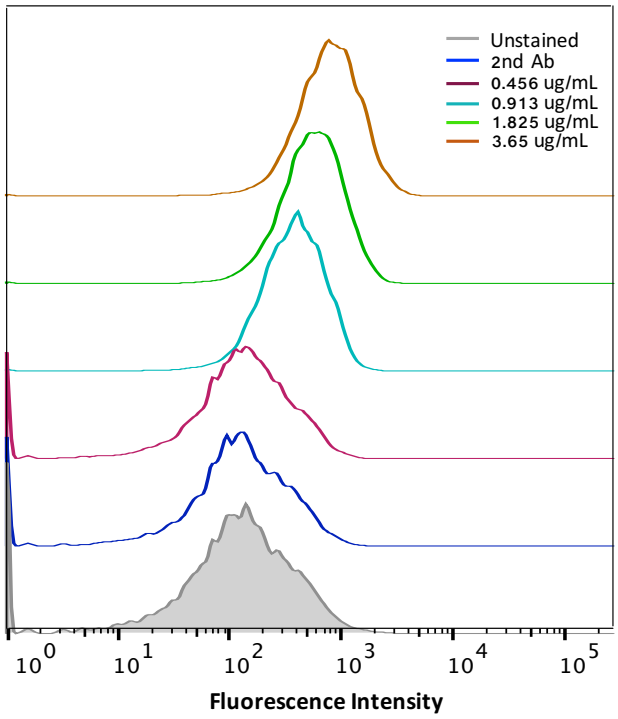

Figure 13: Binding of gO-Fc to fibroblasts is dose-dependent.
Two-fold serial dilutions of one prep of gO-Fc protein were coincubated with HFF. Cell-surface binding was detected by flow cytometry using an Alexa Fluor® 488 conjugated anti-mouse IgG secondary antibody.

3.1.2.3 Blocking of HCMV infection using gO-Fc

Since gO-Fc bound to the surface of HFF, it might be used to block HCMV infection. As depicted in Figure 14, soluble gO-Fc might bind a potential entry receptor on HFF and thus interfere with gO-dependent infection of fibroblasts.

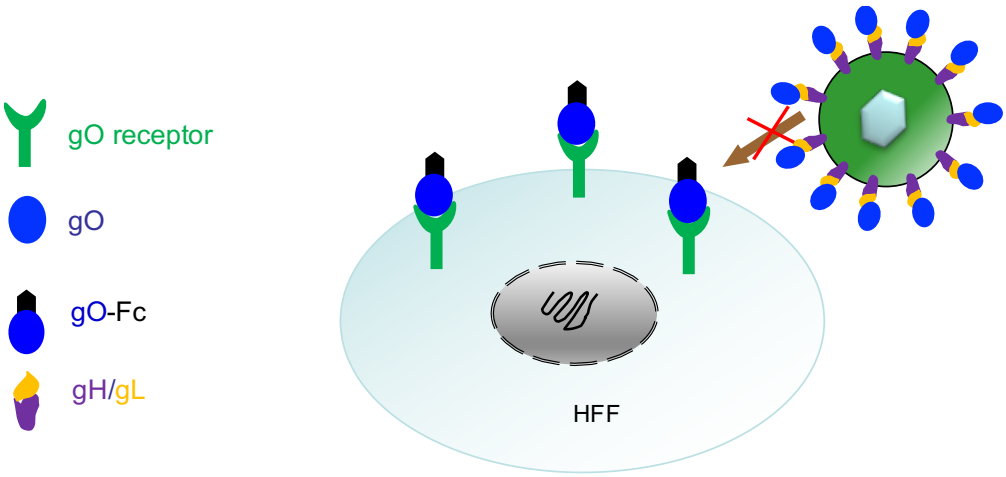

Figure 14: Scheme for an inhibition assay using purified gO-Fc fusion protein.
Pre-incubation of HFF with gO-Fc and binding to cell surface receptors. Infection of HFF mediated by the gH/gL/gO is blocked.

To test this, HFF were preincubated with gO-Fc or as a control IgG Fc alone. HCMV mutants expressing only the gH/gL/gO complex (TB40-UL131stop-Luc) or expressing only the gH/gL/pUL(128,130,131a) complex (TB40-ΔgO-Luc) were used to infect HFF in the presence of gO-Fc or IgG Fc, respectively, followed by removal of the virus inoculum. Infected cells were quantified by measuring luciferase activity in lysates 24h after infection. Preincubation with gO-Fc neither inhibited TB40-Luc nor TB40-ΔgO-Luc (Figure 15). This might have several reasons: i) Binding of gO-Fc to HFF turned out to be temperature sensitive: the binding at 4 ℃ was strong, whereas there was no binding at room temperature. Infection has to proceed at 37 ℃, which probably results in detachment of gO-Fc. ii) gO-Fc binding might be less strong than binding of gH/gL/gO in virions and thus not capable to compete with complexes in virions. iii) The amount of gO-Fc was not sufficient to block all receptors.

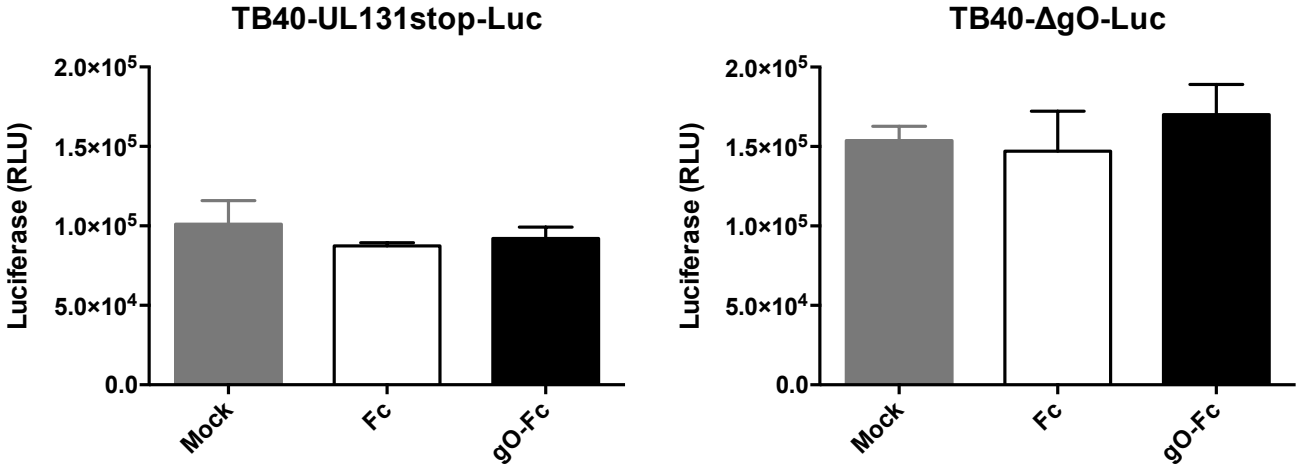

Figure 15: gO-Fc protein does not inhibit HCMV infection.
HFF were preincubated with gO-Fc or as a control IgG Fc on ice for 1 hour, then infected by TB40-UL131stop-Luc or TB40-ΔgO-Luc in the presence of gO-Fc or IgG Fc for 1.5 hours, followed by removal of the virus inocula and 3 washes. Thereafter, cells were fed with medium containg 300 µg/ml PAA. Infected cells were quantified by measuring luciferase activity in lysates 24 h p.i.. Shown are the means ± SD of one experiment assayed in triplicates.

3.1.3 Identification of PDGFRα as a receptor for HCMV gH/gL/gO

HCMV enters host cells through a complex process involving the interaction of cellular receptors and viral glycoproteins [50]. Several cell surface proteins have been reported to interact with HCMV envelope glycoproteins and facilitate the HCMV entry process, however, none of them is currently confirmed to be a functional entry receptor [50].

3.1.3.1 Identification of PDGFRα as a binding partner for HCMV gH/gL/gO

Previous studies have demonstrated that the gH/gL/gO complex mediates binding of HCMV to fibroblasts [68]. Consistent with that, a gO-Fc fusion protein specifically bound to HFF. In a step it was determine whether gO-Fc could precipitate a cellular receptor from extracts of HFF. Co-immunoprecipitation (Co-IP) is a widely used method to identify interaction partners of viral proteins. For a start, it was tested whether gO-Fc can precipitate cell surface proteins from extracts of HFF. HFF were biotinylated with Sulfo-NHS-Biotin and then incubated with equal amounts of either gO-Fc or the control IgG Fc protein, followed by lysis of the cells and precipitation with protein A sepharose beads. Biotinylated proteins were detected by Western blot using peroxidase-conjugated streptavidin. This experiment was repeated several times and a reproducible, but weak biotinylated protein band with a molecular weight of about 180 kDa was detected in the gO-Fc precipitates but not in Fc precipitates. Due to a high background, it was not possible to document this by scanning the Western blot films. Additionally, a silver staining of an SDS-PAGE gel of the same extracts was done but no corresponding band could be detected.

Assuming that binding of virion gH/gL/gO complex to its cellular receptor might be stronger than binding of recombinant gO-Fc, a TB40-BAC4 mutant expressing gH/gL/gO but not the gH/gL/pUL128-131 (TB40-UL131stop [122]) was used for binding to cells and subsequent co-precipitation of host cell proteins. For a preliminary test, TB40-UL131stop [122] virions were lysed to evaluate whether an anti-gH (14-4b) antibody could precipitate the gH/gL/gO complex and associated proteins. As shown in Figure 16, gO could be co-precipitated with gH, indicating that the anti-gH antibody precipitates the gH/gL/gO complex and can thus could be used to precipitate cellular proteins which interact with gH/gL/gO.

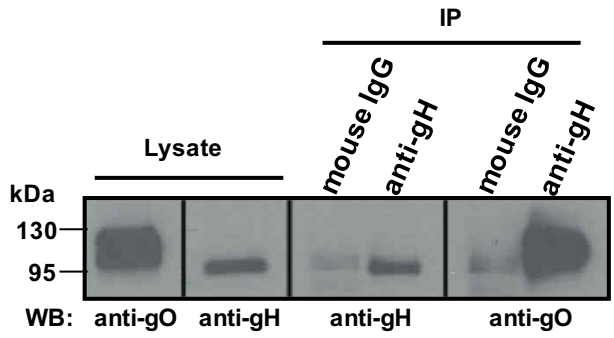

Figure 16: Co-immunoprecipitation of gO and gH from TB40-UL131stop virions.
TB40-UL131stop virions were lysed and gH was precipitated using an anti-gH antibody (14-4b). gO and gH were detected by Western blot analysis using mouse anti-gO antibody (gO.02) and mouse anti-gH antibody (SA4) respectively. A peroxidase-conjugated goat anti-mouse IgG served as detecting antibody. gO and gH were detected in virion lysates and in the precipitates. Mouse IgG served as a control antibody for Co-IP.

Again, a biotinylation assay was performed to detect cell surface binding partners of the gH/gL/gO complex using a similar strategy as for gO-Fc. gH/gL/gO-interacting proteins were precipitated using the above tested mouse anti-gH antibody. HFF cells were labeled with Sulfo-NHS-Biotin, then either cells coincubated with TB40-UL131stop virions on ice followed by lysis of cells and virions bound to cells or virion lysates were mixed with lysates of biotinylated cells. gH was precipitated from these lysates using the mouse anti-gH antibody used above (Figure 17a). A predominant biotinylated band with a molecular weight of about 180kDa could be detected using both approaches but not in lysates of HFF cells only (Figure 17a). The band could also be detected in silver stained gels (Figure 17b). It ran at the same position as the 180 kDa band detected when using gO-Fc for precipitation of cell surface proteins. To identify this protein, the immunoprecipitation approaches were repeated without biotinylation of the HFF cell surface. The 180 kDa band in the silver-stained gel and the corresponding area in the HFF control lane were excised and sent out for nanoHPLC-ESI-MS/MS analysis (Proteome Factory, Berlin). A peptide (KLVYTLTVPEATVKD) derived from platelet-derived growth factor receptor-alpha (PDGFRα) was identified (Figure 17c).

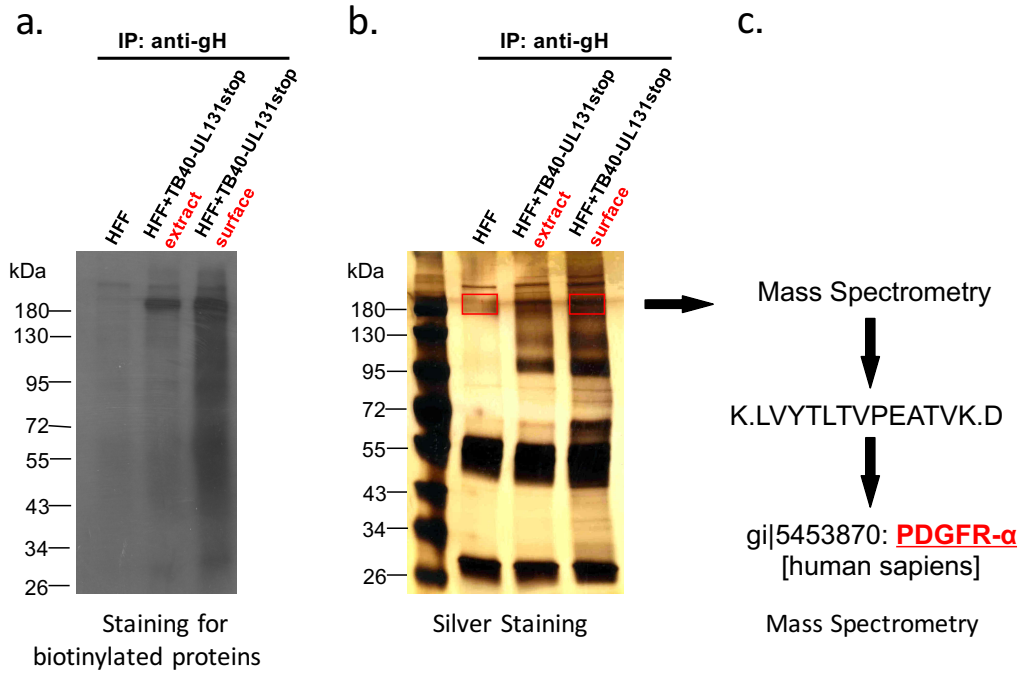

Figure 17: Identification of PDGRFα as a potential cellular receptor for HCMV.
TB40-UL131stop virions were mixed with HFF either before (surface) or after lysis (extract), incubated with the anti-gH antibody (14-4b) and then precipitated with protein A sepharose beads. a. Cell surface proteins were prelabeled with Sulfo-NHS-Biotin before addition of virions or virion extracts. Anti-gH precipitated proteins were analyzed by Western blot using peroxidase-conjugated streptavidin. b. Precipitates were separated by SDS-PAGE and visualized by silver staining using the FireSilver protein gel staining kit. c. Bands excised from silver-stained gels (boxed areas) were sent out for nanoHPLC-ESI-MS/MS analysis and a peptide from human PDGFRα was identified.

3.1.3.2 Confirmation of PDGFRα as a binding partner for gH/gL/gO

To confirm the PDGFRα co-precipitation, the precipitated proteins were additionally subjected to Western blot analysis: precipitation of gH and co-precipitation of gO, PDGFRα and additionally, gB was detected (Figure 18).

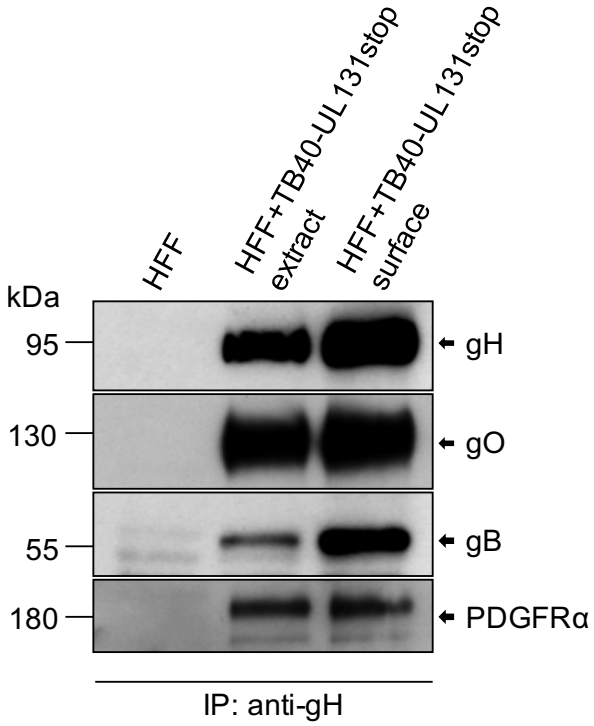

Figure 18: Coprecipitation of gH, gO, gB and PDGFRα.
Precipitates from figure 13 were additionally analyzed by Western blot using anti-gH antibody (SA4), anti-gO antibody (gO.02), anti-gB antibody (2F12) and anti-PDGFRα antibody (C-9) as first antibodies, and a peroxidase-conjugated goat anti-mouse IgG as detecting antibody. Arrows indicate the corresponding proteins.

3.1.3.3 Characterization of the interactions of gH/gL/gO, gB and PDGFRα

A co-precipitation of gB and PDGFRα has been shown before [72]. In addition, it has been shown that gB directly interacts with gH/gL [191]. In line with the previous finding, gB was also detected in our Co-IP samples with the anti-gH antibody. Therefore, it had to be clarified whether the observed interaction of gH/gL/gO, gB and PDGFRα, reflects an interaction of gH/gL/gO with PDGFRα through gB, whether gH/gL/gO binds both PDGFRα and gB, or whether both, gB and gH/gL/gO independently can interact with PDGFRα.

To confirm the co-precipitations, it was tested whether a recombinant PDGFRα-Fc protein could also co-precipitate gH, gO and gB. As shown in Figure 19, PDGFRα-Fc

coprecipitated gO, gH and also gB, whereas PDGFRβ-Fc precipitated none of these proteins. Thus, the interactions are highly specific and promoted by PDGFRα.

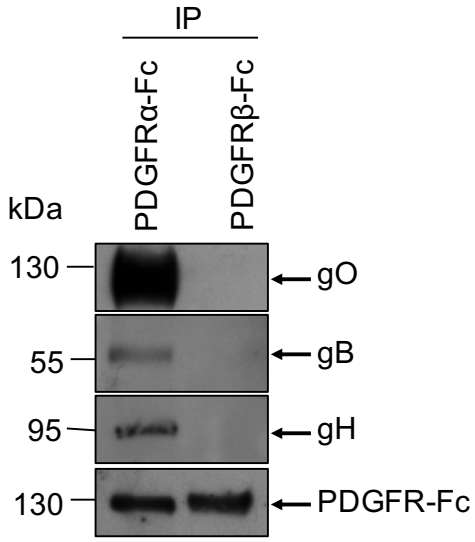

Figure 19: Co-immunoprecipitation of gO, gH, and gB from TB40-UL131stop virions with PDGFR-Fc proteins.
TB40-UL131stop virion lysates were precleared with protein A sepharose beads, co-incubated with either PDGFRα-Fc or PDGFRβ-Fc. Proteins bound to Fc-fusion proteins were precipitated with protein A beads. Coprecipitated proteins were detected by Western blot using corresponding antibodies. Fc-fused proteins were visualized using a peroxidase-conjugated goat anti-human antibody.

It has been described that gH and gB can interact during HCMV entry [97] or in transfected cells [67, 192]. Co-precipitation of gB and gH either using an anti-gH antibody (Figure 18) or PDGFRα-Fc protein (Figure 19) could be confirmed. To test whether there is an interaction between gB and gH in the absence of PDGFRα, co-immunoprecipitation experiments were performed using extracts of cell-free virions. As shown in Figure 20, anti-gH antibody precipitated gH, gO and also gB from purified virions. Anti-gB antibody could only precipitate gB, but not gH or gO. A likely explanation might be that the antibody recognizes an epitope which is also required for the interaction between gB and gH and blocked when complexes are formed. Consequently, only gB which is not in complexes can be precipitated by this antibody. Collectively, these data support the existence of a direct interaction between gB and gH in virions. This interaction very likely is independent of PDGFRα.

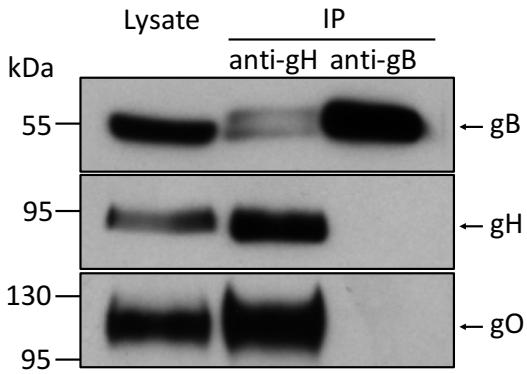

Figure 20: Immunoprecipitation of gH and gB from TB40-UL131stop virions.
TB40-UL131stop virions lysates were precleared with protein A sepharose beads, incubated with either anti-gH antibody (14-4B) or anti-gB antibody (SM5-1), which were then precipitated with protein A sepharose beads. Virion lysates and immunoprecipitates were detected by Western blot using corresponding first antibodies and a peroxidase-conjugated goat anti-mouse IgG (Kappa light chain) for gB and a peroxidase-conjugated goat anti-mouse IgG for gH and gO as second antibodies.

The experiments were replaced using wild type TB40 virus to test reproducibility in a virus expressing both the gH/gL/gO and gH/gL/pUL(128,130,131a) complexes. Figure 21 shows that PDGFRα, but not PDGFRβ precipitated gO and gB also from TB40-BAC4 virion lysates. Anti-gH antibody co-precipitated gB, gH and gO from mixed lysates of virions and cells. And again, anti-gB antibody only precipitated gB.

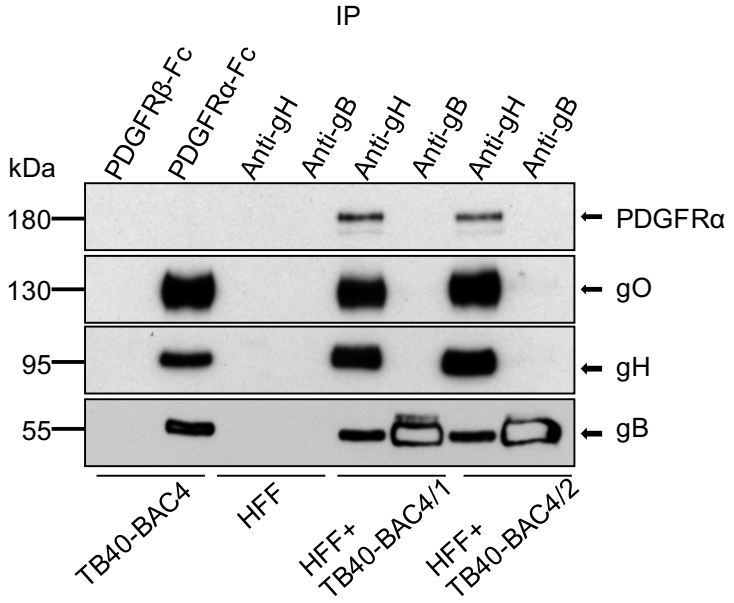

Figure 21: Co-immunoprecipitation of gH, gO, gB and PDGFRα from lysates of TB40-BAC4 virions or TB40-BAC4 virions mixed with fibroblasts.
TB40 virions lysates or mixtures of TB40 virions lysates and HFF lysates were incubated with PDGFR-Fc proteins or anti-gH antibody (14-4b) or anti-gB antibody (SM5-1), and then precipitated with protein A sepharose beads. Immunoprecipitates were detected by Western blot analysis using the corresponding first antibodies and a peroxidase-conjugated goat anti-mouse IgG (Kappa light chain) for gB and a peroxidase-conjugated goat anti-mouse IgG for gH, gO and gB as second antibodies. Fc-fused proteins were visualized using a peroxidase-conjugated goat anti-human antibody.

3.1.3.4 PDGFRα and HCMV gO interact directly

To find out whether gO can directly interact with PDGFRα, purified gO-Fc protein was co-incubated with HFF on ice, and then crosslinked by adding water-dissolved DTSSP (membrane-impermeable protein crosslinker) into the mixture. After the crosslink, cells were lysed and proteins precipitated with protein A sepharose beads. As shown in Figure 22, gO-Fc precipitated PDGFRα from HFF after crosslink whereas an interaction with PDGFRα in the absence of DTSSP was hardly detectable. This strongly suggests a direct interaction between gO and PDGFRα on the cell surface.

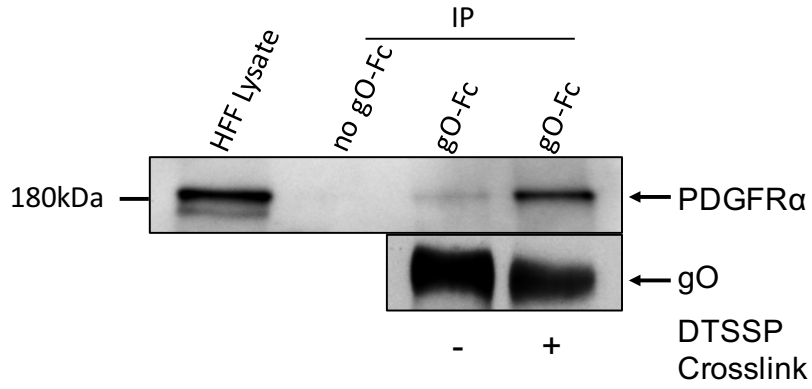

Figure 22: Crosslink of gO-Fc and PDGFRα on the surface of HFF.
HFF were detached with versene and incubated with or without gO-Fc on ice for 90 min. Samples were crosslinked or not with 2 mM DTSSP on ice for 90 min. Cells were lysed and Fc proteins precipitated using protein A sepharose beads. Precipitates were detected by Western blot analysis using the corresponding first antibodies and a peroxidase-conjugated goat anti-mouse IgG as the second antibody.

3.2 The role of PDGFRα in HCMV infection

PDGFRα has been reported to enhance HCMV infection [72]. Additionally, HCMV infection has been shown to result in phosphorylation of PDGFRα, yet inhibition studies with anti-PDGFRα antibody, PDGFRα ligand or inhibitors of phosphorylation were inconclusive [72, 74]. Thus, to date, it is still not clear whether PDGFRα serves as an entry receptor or as a coreceptor promoting entry by providing a costimmulation signal for HCMV host cells.

3.2.1 Inhibition of infection with soluble PDGFRα protein

HCMV infection of fibroblasts has been shown to be mediated by the gH/gL/gO complex [68]. If the entry process depends on an interaction of PDGFRα and gH/gL/gO, preincubation of virus with soluble PDGFRα protein might be able to inhibit infection. To evaluate that, TB40-Luc virions were preincubated with recombinant PDGFRα-Fc protein

(524 aa long N-terminus of human PDGFRα fused to human IgG1 Fc, R&D Systems) and then subjected to infection of HFF. Twenty-four hours post infection (p.i.), virus entry was quantified by measuring the luciferase activities of TB40-Luc. As shown in Figure 23, PDGFRα-Fc blocked TB40-Luc infection in a dose-dependent manner. Blocking could be saturated. PDGFRβ-Fc, which was used as a control, had no effect, indicating that HCMV entry into HFF specifically relies on a gH/gL/gO - PDGFRα interaction.

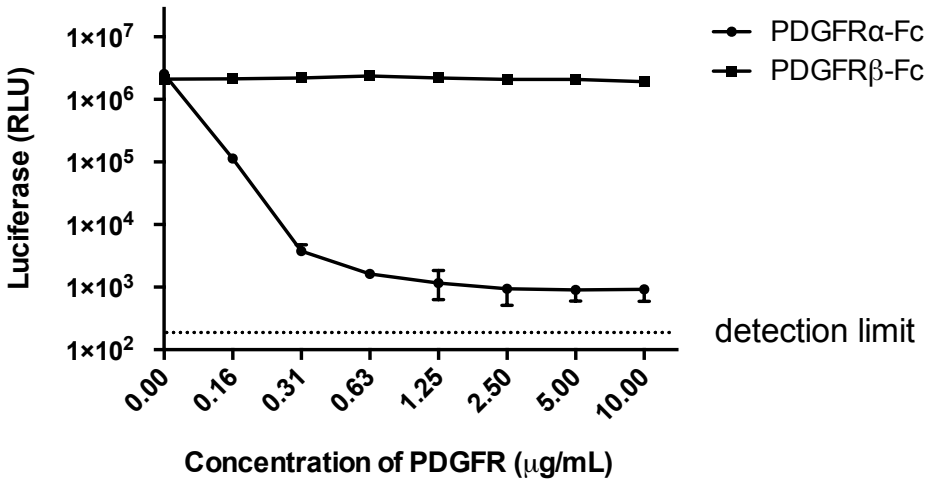

Figure 23: PDGFRα-Fc blocks HCMV infection of HFF.
HFF cells were plated in 96-well plates one day before infection. TB40-Luc virus was preincubated with the indicated amounts of soluble PDGFRα-Fc protein or as a control PDGFRβ-Fc for one hour at 4°C. Cells were infected with the virus-PDGFR-Fc mixtures using centrifugal enhancement (2000rpm, 30min; RT) followed by an incubation at 37℃ for 1h. Then cell layers were washed 3 times with PBS and incubated with medium containing PAA. Luciferase activity was measured 24h post infection (p.i.). Shown are means ± SD of one experiment performed in triplicates.

To confirm that neutralization of HCMV by PDGFRα is gO-dependent, TB40-ΔgO-Luc virus (Figure 24b), which lacks gO and expresses only the gH/gL/pUL(128,130,131a) complex, was tested in parallel with TB40-Luc virus (Figure 24a) following the same strategy as above. Amounts of TB40-ΔgO-Luc virus and TB40-Luc virus were adapted to give a similar initial infection capacity on HFF. Notably, PDGFRα-Fc specifically blocked TB40-Luc infection but not TB40-ΔgO-Luc infection of HFF, suggesting that PDGFRα functions as a gH/gL/gO-specific receptor.

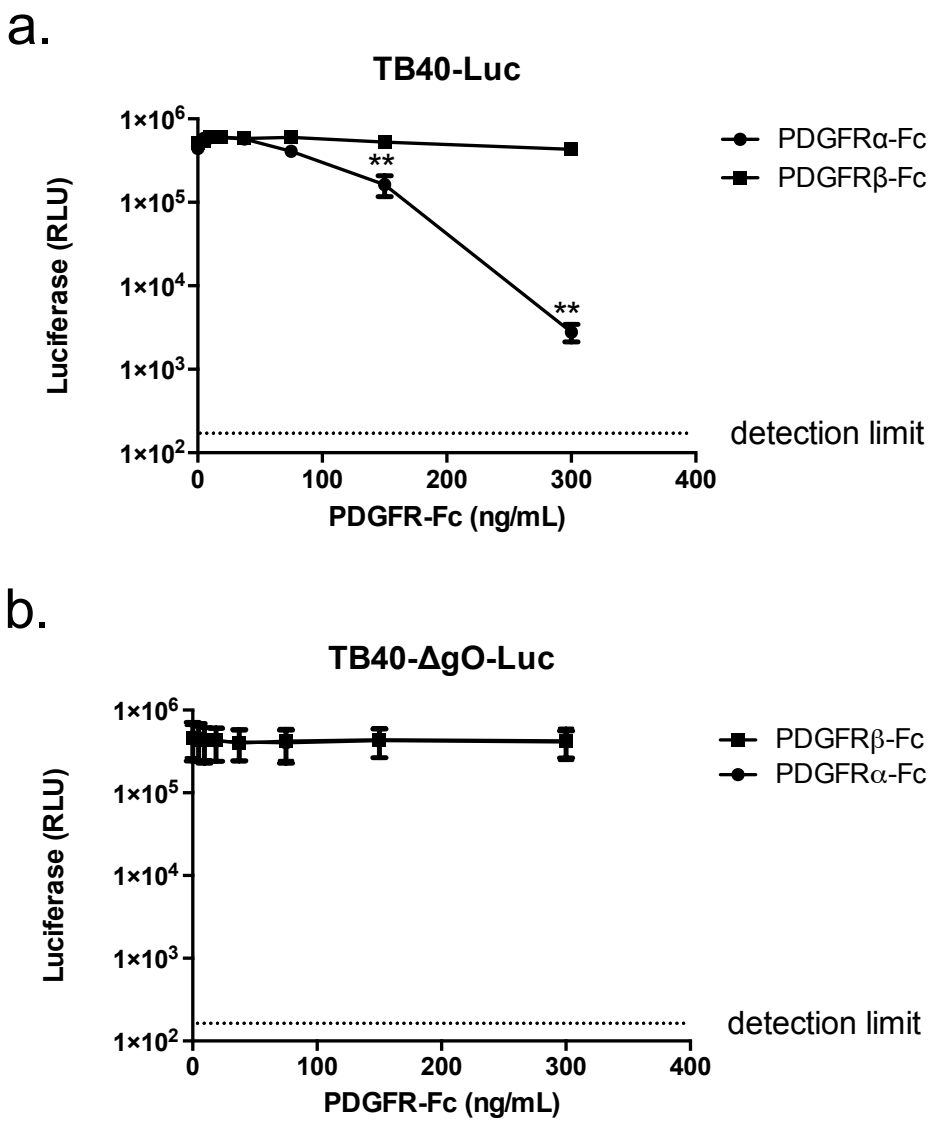

Figure 24: PDGFRα-Fc neutralizes TB40-Luc but not TB40-ΔgO-Luc infection of HFF.
HFF cells were plated in a 96-well plate one day before infection. TB40-Luc (a) and TB40-ΔgO-Luc (b) virus were preincubated with the indicated amounts of soluble PDGFRα-Fc protein or as a control PDGFRβ-Fc for one hour at 4°C. Cells were infected with the virus-PDGFR-Fc mixtures using centrifugal enhancement (2000rpm, 30min; RT) followed by an incubation at 37℃ for 1h. Then cell layers were washed 3 times with PBS and incubated with medium containing PAA. Luciferase activity was measured 24h p.i.. Shown are means ± S.E. of 3 independent experiments assayed in triplicates. Unpaired student's t-test was performed for statistical analysis. (** denotes $0.01<p<0.01$)

The inability of PDGFRα-Fc protein to block infection of HFF with TB40-ΔgO confirms earlier findings [118] that entry via the pentameric complex relies on an alternative receptor. In line with that, infection with wildtype virus TB40-Luc which expresses both gH/gL/gO and gH/gL/pUL(128,130,131a) could not be completely inhibited (Figure 23), indicating a residual infection due to the pentameric complex. To verify this, TB40-UL131stop-Luc [122], a virus mutant lacking the pentameric complex was co-incubated with PDGFRα-Fc in

parallel with wildtype TB40-Luc. As shown in Figure 25, TB40-UL131stop-Luc infection, but not TB40-Luc could be completely inhibited, supporting that the residual infection is gH/gL/pUL(128-UL131a)-dependent entry, which is independent of PDGFRα.

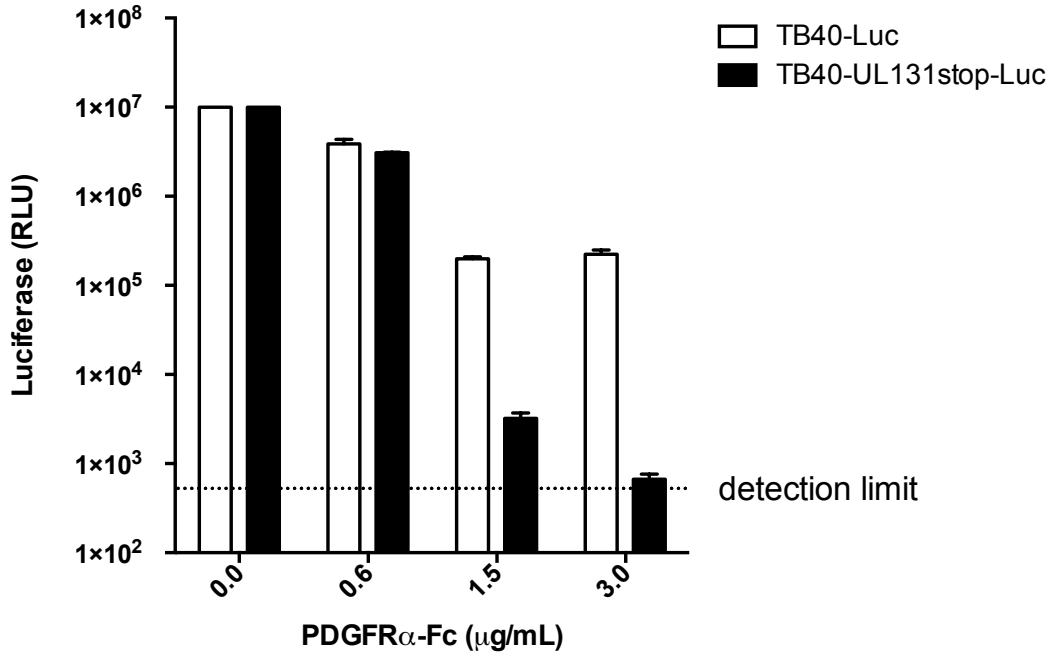

Figure 25: PDGFRα-Fc completely blocks TB40-UL131stop-Luc infection of HFF, but not TB40-Luc infection.

HFF cells were plated in a 96-well plate one day before. TB40-Luc and TB40-UL131stop-Luc viruses were preincubated with the indicated amounts of soluble PDGFRα-Fc protein or as a control PDGFRβ-Fc for one hour at 4°C. Cells were infected with the virus-PDGFR-Fc mixtures using centrifugal enhancement (2000rpm, 30min; RT) followed by an incubation at 37℃ for 1h. Then cell layers were washed 3 times with PBS and incubated with medium containing PAA. Luciferase activity was measured 24h p.i.. Shown are the means ± SD of one experiment performed in triplicates.

3.2.2 gH/gL/gO determines infection of fibroblast cultures with free virus, but not cell-associated spread

HCMV spread in fibroblast cultures is determined by the gH/gL/gO complex and is predominantly driven by supernatant virus [122]. Deletion of HCMV gO results in release of hardly infectious virus particles and shifts the spread pattern from supernatant-driven to cell-associated spread [107].

Infection of fibroblasts with free virus can be effectively inhibited with soluble PDGFRα (Figure 23 - 25). To study whether also cell-associated spread in cell culture is PDGFRα-dependent, co-culture experiments were performed. TB40-BAC4 infected HFF were either mixed with uninfected HFF or HUVEC, and spread of infection followed in the presence or

absence of PDGFRα-Fc or as a control PDGFRβ-Fc or anti-pUL131a antibody, which specifically blocks gH/gL/pUL(128, 130, 131a)-dependent spread [94]. Spread of infection was monitored by staining for the HCMV immediate-early protein (IE1). For HCMV spread in HFF culture, only PDGFRα-Fc specifically reduced the number of infected cells per focus (Figure 26a and Figure 26b) to a level reminiscent to the effect of methylcellulose overlays, a treatment which restricts cell-free virus spread. This suggests that the reduced infection in fibroblast cultures is likely due to a PDGFRα-dependent neutralization of cell-free virus. The observation that the anti-pUL131a antibody had no effect on focus size in HFF, suggests that gH/gL/gO can also promote cell-associated spread independent of PDGFRα. Spread in HUVEC cultures was abolished by anti-pUL131a antibody but not by PDGFRα (Figure 26a and 26c), supporting that HCMV spread in EC cultures is determined by gH/gL/pUL(128, 130, 131a) and independent of PDGFRα.

To conclude, gH/gL/gO likely promotes entry of cell-free virus through a PDGFRα-dependent pathway and cell-associated virus spread through a PDGFRα-independent pathway.

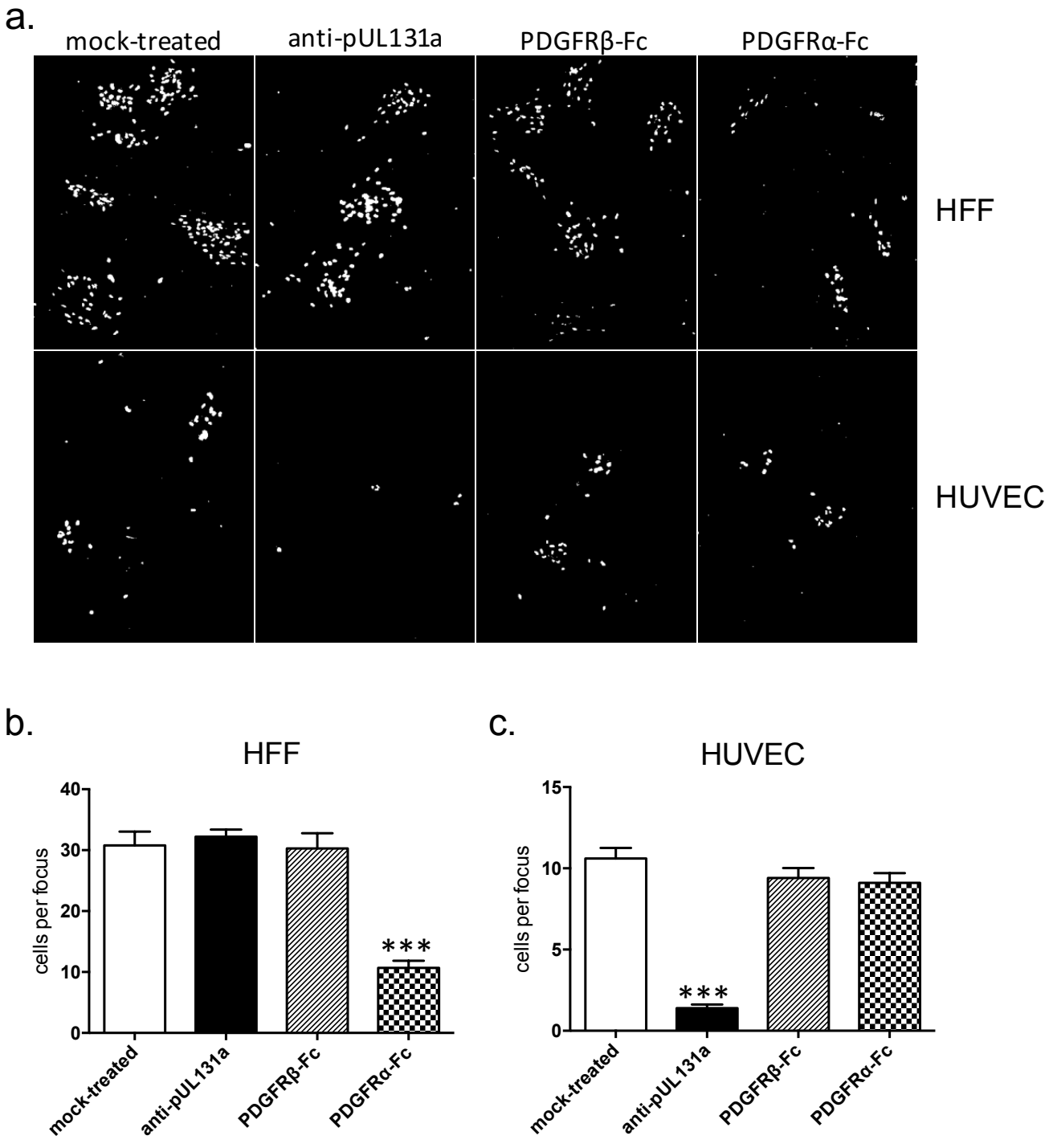

Figure 26: PDGFRα-Fc does not inhibit cell-associated spread of HCMV in fibroblast cultures.
HFF were infected with TB40-Luc at an MOI of 10. 150 infected cells/well were then mixed with 1.5×10^4 HFF/well or 2×10^4 HUVEC/well and seeded in 96-well plates. Supernatants were removed after 12 h and fresh medium containing anti-pUL131a serum or PDGFR-Fc proteins was added. These media were exchanged every second day. Cells were fixed after 5 days and infected cells were visualized by antibodies directed against HCMV IE1 and a goat anti-mouse Alexa Fluor® 488 antibody. a) representative microscopic fields. b) and c) IE1 positive cells of 10 randomly chosen foci were counted for each group. The error bars in b and c represent means ± SD. Mann-Whitney Rank Sum test was performed for statistical analysis (*** denotes $p<0.001$)

3.2.3 The infection capacity of HCMV for its host cells correlates with the abundance of PDGFRα

Infection of cells with HCMV expressing only gH/gL/gO complex is highly restricted [114]. Mainly fibroblasts are susceptible to HCMV infection [68]. To find out whether this correlates with PDGFRα levels, PDGFRα protein levels of several HCMV-permissive cell types were assessed by Western blot analysis. PDGFRα was found to be abundantly expressed in fibroblasts (HFF and MRC5) but not detectable in epithelial cells (293 and ARPE-19) and EC (HUVEC) (Figure 27), coinciding with the observation that in cell culture, only fibroblasts are susceptible for HCMV lacking the pentameric complex and expressing only the gH/gL/gO complex [93, 94]. Additionally, this fits the observation that gO-Fc specifically binds to HFF, but not to HUVEC (Figure 12).

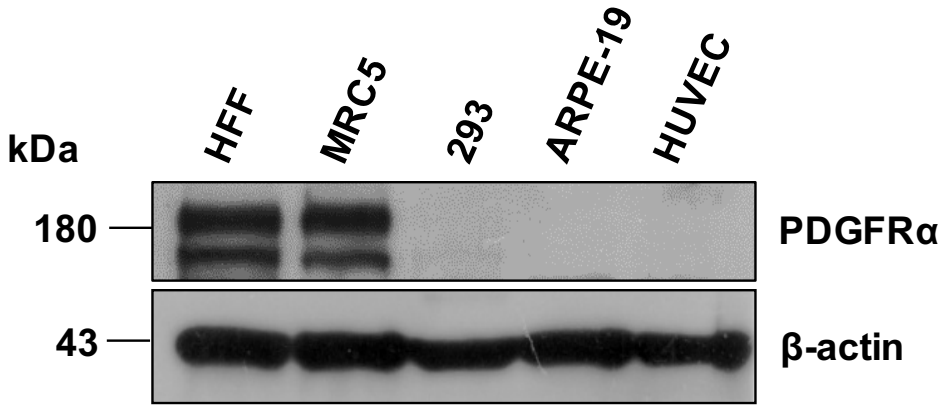

Figure 27: PDGFRα levels in different cell types.
Cell extracts were analyzed for PDGFRα levels or as a loading control β-actin by Western blot analysis using the corresponding first antibodies and a peroxidase-conjugated goat anti-mouse IgG as second antibody.

Although there seems to be a correlation between expression levels of PDGFRα and susceptibility to binding of gO-Fc protein to cell surfaces (Figure 9), TB40-UL131stop infection of different cell types may also be shaped by cell type-specific costimulatory cell surface proteins which affect HCMV entry. To directly determine in one specific cell line that there is a correlation of PDGFRα levels and HCMV entry, 293 cells, which do not express detectable levels of PDGFRα (Figure 27, Figure 28a and Figure 28b), were transfected with a plasmid expressing PDGFRα.

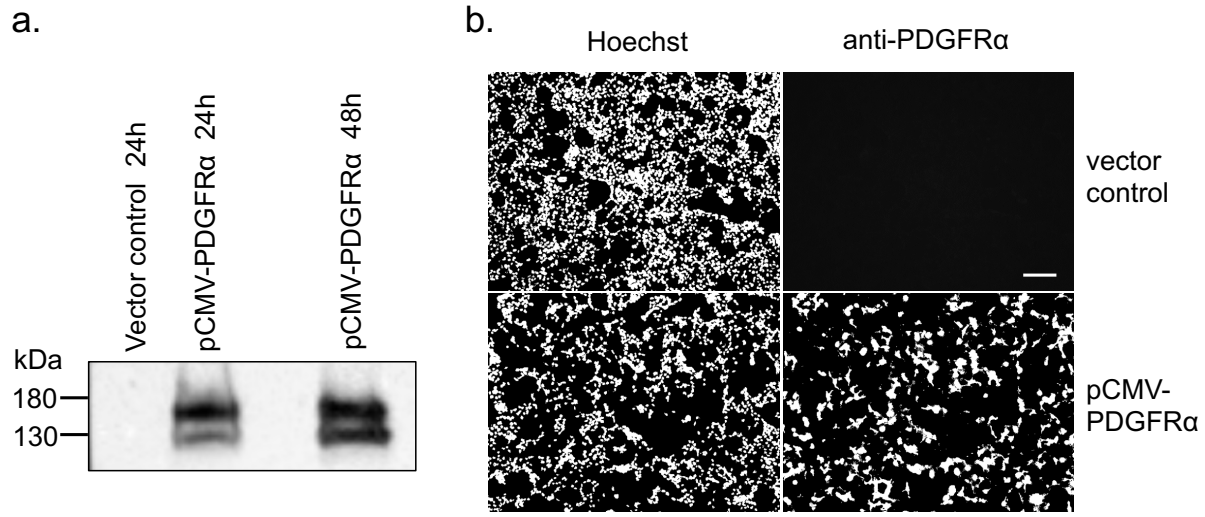

Figure 28: Over-expression of PDGFRα in 293 cells.
293 cells were transfected with pCMV-PDGFRα or a vector control (pCR3.1). a) lysates of cells collected 24 h and 48 h after transfection were analyzed by Western blot using a mouse-anti-PDGFRα antibody and a peroxidase-conjugated goat anti-mouse IgG. b. Transfected cells were fixed at 24 h after transfection, and either stained with Hoechst 33258 to visualize nuclei or by indirect immunofluorescence staining using a mouse-anti-PDGFRα antibody and an Alexa Fluor-488-conjugated goat anti-mouse IgG. Scale bar, 200 µm.

Control- and PDGFRα- transfected cells were infected with TB40-Luc, TB40-UL131stop-Luc or TB40-ΔgO-Luc. Infections were adjusted prior infection. TB40-UL131stop-Luc, lacking the pentameric complex can hardly infect epithelial cells which is reflected in Figure 29a. TB40-ΔgO-Luc amounts were adjusted to result in a infection of mock-transfected 293 cells comparable TB40-Luc. Over-expression of PDGFRα strongly enhanced infection with both TB40-Luc and TB40-UL131stop-Luc viruses (Figure 29a). In contrast, over-expression of PDGFRα had no impact on infection of TB40-ΔgO-Luc virus (Figure 29b). Again, these data suggest that gO-dependent entry of HCMV correlates with PDGFRα levels in host cells.

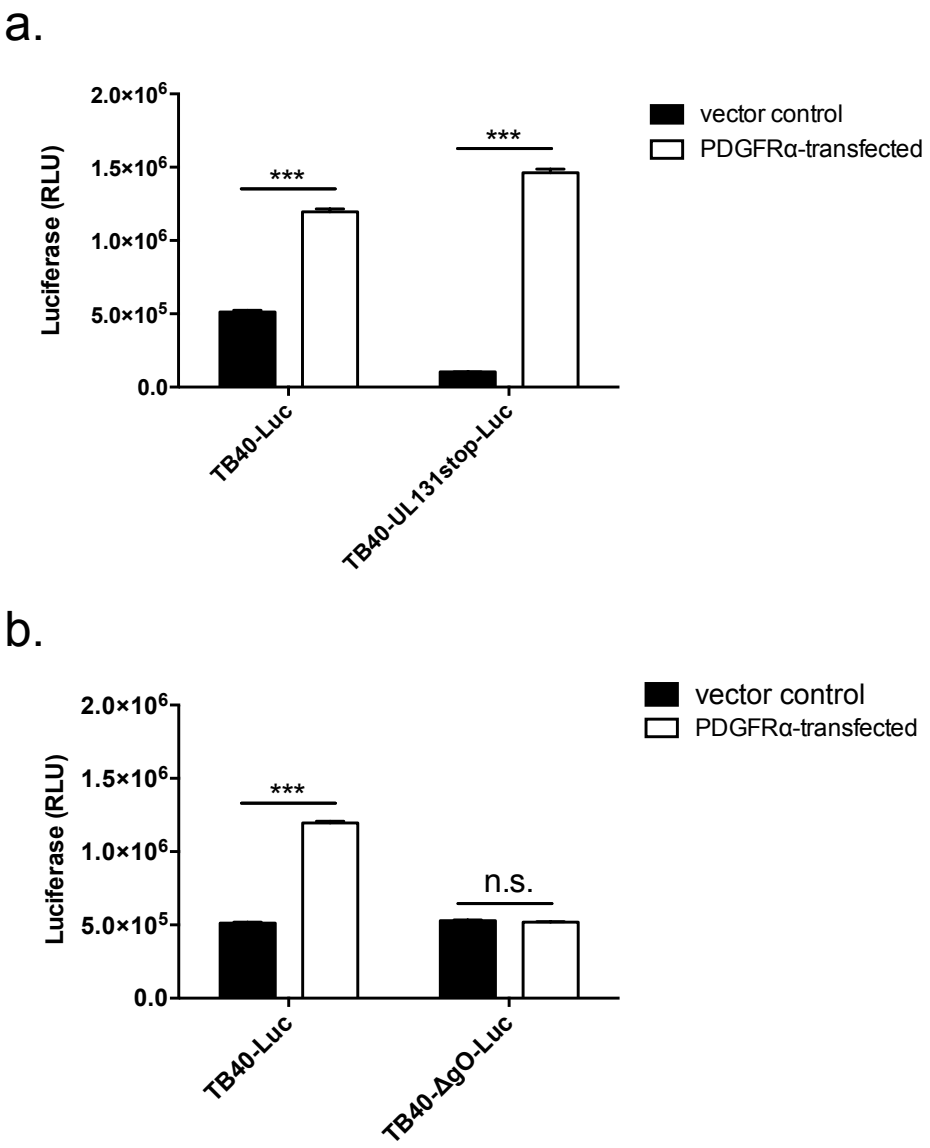

Figure 29: PDGFR-overexpression enhances HCMV infection in a gO-dependent manner.
293 cells were transfected with pCMV-PDGFRα (Sino Biological Inc.) or a vector control (pCR3.1), and 2 days later infected with a) TB40-Luc or TB40-UL131stop-Luc or b) TB40-Luc or TB40-ΔgO-Luc. Cells were lysed at 24 h.p.i and analyzed by a luciferase assay. Shown are means +/- S.E.M. of 3 independent experiments done in triplicates. Unpaired student's t-test was performed for statistical analysis. (n.s. denotes $p>0.05$; *** denotes $p<0.001$)

3.2.4 Inhibition of HCMV infection with PDGFRα ligand

Several natural ligands of PDGFRα bind to its extracellular domain with high affinity. Therefore, they are good candidates to further confirm a gH/gL/gO-PDGFRα interaction. To test whether PDGF-BB, a ligand of PDGFRα, can interfere with HCMV entry into fibroblasts, HFF were preincubated with PDGF-BB, and then infected with TB40-Luc, TB40-UL131stop-Luc or TB40-ΔgO-Luc in the presence of PDGF-BB. To inactivate not penetrated virions, cells were washed 3 times with PBS, pH 3.0. Twenty four h p.i, infection

was quantified by a luciferase assay. Infection of HFF by TB40-Luc was about 50 % reduced, TB40-UL131stop-Luc infection was about 30 % reduced, and TB40-ΔgO-Luc infection was not affected (Figure 30). Thus again, only gH/gL/gO-positive HCMV showed a PDGFRα-dependent infection pattern.

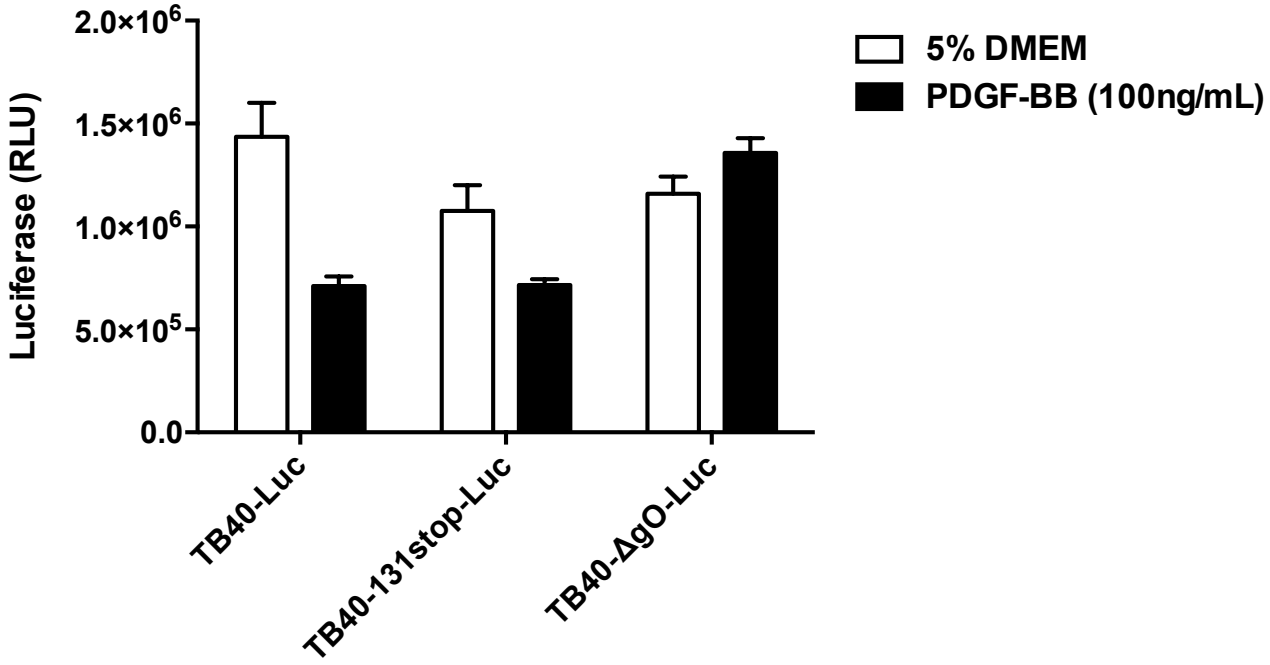

Figure 30: PDGF-BB inhibits TB40-Luc and TB40-UL131stop-Luc but not TB40-ΔgO-Luc entry into HFF.

HFF cells are preincubated with PDGF-BB or as a control 5% DMEM for 15min and then infected with TB40-Luc, TB40-UL131stop-Luc and TB40-ΔgO-Luc in the absence (controls) or presence of PDGF-BB. Infection was performed with centrifugal enhancement followed by 1 h incubation at 37 ℃. After infection, cells were washed 3 times with PBS (pH 3.0) to inactivate and remove free virus and cell surface-bound virus and then cultivated with medium containing PAA. 24 h p.i., cells were lysed and analyzed by a luciferase assay. Shown are means +/- SD of one experiment performed in triplicates.

A previous study has suggested that activation of PDGFRα is required for HCMV infection [72]. Thus, pre-stimulation of host cells with a ligand of PDGFRα which activates PDGFRα might promote HCMV entry into host cells. To investigate this, cells were preincubated with PDGF-BB and infected in the absence of PDGF-BB. Infection was slightly elevated independent whether virions contained gH/gL/gO complex or not (Figure 31). If activation of PDGFRα was essential for gH/gL/gO- or gH/gL/pUL(128, 130, 131a)-dependent entry, one would have expected a stronger enhancement of infection.

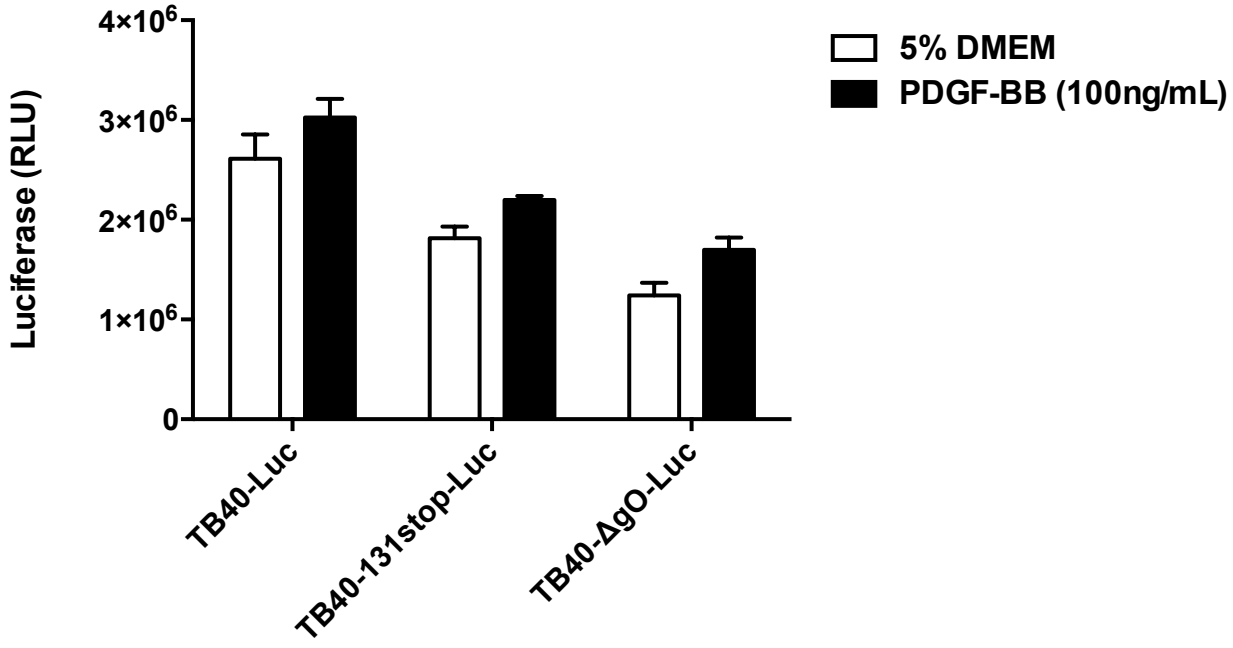

Figure 31: PDGF-BB stimulation has hardly any effect on TB40-Luc, TB40-UL131stop-Luc and TB40-ΔgO-Luc infections of HFF.
HFF cells are preincubated with PDGF-BB or as a control 5% DMEM for 15min and then infected with TB40-Luc, TB40-UL131stop-Luc and TB40-ΔgO-Luc in the absence of PDGF-BB. Infection was performed with centrifugal enhancement followed by 1 h incubation at 37 ℃. After infection, cells were washed 3 times with 5% DMEM to remove free virus and then fed with medium containing PAA. At 24 h p.i., cells were lysed and analyzed by a luciferase assay. Shown are means +/- SD of one experiment performed in triplicates.

It has been reported before that imatinib mesylate, a tyrosine kinase inhibitor, can substantially inhibit HCMV infection by blocking the kinase activity of PDGFRα and abolishing downstream activation pathways in U87 glioma and human embryonic lung (HEL) cells [72]. In contrast, a second study found that the effect of imatinib mesylate on HCMV entry was not specific for HCMV but could also be observed for HSV-1, and thus very likely resulted in a general down-regulation of cellular signaling pathways [74]. To decide whether imatinib mesylate has a specific effect on HCMV entry and whether this effect is gO-dependent, HFF were pretreated with imatinib mesylate and then infected with TB40-Luc, TB40-UL131stop-Luc or TB40-ΔgO-Luc. Virus entry was quantified by evaluating infection using a luciferase assay. Both TB40-Luc and TB40-UL131stop-Luc were slightly inhibited, while no impact was observed for TB40-ΔgO-Luc infection (Figure 32). This could indicate that activation might play a role in gH/gL/gO-dependent entry.

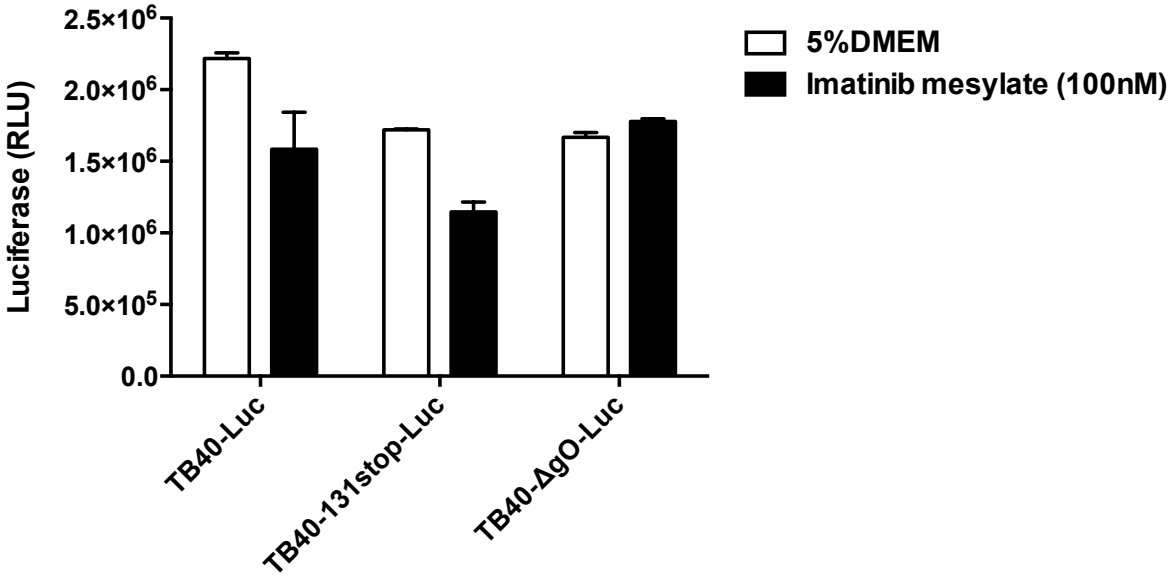

Figure 32: Imatinib mesylate inhibits TB40-Luc and TB40-UL131stop-Luc but not TB40-∆gO-Luc infections of HFF.
HFF cells were pretreated with imatinib mesylate or as a control 5% DMEM for 1 h and then infected with wildtype TB40-Luc, TB40-UL131stop-Luc or TB40-∆gO-Luc for 90 min in the presence of imatinib mesylate. Free virus was removed by washing the cells 3 times with 5% DMEM. Cells were cultured in fresh medium containing PAA and imatinib mesylate. At 24 h p.i., cells were lysed and analyzed by a luciferase assay. Shown are means +/- SD of one experiment performed in triplicates.

In summary, data reveal that gH/gL/gO-dependent entry and PDGFRα-dependent entry are congruent. PDGFRα thus very likely is the entry receptor used by gH/gL/gO. The restricted numbers of experiments studying the role of PDGFRα phosphorylation in gH/gL/gO-dependent entry do not yet allow a final conclusion whether gH/gL/gO-dependent entry is phosphorylation-dependent.

3.3 The role of the gH/gL/gO complex in MCMV infection

The infection of mice with murine cytomegalovirus (MCMV), serves as a model for the human HCMV infection. MCMV encodes functional homologues of the HCMV gH/gL/gO and gH/gL/pUL(128, 130, 131a) complexes, namely a gH/gL/gO (m74) complex [165] and a gH/gL/MCK-2 (m131/129) complex [166].

3.3.1 The role of deletion of gO in MCMV infection of different cell types

Infection capacities of HCMV for different cell types are gH/gL/gO dependent (Figure 8). To find out whether ΔgO mutants of MCMV also show cell type specific changes in infection

capacities, MCMV infection of different cell types was analyzed. For all experiments, MCMV 3.3WT which is a BAC clone of the MCMV strain Smith (pSM3fr-MCK-2fl) [185] and mutants therefore were used. Δm74 is a gO-deletion mutant lacking the 532 N-terminal base pairs of m74 and m74stop is a gO-stop mutant with a stop cassette at nucleotide position 120 nt [165]. ΔgO-gO^{trans} virions are phenotypically WT-like virions carrying gH/gL/gO complexes in the envelope. They were generated by propagation of Δm74 virions in NIH3T3 cells expressing gO [166]. Primary embryonic fibroblasts (MEF), a fibroblast cell line (NIH3T3), lung epithelial cells (TCMK-1), EC (MHEC-5T), and macrophages (ANA-1) were infected with wildtype MCMV (3.3WT), ΔgO mutants (Δm74 and m74stop), and a gO-transcomplementated ΔgO virus (ΔgO-gO^{trans}). For all viruses, infection was normalized to infection of MEF which was arbitrarily set to 1. Compared to WT virus, both ΔgO mutants showed reduced infection capacities for NIH3T3 and TCMK-1. Transcomplementation reverted this phenotype (Figure 33a). Infection of ANA-1 was not affected by deletion of gO (Figure 33b). Strikingly, infection of MHEC-5T was enhanced by deletion of gO. This enhancement was not completely reversed by transcomplementation (Figure 33a), a phenomenon that might due to non-wildtype gO levels in transcomplemented virions.

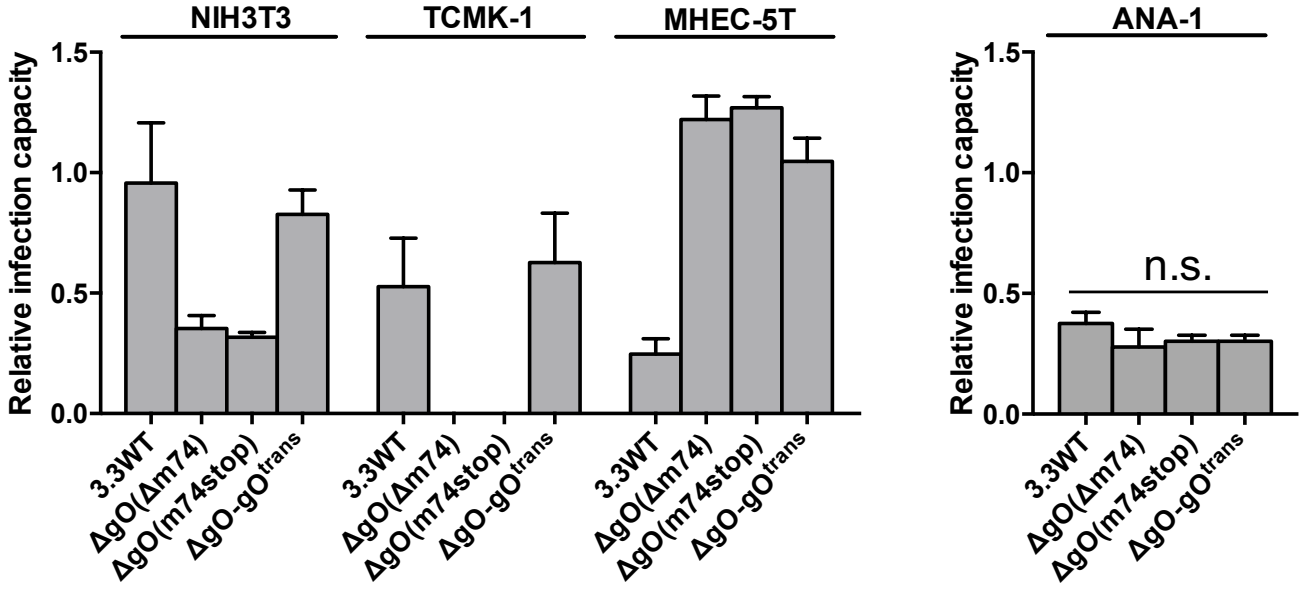

Figure 33: Comparison of the relative infection capacities of MCMV 3.3WT, ΔgO mutants and ΔgO-gO^{trans} for different cell types in culture.

MEF, NIH3T3, TCMK-1, MHEC-5T and ANA-1 cells were infected with 3.3WT, Δm74, m74stop or ΔgO-gO^{trans}. Infection capacities were determined (a) 4h p.i. by indirect immunofluorescence (data from Ilija Brizic) or (b) 16 h p.i. by intracellular FACS analysis specific for MCMV immediate-early 1 protein (ie1). Bars represent means +/- SD of at least three independent experiments. Unpaired student's t-test was performed for statistical analysis. (n.s. denotes p>0.05)

In conclusion, MCMV lacking gO shares infection patterns with gO-null HCMVs when infection of different cell types all compared. Viruses lacking gH/gL/gO show low infection capacities for epithelial cells and fibroblasts and a relatively increased infection capacity for EC.

3.3.2 MCMV produced in MEF or NIH3T3 cells have different infection capacities

MEF and NIH3T3 cells are two extensively used cell types for production of MCMV in cell culture. Thus, it is of high importance to study whether viruses produced from the two cell types have similar qualities.

When comparing the infection capacities of WT MCMV either derived from MEF or NIH3T3 cells on macrophages, MEF-derived virus showed a lower capacity to infect ANA-1 than NIH3T3-derived virus (Figure 34). A reduced infection capacity for ANA-1 cells has also been observed for MCMV lacking MCK-2 [166].

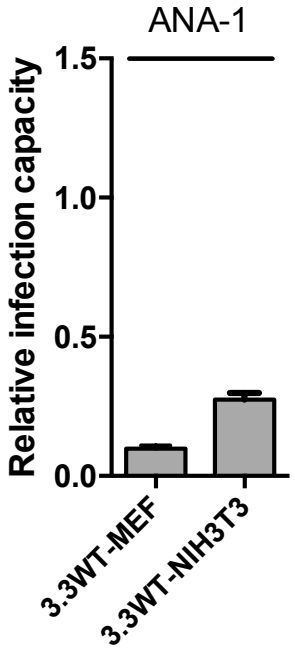

Figure 34: Comparison of macrophage infection capacities of WT MCMV derived from MEF or NIH3T3 cells.
MCMV derived from MEF (3.3WT-MEF) or NIH3T3 cells (3.3WT-NIH3T3) were used to infect ANA-1. Infection capacities were determined 16 h p.i. by intracellular FACS analysis specific for MCMV ie1 protein. Infection was normalized to the number parallely of infected MEF. Shown are means +/- SD of one representative experiment out of 2 assayed in triplicates.

To further investigate the infection capacities of MEF- and NIH3T3-derived virus, infection of additional cell types was analyzed. MEF, NIH3T3, TCMK-1 and MHEC-5T cells were infected with supernatant viruses derived from MEF and NIH3T3 cells. Infection capacities were evaluated by staining for MCMV ie1 protein. MEF-derived and NIH3T3-derived MCMV showed similar infection capacities for NIH3T3 and TCMK-1 cells. NIH3T3-derived virus showed a higher relative infection capacity for EC than MEF-derived virus (Figure 35).

For HCMV, it has also been reported that different cell types produce virus progenies which differ in their infection capacities for different cell types. This has been attributed to different ratios of gH/gL complexes in virions [102, 122].

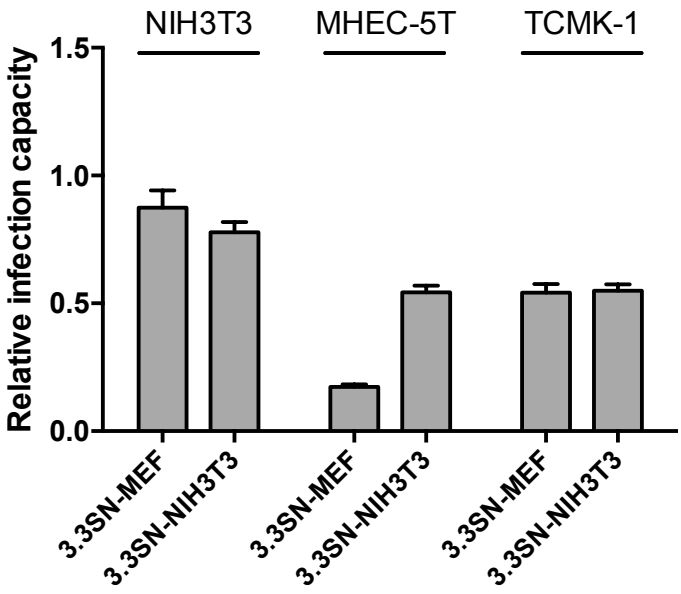

Figure 35: Comparison of infection capacities of supernatant virus-derived from MCMV-infected MEF and NIH3T3 cells.
MCMV derived from MEF (3.3WT-MEF) or NIH3T3 cells (3.3WT-NIH3T3) were used to infect MEF, NIH3T3, MHEC-5T or TCMK-1 cells. Infection capacities were determined 4h p.i. by indirect immunofluorescence specific for MCMV ie1 protein. Infection was normalized to the number of parallely infected MEF. Shown are means +/- SD of one representative experiment out of two assayed in triplicates.

To exclude that the observed discrepancy between MEF- and NIH3T3-derived virus was not caused by the way virus was collected, different virus preparation methods: i) precleared supernatant virus, ii) pelleted virus and iii) sucrose cushion-purified virus. Pellets were prepared by high speed centrifugation of supernatants of infected MEF or NIH3T3 cells. For preparation of sucrose cushion-purified virus, those pellets are further purified through 15 % sucrose cushions. All three virus preparations showed a discrepancy for the

infection capacity for EC (Figure 35, 36a and 36b), although it appeared less pronounced for the sucrose-cushion purified viruses (Figure 36b).

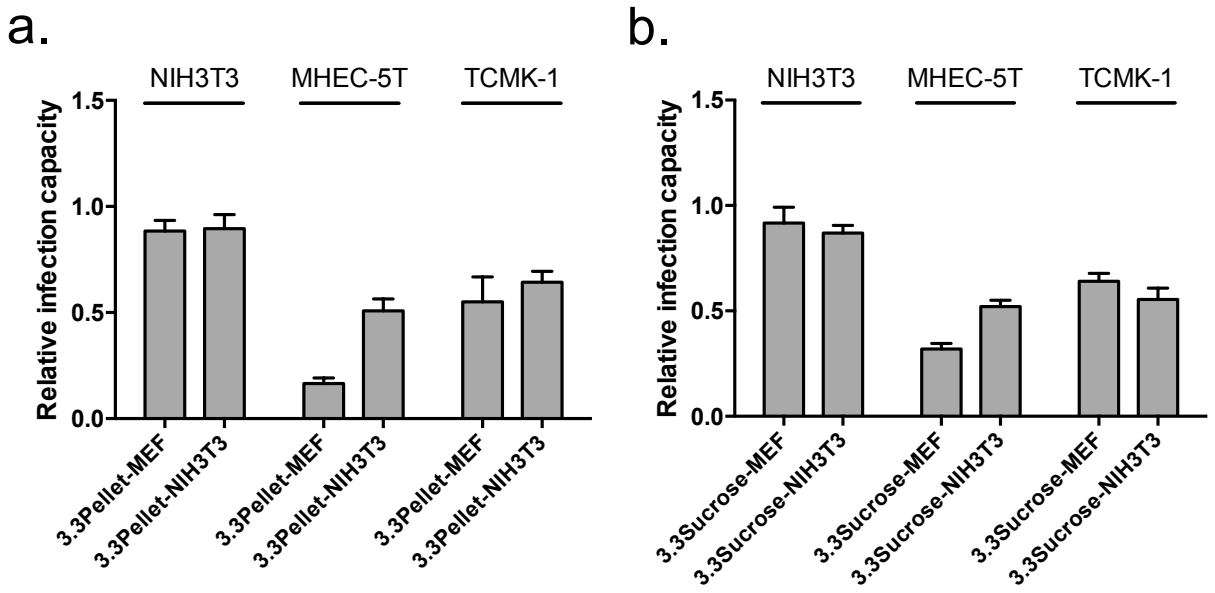

Figure 36: Comparison of infection capacities of virus pellets and sucrose-cushion purified virions. Virus pellets (a) and sucrose-cushion-purified viruses (b) derived from MEF (3.3SN-MEF) or NIH3T3 cells (3.3SN-NIH3T3) were used to infect MEF, NIH3T3, MHEC-5T or TCMK-1 cells. Infection capacities were determined 4h p.i. by indirect immunofluorescence analysis specific for MCMV ie1 protein. Infection was normalized to the number of parallely infected MEF. Shown are means +/- SD of one representative experiment out of two assayed in triplicates.

To test whether virus produced by other cell types also show discrepant infection capacities, virus produced from TCMK-1, MHEC-5T and fibroblasts was tested on MHEC-5T and TCMK-1. Only virus produced from NIH3T3 has a higher infection capacity for MHEC-5T cells (Figure 37).

The discrepancy between MEF- and NIH3T3-derived virus might be due to different ratios of gH/gL/gO and gH/gL/MCK-2 complexes. To analyze this, one would need to compare the gO and MCK-2 levels of those virus particles. However, lack of an antibody against MCMV gO hinders further investigation of this issue. Thus, the next step to address this issue would be to produce an antibody against MCMV gO.

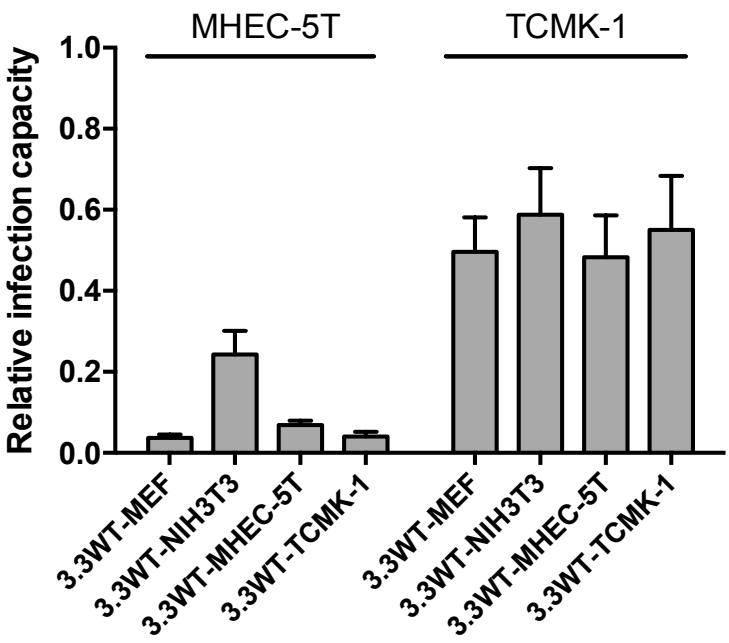

Figure 37: Comparison of infection capacities of supernatant virus from MCMV-infected MEF, MHEC-5T and TCMK-1 cells.

MCMV from MEF, NIH3T3, MHEC-5T or TCMK-1 cells were used to infect MEF, NIH3T3, MHEC-5T or TCMK-1 cells. Infection capacities were determined 4h p.i. by indirect immunofluorescence analysis specific for MCMV ie1 protein. Infection was normalized to the number of parallely infected MEF. Shown are means +/- SD of one experiment assayed in triplicates.

4 Discussion

HCMV is highly prevalent worldwide, causing morbidity and mortality in immunocompromised individuals and birth defects after congenital infection [13]. Up to now, there is still no approved vaccine against HCMV available on the market and the treatments are restricted. Viral infection starts with successful entry into host cells which relies on interactions between host cell receptors and viral envelope glycoprotein complexes. The specificity of the virus-receptor interaction is a pivotal determinant of virus cell tropism and host range. Therefore, investigation of host cell receptors for HCMV entry may contribute to the development of vaccines and anti-virals. In the last three decades, many studies aimed at identifying and characterizing host cell receptors for HCMV. However, so far, none of the reported proteins could be confirmed to be functional entry receptors.

In cell culture it has been shown that cell type-specific HCMV infection and thus recognition of cell-type-specific receptors are promoted by the envelope glycoprotein complexes gH/gL/gO and gH/gL/pUL(128, 130, 131a) [50, 68, 118].

This study concentrated on the identification of a host cell receptor for gH/gL/gO and the role of gH/gL/gO in HCMV infection in cell culture. Previous studies have shown that gO-null mutants produced only small plaques in fibroblast culture and that titers of gO-null progeny virus were 1000 fold lower than those of wildtype HCMV [107]. gO has also been reported to contribute to HCMV release by taking part in the secondary envelopment of virions [106]. Cellular receptors of the gH/gL/gO complex are considered to be fibroblast-specific [68]. Additionally, a general role of the gH/gL/gO complex in enhancing infection of all cell types was reported [104]. Recently, a study of MCMV mutants in mice specified an essential role for gO in entry into first target cells during the primary infection in vivo [109].

4.1 A switch of tools - from gO-Fc fusion proteins to virus particles for identification of the cellular receptor of the gH/gL/gO complex

Utilization of IgG-Fc fusion proteins to fish protein binding partners and to purify them by using protein A or G beads is a widely used method for identification of viral receptors [53, 189, 193, 194]. The starting point here was to produce an IgG Fc-fused HCMV gO protein

(gO-Fc) as a tool to investigate the role of gO in HCMV infection and to identify a host cell receptor for the gH/gL/gO complex. To avoid an Fc-specific interaction with Fcγ-binding proteins in the viral envelope or on host cells [195, 196], mouse IgG2b-Fc, which has been shown not to bind to HCMV Fc receptors, [197] was used as a fusion tag.

The gO-Fc protein specifically bound to cells whose infection is predominantly dependent on the gH/gL/gO complex, but not to cells whose infection is mainly driven by the gH/gL/pUL(128-131a) complex. When testing whether gO-Fc could compete with binding of HCMV virions to HFF and consequently inhibit infection, no block of infection could be observed. Several reasons might account for that: 1) The yield of gO-Fc was low and preparation only with 3-16 µg/ml could be produced. For comparison, EBV gp42-Fc fusion protein could inhibit EBV infection of host cells through the EBV gH/gL/gp42 complex only when the gp42-Fc preparations showed concentrations of 10 µg/ml or more [53]. Therefore, the amount of HCMV gO-Fc might not have been sufficient to block all receptors on the surface of HFF. 2) Binding of gO-Fc on cell surfaces was temperature- and detergent-sensitive and could be easily reversed, reflecting a very weak interaction between the gO-Fc protein and its binding partner on HFF. If the gH/gL/gO complex in virions bound with a much higher affinity to the cellular receptor than gO-Fc protein, it would substitute the gO-Fc protein. This could also be the reason why in coprecipitation experiments using gO-Fc no cellular binding partner for gO could be deleted. Hence, an alternative strategy was used to identify the cellular receptor for the gH/gL/gO complex: coincubation of fibroblasts with HCMV virions followed by precipitation of gH and proteins bound to gH. To avoid precipitation of proteins interacting with the gH/gL/pUL(128, 130, 131a) complex, TB40-UL131stop, an HCMV mutant lacking the gH/gL/pUL(128, 130, 131a) complex, was used.

4.2 PDGFRα as a binding partner for gH/gL/gO

To date, a number of different host cell surface proteins have been shown to enhance HCMV infection of cells in culture. Previous studies have already proposed a connection between PDGFRα and HCMV entry. It has been observed that binding of HCMV to host cells induced phosphorylation of PDGFRα and activation of downstream molecules [72]. Knockdown of PDGFRα, or treatment with a PDGFRα ligand (PDGF-AA), a tyrosine-kinase inhibitor (imatinib mesylate), or a PDGFRα-neutralizing antibody all inhibited HCMV infection. Additionally, a gB-PDGFRα interaction was observed in cells expressing

recombinant gB [72]. Therefore, it has been claimed that activation of PDGFRα plays a vital role in mediating HCMV entry [72]. Yet, another study contested this claim based on the observation that although overexpression of PDGFRα highly enhanced HCMV infection, virus entry was not affected by preincubating cells with anti-PDGFRα antibodies, PDGF-AA, or by knockdown of PDGFRα [74].

Here, it could be shown that PDGFRα is indeed an entry receptor for HCMV and that not gB, but gH/gLgO is the binding partner on virions. To precipitate specific cell surface proteins binding the gH/gL/gO complex, TB40-UL131stop virions were mixed with cell surface-biotin-labeled HFF. Two approaches were used, 1) virions and HFF cells were lysed independently and then mixed, or 2) virions and HFF were coincubated and then cells and bound virions were lysed. Precipitation of gH from these lysates resulted in co-precipitation of gH, gO and a cellular 200 kDa biotinylated protein, indicating a successful precipitation of a specific cell surface protein. Subsequent mass spectrometry analysis of this protein identified it as PDGFRα. Using IgG Fc-fused PDGFR protein, gO, gH and gB could be co-precipitated by PDGFRα-Fc protein but not by PDGFRβ-Fc, demonstrating a highly specific interaction with PDGFRα. PDGFRα could also be co-precipitated by using the gO-Fc protein, indicating that PDGFRα directly interacts with gO.

4.3 gB and PDGFRα

The envelope glycoproteins gB and gH/gL are conserved within the family of *Herpesviridae*. They form the core fusion complex necessary for viral entry into host cells [45]. HCMV gB is essential for virion fusion with the host cell plasma membrane and cell-to-cell spread of virus [198], but it is not involved in recognition of entry receptors [75]. It has recently been reported that HCMV gB interacts with gH/gL to form stable gH/gL/gB complexes that are incorporated into virions independent of membrane fusion or receptor binding [191]. Here, a Co-IP of gB, gH and PDGFRα was achieved by using either the PDGFRα-Fc protein or anti-gH antibody to precipitate protein complexes. A previous study had shown that PDGFRα binds to recombinant HCMV gB [72]. This raised the question whether the Co-IP of gH, gO, PDGFRα and additionally gB reflect an interaction of the gH/gL/gO complex with gB bound to PDGFRα, or interactions of gH/gL/gO with PDGFRα and independently also with gB, or whether gB and gH/gL/gO both independently bind to PDGFRα. To test this, Co-IP experiments using virus lysates of an HCMV mutant lacking gH/gL/gO should be

performed to test whether anti-gH antibody and recombinant PDGFRα-Fc protein precipitate gB also in the absence of gO. To test whether anti-gB antibodies could also co-precipitate gH and/or PDGFRα, several anti-gB antibodies were used to precipitate binding partners of gB, however, only gB was precipitated. This very likely reflects that the anti-gB antibodies used bind to a gB epitope which is involved in the formation of gB-gH complexes. In line with this observation, a previous study using a gB-specific antibody also failed to precipitate recombinant gH/gL/gB complexes formed in transfected cells [67].

Overexpression of gB in host cells can overcome the fusion deficiency of gB-null expressing virus [75], suggesting that gB is a fusion promotor rather than a receptor-binding protein. In summary, all data suggest that the co-precipitation of gB and PDGFRα is mediated by gH. In accordance with previous studies, a possible model of HCMV entry might be that the gH/gL complexes recognize different receptors on different cell types, for instance, gH/gL/gO recognizes PDGFRα, and subsequently activate gB to initiate fusion [75].

4.4 gO-dependent infection correlates with PDGFRα-dependent infection

It has been shown that HCMV infection of fibroblasts is dependent on the gH/gL/gO complex [68, 107]. PDGFRα has been reported to be essential for efficient HCMV infection of fibroblasts [72]. Overexpression of PDGFRα in different host cell types markedly boosted entry of both wildtype HCMV and mutants lacking gH/gL/pUL(128, 130, 131a) [72, 74, 199], suggesting that gH/gL/gO contributes to PDGFRα-enhanced entry. HCMV enters fibroblasts through direct fusion with the plasma membrane at neutral pH [21], whereas it enters epithelial cells and EC through macropinocytosis which involves internalization of virions into endosomes and subsequent low pH-dependent fusion with endosomal membranes [22, 50]. When entering epithelial cells overexpressing PDGFRα, virus entry switched to pH-independent fusion [74].

4.4.1 Soluble PDGFRα or PDGFRα ligand can block infection of HCMV expressing gO

A convenient and reliable strategy to evaluate HCMV infection has been established by using luciferase-labeled HCMVs [122]. These luciferase-expressing viruses were used here for blocking experiments. Preincubating of soluble PDGFRα protein with virions or PDGFRα ligand PDGF-BB with host cells efficiently blocked entry of gH/gL/gO-positive HCMV into

HFF, while the same treatment did not affect TB40-ΔgO-Luc entry. This suggests that the inhibition relies on a gH/gL/gO-PDGFRα interaction. Intriguingly, the treatment with soluble PDGFRα protein could completely block infection of TB40-UL131stop-Luc, yet, when wildtype TB40-Luc was used a residual infection was observed. This could be explained that infection with the UL131stop mutant completely relies on the gH/gL/gO complex whereas wildtype HCMV infection partially depends on gH/gL/pUL(128, 130, 131a). The observed low residual infection (2.2%) of TB40-Luc indicates that HCMV infection is predominantly dependent on the gH/gL/gO complex.

4.4.2 The infection capacity of HCMV correlates with the abundance of PDGFRα in host cells

It has been shown that the binding capacity of HCMV virions for fibroblasts is much higher than for other cell types tested [40, 41]. Combined with the observation that fibroblasts show abundant PDGFRα level in contrast to epithelial cells and EC. This indicates a correlation between the infection capacity of HCMV and the abundance of PDGFRα in host cells. In this study, gO was found to directly interact with PDGFRα. Additionally, recombinant gO-Fc protein bound much better to fibroblasts than to EC which correlates with the PDGFRα level of these cells. Overexpression of PDGFRα in different cell types (including epithelial cells) promoted entry of both wildtype HCMV and HCMV lacking the pentameric complex [72, 74]. In line with that, infection of 293 cells transfected with a vector expressing PDGFRα showed an enhanced entry of gO-positive HCMV when compared to non-transfected 293 cells, supporting that enhancment of HCMV infection is gH/gL/gO-dependent and correlates with the abundance of cellular PDGFRα. It has been shown in cells transfected with vectors expreeing gB and gH/gL that overexpression of PDGFRα did not enhance gB, gH/gL-induced cell-cell fusion [74], indicating that PDGFRα-enhanced entry was not dependent on gB or gH/gL dimer. All these data support PDGFRα as a bona fide entry receptor for the HCMV gH/gL/gO complex.

4.4.3 The gH/gL/gO complex shapes HCMV entry in cell culture

Previous reports revealed that HCMV spread in EC cultures exhibits a cell-associated focal pattern and is gH/gL/pUL(128, 130, 131a)-dependent, while spread in fibroblast cultures is homogeneous and driven by supernatant virus [122]. Interestingly, the spread pattern of gO-null virus in fibroblast cultures was strictly cell associated and produced only small plaques [106, 122]. This suggests supernatant-driven spread in fibroblast cultures is driven

by gH/gL/gO complex. In this study, infection of cells with preincubation of virus particles with recombinant PDGFRα completely blocked virus expressing only the gH/gL/gO complex, whereas preincubation of virus expressing both gH/gL complexes could not be blocked completely. In addition, incubation of PDGFRα protein with HCMV infected cells restricted virus spread in fibroblasts and produced smaller plaques, whereas the same treatment had no effect on virus spread in EC which is driven by the gH/gL/pUL(128, 130, 131a) complex. This spread pattern of HCMV in fibroblast culture was similar to spread of gO-null virus. Specifically, an antibody against the pentameric complex halted virus spread in EC but had no effect on virus spread in fibroblasts which express abundant PDGFRα. Coupled with previous data, it can be concluded that HCMV infection of cells with free virus is mainly driven by the gH/gL/gO complex, provided the cells abundantly express PDGFRα on their surface. Virus spread in EC cultures neither depends on PDGFRα nor on the gH/gL/gO complex, but depends on the gH/gL/pUL(128, 130, 131a) complex.

In summary, the relative abundances of viral gH/gL/gO and cellular PDGFRα shape the cell tropism of HCMV. For instance, for HCMV particles with high levels of gH/gL/gO, the PDGFRα level of target cells will be the major determinant for cell tropism. The gH/gL/pUL(128, 130, 131a) complex determines HCMV entry into cells which scarcely express PDGFRα.

This should be taken into account when characterizing the HCMV cell tropism in cell culture. Cell culture conditions [200, 201] and transforming antigens [199] may alter the cellular expression level of PDGFRα and thus affect the infection capacities of HCMV for these cells. For example, expression of PDGFRα could be downregulated by suramin treatment or 3D-culture and upregulated by interleukin-1 β [200, 201]. In addition, expression of oncogenic alleles like simian virus 40 T antigen in human cells reduced the abundance of PDGFRα and thus inhibited HCMV infection [199]. Thus, due to the complexity and dynamic tendency, it is difficult to predict the HCMV *in vivo* tropism from cell culture studies.

4.5 PDGFRα-dependent entry ans PDGFRα activation

Virus entry can trigger receptor-mediated signaling in host cells. For HCMV, activation of the PI3K and MAPK signaling pathway has been reported in a number of different cell types

including fibroblasts [71, 139], monocytes [202, 204] and EC [203]. It has been reported that gH/gL/pUL(128, 130, 131a) is required for activation of the integrin/Src/paxillin pathway required for entering monocytes [204]. HCMV gB and gH are both considered to be involved in signaling pathways by binding cell surface integrins and EGFR [139, 204, 205].
A prerequisite for activation of PDGFRα is homodimerization or heterodimerization with PDGFRβ [206]. Phosphorylation of PDGFRα by HCMV has been detected upon HCMV infection by using an antibody that recognizes the heterodimeric PDGFRα/β complex [72, 207]. By using the tyrosine kinase inhibitor imatinib mesylate, phosphorylation of PDGFRα by HCMV in human embryonic lung fibroblasts (HELs) was inhibited [72]. Another study demonstrated that imatinib mesylate inhibited not only HCMV but also HSV-1, suggesting a non-specific role in inhibiting on herpesvirus infection [74]. Here, HCMV infection of HFF could only be slightly inhibited with imatinib mesylate. In summary, one study showed that imatinib mesylate was able to block phosphorylation of PDGFRα but it was not tested whether imatinib mesylate could also block HCMV infection [72], whereas the other study showed that HCMV infection of ARPE-19 cells could be inhibited by imatinib mesylate [74]. Thus, the observed discrepancy might due to cell type-specific PDGFRα-activation patterns.

4.6 HCMV infection and its association with glioblastoma or coronary heart disease

HCMV has been proposed to play a role in the pathogenesis of glioblastoma more than a decade ago. Based on the observation that viral proteins and nucleic acids of HCMV have been occasionally detected in tumor cells [208], a debate has been started whether HCMV could serve as a therapeutic target for treatment of glioblastoma. It has also been claimed that HCMV infection results in the formation of atherosclerosis as several HCMV proteins or DNA could be detected in various cells of atherosclerotic vessel walls [209]. Both the atherosclerotic lesions and the glioblastoma express high levels of PDGFRα, suggesting that they might rather serve as good targets for HCMV infection than being caused by HCMV. Supporting this, a recent clinical trial using valganciclovir as an adjuvant therapy for glioblastoma failed to prove a beneficial effect on either tumor growth or overall survival [210]. Thus, the correlation between HCMV and atherosclerosis and glioblastoma may just reflect a PDGFRα-driven susceptibility to HCMV infection.

4.7 The gH/gL/gO-PDGFRα complex

As PDGFRα is used by different strains of HCMV for entry [72, 74, 199], the binding site of gO very likely is within the most conserved region of gO, aa 100 to aa 270 [102]. One can imagine several options how the gH/gL/gO complex binds to PDGFRα: i) PDGFRα possesses 5 immunoglobulin-like (IgG-like) repeats in its extracellular domain [211] and PDGFs bind to the second IgG-like region of PDGFRα [211]. It has been reported that the PDGFRα ligand PDGF-AA competes with HCMV and causes significant inhibition of HCMV entry into fibroblasts [72]. Accordingly, in this thesis, the PDGFRα ligand PDGF-BB was found to be able to interfere with HCMV entry into fibroblasts. These data suggest that the gO binding site on PDGFRα could be within or overlap with the second IgG-like region of PDGFRα. ii) Another potential mechanism of the ligand-dependent block might be that the ligand-induced dimerization of PDGFRα interferes with the binding of gH/gL/gO. In other words, gH/gL/gO might only bind PDGFRα in a monomeric form.

4.8 A model for gH/gL/gO-dependent entry of HCMV

It has previously been shown that HCMV infection of fibroblasts depends on the gH/gL/gO complex and that fibroblasts possess a receptor for gH/gL/gO [68]. Here, it could be demonstrated that fibroblasts abundantly express PDGFRα which is recoginized by gH/gL/gO, and are therefore a dominant target for HCMV. Current data indicate that HCMV gB acts as a fusion trigger which is required for entry into all cell types [50] rather than a receptor-binding protein [75]. It has been reported that gB is able to bind integrins and induce subsequent integrin signaling which has a crosstalk with PDGF signaling [70, 139, 141]. This could at least partially explain the observed activation of cellular signaling pathways upon HCMV infection. In addition, gB can bind gH during entry [97]. Collectively, this supports a model of HCMV entry initiated by an interaction of PDGFRα and gH/gL/gO (Figure 38). HCMV gH/gL/gO interacts with PDGFRα on the cell surface upon virion attachment, which may or may not induce the phosphorylation of PDGFRα. A subsequent conformational change of the gB-gH/gL/gO complex moves gB closer to the host cell membrane. There, gB induces direct fusion of virion membrane with the plasma membrane (Figure 38).

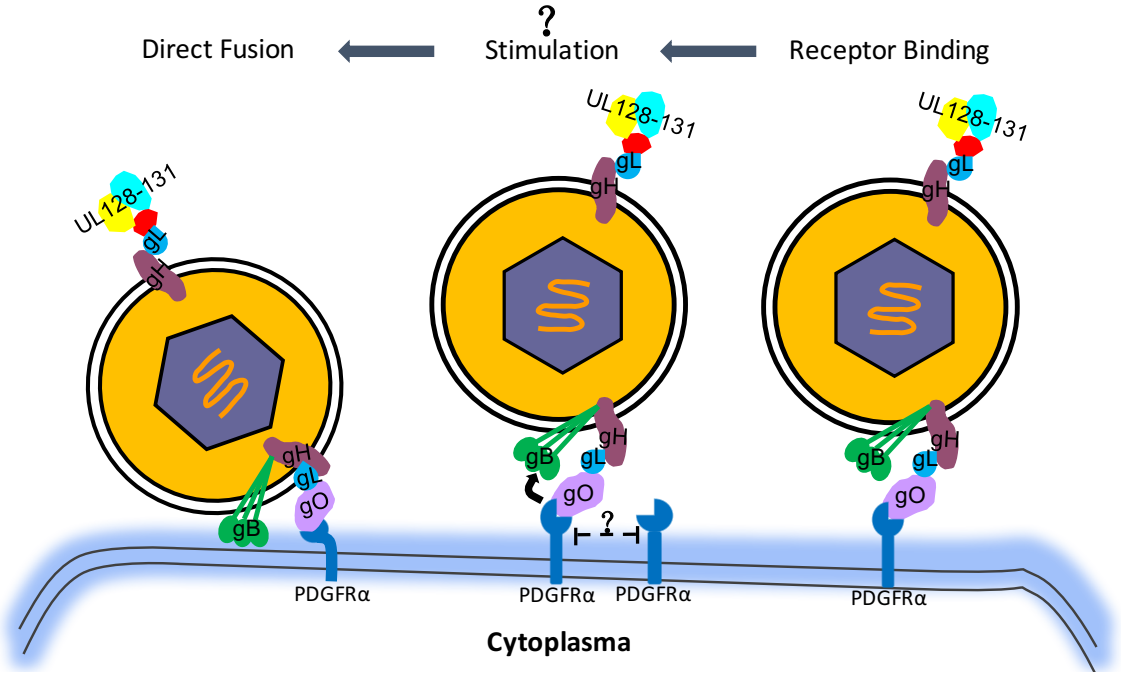

Figure 38: Model of PDGFRα-mediated HCMV entry with cell free virus.
gH/gL/gO binds to PDGFRα upon attachment of virions to the cell surface. Depending on the cell type, this interaction may cause phosphorylation and dimerization of PDGFRα. The gH/gL/gO-PDGFRα interaction then induces a conformational change of the the gB-gH/gL/gO complex and moves gB closer to the cell membrane, which subsequently induces direct fusion between virus envelope and the plasma membrane.

4.9 MCMV as a model to study the gH/gL/gO complex

MCMV serves as a model for HCMV and its infection resembles in many aspects of HCMV infection, including cell and organ tropism, pathogenesis during acute infection, establishment of latency, and reactivation after immunosuppression [152, 212, 213]. MCMV also forms two gH/gL complexes, gH/gL/m74 which is functionally homologous to HCMV gH/gL/gO, and gH/gL/MCK2 [165, 166].

4.9.1 Infection properties of MCMV gO-null mutants

Previous studies revealed that m74 knockout mutants of MCMV exhibit spread patterns in cell culture which are comparable to spread patterns of gO knockout mutants of HCMV [122]. When comparing the infection capacities of m74-null virus on different cell types in cell culture, deletion of m74 reduced virus entry into fibroblasts and showed a relative enhancement of entry into EC [109], infection properties which gO-null mutants of HCMV also exhibit [122]. Yet, m74-null MCMV showed a pronounced reduction of entry into

epithelial cells [109], whereas gO-null HCMV exhibited an enhancement of entry into epithelial cells. These distinct infection properties of HCMV and MCMV in cell culture might rather be cell line-specific or dependent on culture conditions rather than being cell type-specific.

4.9.2 Infection capacities of MCMV progenies derived from different cell types

Here, it was described that MCMV progenies from two types of fibroblasts, MEF and NIH3T3, had different infection capacities for different cell types. NIH3T3-derived virus showed a relatively higher capacity to infect EC and macrophages than MEF-derived virus. Analysis of different MCMV progenies from MEF, NIH3T3, TCMK-1 and MHEC-5T also emphasized that NIH3T3-derived progenies infect EC more efficiently than MCMV progenies from other cell types. Cell-type specific differences of virus progenies have also been found for HCMV. They have been shown to correlate with the relative ratios of the gH/gLgO and gH/gL/pUL(128, 130, 131a) complexes in virions [122]. These ratios are determined by the cell type in which the virus is propagated and they affect the pattern of HCMV tropism [122]. The mechanism for MCMV may be similar and the relative abundances of the MCMV gH/gL complexes in virions may also determine the cell tropism of MCMV (Figure 39).

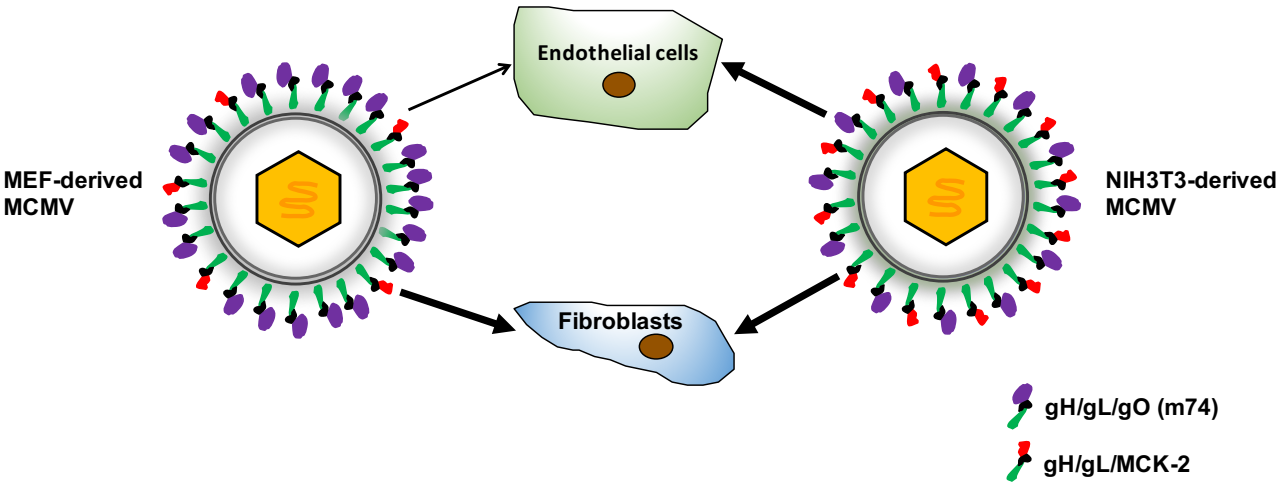

Figure 39: Cell tropism for MEF- or NIH-produced MCMV.
This model proposes that MEF-derived (left) and NIH3T3-derived (right) MCMV contain different amounts of gH/gL/m74 and gH/gL/MCK-2 complexes, thus, show different infection capacities for different cell types. The strength of arrows represent the infection capacity.

4.9.3 How could the model be verified?

MCMV encodes m74 and MCK-2 which are incorporated into different gH/gL complexes and serve as functional homologues to HCMV gH/gL/gO [165] and gH/gL/pUL(128, 130, 131a), respectively [166]. Both the gH/gL/m74 and gH/gL/MCK-2 complexes function as MCMV entry mediators, and changes in the relative ratios of the two complexes in virions may affect the infection properties. To verify the above model, antibodies recognizing m74 and MCK-2 are required to evaluate the abundancies of the MCMV gH/gL complexes in virions released from different cells. However, currently no m74-specific antibody is available. The next step would be to generate an anti-m74 antibody which will include cloning and expression of m74, and immunization of rabbits or mice. If differences are found or verified, this would support MCMV as a good model to study role of HCMV gH/gL complexes.

4.10 Conclusion and perspectives

In this work, PDGFRα has been identified as a binding partner for the HCMV gH/gL/gO complex by looking for protein binding partner of HCMV virions on the cell surface of fibroblasts. The surface expression levels of PDGFRα very likely determine the HCMV entry pathway. When HCMV infects cells with high level of PDGFRα, such as fibroblasts, infection is mainly driven by gH/gL/gO, whereas infection of cells expressing low level of PDGFRα, such as epithelial cells and EC, is mainly driven by gH/gL/pUL(128, 130, 131a). gH/gL/gO promotes entry of free virus through a PDGFRα-dependent pathway and cell-associated virus spread through a PDGFRα-independent pathway.

It has been shown that the gH/gL/m74 complex of MCMV determines virus entry into first target cells during primary MCMV infection of the mouse [109]. Transferred to HCMV infections in vivo, the gH/gL/gO-PDGFRα interaction may thus also play a pivotal role in primary HCMV infection. The gH/gL/gO-PDGFRα interaction, may determine horizontal dissemination via free virus in body fluids like breast milk or urine. This renders the gH/gL/gO-PDGFRα interaction a potential target for HCMV vaccines, new therapeutic avenues and facilitate screening of small-molecule antagonists to block HCMV entry during primary infections. Molecules targeting gO may become an important new group of potential antivirals. A number of antibodies, peptides and small compounds have been

shown to bind to PDGFRα. Alternatively, soluble PDGFRα, or peptides derived from PDGFRα may interfere with viral spread in an infected individual. Mapping of the gH/gL/gO-PDGFRα interaction site would be very helpful in the design of future treatments of HCMV infection and disease.

5 References

1. Davison, A.J., Overview of classification, in Human Herpesviruses: Biology, Therapy, and Immunoprophylaxis, A. Arvin, et al., Editors. 2007: Cambridge.

2. Rowe, W.P., et al., Cytopathogenic agent resembling human salivary gland virus recovered from tissue cultures of human adenoids. Proc Soc Exp Biol Med, 1956. **92**(2): p. 418-24.

3. Smith, M.G., Propagation in tissue cultures of a cytopathogenic virus from human salivary gland virus (SGV) disease. Proc Soc Exp Biol Med, 1956. **92**(2): p. 424-30.

4. Craig, J.M., et al., Isolation of intranuclear inclusion producing agents from infants with illnesses resembling cytomegalic inclusion disease. Proc Soc Exp Biol Med, 1957. **94**(1): p. 4-12.

5. Cannon, M.J., D.S. Schmid, and T.B. Hyde, Review of cytomegalovirus seroprevalence and demographic characteristics associated with infection. Rev Med Virol, 2010. **20**(4): p. 202-13.

6. Pomeroy, C. and J.A. Englund, Cytomegalovirus: epidemiology and infection control. Am J Infect Control, 1987. **15**(3): p. 107-19.

7. Ljungman, P., Cytomegalovirus infections in transplant patients. Scand J Infect Dis Suppl, 1996. **100**: p. 59-63.

8. Hamprecht, K., R. Goelz, and J. Maschmann, Breast milk and cytomegalovirus infection in preterm infants. Early Hum Dev, 2005. **81**(12): p. 989-96.

9. Syggelou, A., et al., Congenital cytomegalovirus infection. Ann N Y Acad Sci, 2010. **1205**: p. 144-7.

10. Barami, K., Oncomodulatory mechanisms of human cytomegalovirus in gliomas. J Clin Neurosci, 2010. **17**(7): p. 819-23.

11. Cheng, J.L., et al., Cytomegalovirus Infection Causes an Increase of Arterial Blood Pressure. Plos Pathog, 2009. **5**(5).

12. Mercorelli, B., et al., Early inhibitors of human cytomegalovirus: state-of-art and therapeutic perspectives. Pharmacol Ther, 2011. **131**(3): p. 309-29.

13. Mocarski, E.S., Shenk, T., and Pass, R.E., *Cytomegaloviruses*. 5th ed. Fields Virology. 2007, Philadelphia: Lippincott Williamy & Wilkins. 2702-2757.

14. Salzberger, B., et al., Neutropenia in allogeneic marrow transplant recipients receiving ganciclovir for prevention of cytomegalovirus disease: risk factors and outcome. Blood, 1997. **90**(6): p. 2502-8.

15. Emery, V.C. and P.D. Griffiths, Prediction of cytomegalovirus load and resistance patterns after antiviral chemotherapy. Proc Natl Acad Sci U S A, 2000. **97**(14): p. 8039-44.

16. Schleiss, M.R., Cytomegalovirus vaccine development. Curr Top Microbiol Immunol, 2008. **325**: p. 361-82.

17. Murphy, E., et al., Coding potential of laboratory and clinical strains of human cytomegalovirus. Proc Natl Acad Sci U S A, 2003. **100**(25): p. 14976-81.

18. Davison, A.J., Comparative analysis of the genomes, in Human Herpesviruses: Biology, Therapy, and Immunoprophylaxis, A. Arvin, et al., Editors. 2007: Cambridge.

19. Varnum, S.M., et al., Identification of proteins in human cytomegalovirus (HCMV) particles: the HCMV proteome. J Virol, 2004. **78**(20): p. 10960-6.

20. Smith, J.D. and E. de Harven, Herpes simplex virus and human cytomegalovirus replication in WI-38 cells. II. An ultrastructural study of viral penetration. J Virol, 1974. **14**(4): p. 945-56.

21. Compton, T., R.R. Nepomuceno, and D.M. Nowlin, Human cytomegalovirus penetrates host

cells by pH-independent fusion at the cell surface. Virology, 1992. **191**(1): p. 387-95.

22. Ryckman, B.J., et al., Human cytomegalovirus entry into epithelial and endothelial cells depends on genes UL128 to UL150 and occurs by endocytosis and low-pH fusion. J Virol, 2006. **80**(2): p. 710-22.

23. Ogawa-Goto, K., et al., Microtubule network facilitates nuclear targeting of human cytomegalovirus capsid. J Virol, 2003. **77**(15): p. 8541-7.

24. Dohner, K., C.H. Nagel, and B. Sodeik, Viral stop-and-go along microtubules: taking a ride with dynein and kinesins. Trends Microbiol, 2005. **13**(7): p. 320-7.

25. Stinski, M.F., Sequence of protein synthesis in cells infected by human cytomegalovirus: early and late virus-induced polypeptides. J Virol, 1978. **26**(3): p. 686-701.

26. Gibson, W., Structure and assembly of the virion. Intervirology, 1996. **39**(5-6): p. 389-400.

27. Sanchez, V., et al., Accumulation of virion tegument and envelope proteins in a stable cytoplasmic compartment during human cytomegalovirus replication: characterization of a potential site of virus assembly. J Virol, 2000. **74**(2): p. 975-86.

28. Sanchez, V., E. Sztul, and W.J. Britt, Human cytomegalovirus pp28 (UL99) localizes to a cytoplasmic compartment which overlaps the endoplasmic reticulum-golgi-intermediate compartment. J Virol, 2000. **74**(8): p. 3842-51.

29. Craighead, J.E., R.E. Kanich, and J.D. Almeida, Nonviral microbodies with viral antigenicity produced in cytomegalovirus-infected cells. J Virol, 1972. **10**(4): p. 766-75.

30. Jean Beltran, P.M. and I.M. Cristea, The life cycle and pathogenesis of human cytomegalovirus infection: lessons from proteomics. Expert Rev Proteomics, 2014. **11**(6): p. 697-711.

31. Sinzger, C. and G. Jahn, Human cytomegalovirus cell tropism and pathogenesis. Intervirology, 1996. **39**(5-6): p. 302-19.

32. Wiley, C.A. and J.A. Nelson, Role of human immunodeficiency virus and cytomegalovirus in AIDS encephalitis. Am J Pathol, 1988. **133**(1): p. 73-81.

33. Sinzger, C., et al., Fibroblasts, epithelial cells, endothelial cells and smooth muscle cells are major targets of human cytomegalovirus infection in lung and gastrointestinal tissues. J Gen Virol, 1995. **76 (Pt 4)**: p. 741-50.

34. Sinzger, C., et al., Hepatocytes are permissive for human cytomegalovirus infection in human liver cell culture and In vivo. J Infect Dis, 1999. **180**(4): p. 976-86.

35. Gerna, G., et al., Human cytomegalovirus infection of the major leukocyte subpopulations and evidence for initial viral replication in polymorphonuclear leukocytes from viremic patients. J Infect Dis, 1992. **166**(6): p. 1236-44.

36. Ibanez, C.E., et al., Human cytomegalovirus productively infects primary differentiated macrophages. J Virol, 1991. **65**(12): p. 6581-8.

37. Percivalle, E., et al., Circulating endothelial giant cells permissive for human cytomegalovirus (HCMV) are detected in disseminated HCMV infections with organ involvement. J Clin Invest, 1993. **92**(2): p. 663-70.

38. Revello, M.G. and G. Gerna, Human cytomegalovirus tropism for endothelial/epithelial cells: scientific background and clinical implications. Rev Med Virol, 2010. **20**(3): p. 136-55.

39. Sinclair, J. and P. Sissons, Latency and reactivation of human cytomegalovirus. J Gen Virol, 2006. **87**(Pt 7): p. 1763-79.

40. Taylor, H.P. and N.R. Cooper, Human cytomegalovirus binding to fibroblasts is receptor

mediated. J Virol, 1989. **63**(9): p. 3991-8.

41. Shanley, J.D., D. Biegel, and J.S. Pachter, A rapid and sensitive radioimmunoassay for the detection of human cytomegalovirus binding and infection of human fibroblasts. J Virol Methods, 1996. **58**(1-2): p. 121-9.

42. Neyts, J., et al., Sulfated polymers inhibit the interaction of human cytomegalovirus with cell surface heparan sulfate. Virology, 1992. **189**(1): p. 48-58.

43. Compton, T., D.M. Nowlin, and N.R. Cooper, Initiation of human cytomegalovirus infection requires initial interaction with cell surface heparan sulfate. Virology, 1993. **193**(2): p. 834-41.

44. Kari, B. and R. Gehrz, Structure, composition and heparin binding properties of a human cytomegalovirus glycoprotein complex designated gC-II. J Gen Virol, 1993. **74 (Pt 2)**: p. 255-64.

45. Connolly, S.A., et al., Fusing structure and function: a structural view of the herpesvirus entry machinery. Nat Rev Microbiol, 2011. **9**(5): p. 369-81.

46. Hetzenecker, S., A. Helenius, and M.A. Krzyzaniak, HCMV Induces Macropinocytosis for Host Cell Entry in Fibroblasts. Traffic, 2016. **17**(4): p. 351-68.

47. Bodaghi, B., et al., Entry of human cytomegalovirus into retinal pigment epithelial and endothelial cells by endocytosis. Invest Ophthalmol Vis Sci, 1999. **40**(11): p. 2598-607.

48. Sinzger, C., Entry route of HCMV into endothelial cells. J Clin Virol, 2008. **41**(3): p. 174-9.

49. Tiwari, V. and D. Shukla, Nonprofessional phagocytosis can facilitate herpesvirus entry into ocular cells. Clin Dev Immunol, 2012. **2012**: p. 651691.

50. Vanarsdall, A.L. and D.C. Johnson, *Human cytomegalovirus entry into cells.* Curr Opin Virol, 2012. **2**(1): p. 37-42.

51. Haspot, F., et al., Human cytomegalovirus entry into dendritic cells occurs via a macropinocytosis-like pathway in a pH-independent and cholesterol-dependent manner. PLoS One, 2012. **7**(4): p. e34795.

52. Campadelli-Fiume, G., et al., The multipartite system that mediates entry of herpes simplex virus into the cell. Rev Med Virol, 2007. **17**(5): p. 313-26.

53. Wang, X., et al., Epstein-Barr virus uses different complexes of glycoproteins gH and gL to infect B lymphocytes and epithelial cells. J Virol, 1998. **72**(7): p. 5552-8.

54. Britt, W.J. and M. Mach, Human cytomegalovirus glycoproteins. Intervirology, 1996. **39**(5-6): p. 401-12.

55. Britt, W.J., Neutralizing antibodies detect a disulfide-linked glycoprotein complex within the envelope of human cytomegalovirus. Virology, 1984. **135**(2): p. 369-78.

56. Britt, W.J. and D. Auger, Synthesis and processing of the envelope gp55-116 complex of human cytomegalovirus. J Virol, 1986. **58**(1): p. 185-91.

57. Britt, W.J. and L.G. Vugler, Processing of the gp55-116 envelope glycoprotein complex (gB) of human cytomegalovirus. J Virol, 1989. **63**(1): p. 403-10.

58. Meyer, H., Y. Masuho, and M. Mach, The gp116 of the gp58/116 complex of human cytomegalovirus represents the amino-terminal part of the precursor molecule and contains a neutralizing epitope. J Gen Virol, 1990. **71** (10): p. 2443-50.

59. Spaete, R.R., et al., Sequence requirements for proteolytic processing of glycoprotein B of human cytomegalovirus strain Towne. J Virol, 1990. **64**(6): p. 2922-31.

60. Eickmann, M., et al., Effect of cysteine substitutions on dimerization and interfragment linkage of human cytomegalovirus glycoprotein B (gp UL55). Arch Virol, 1998. **143**(10): p. 1865-80.

61. Lopper, M. and T. Compton, Disulfide bond configuration of human cytomegalovirus glycoprotein B. J Virol, 2002. **76**(12): p. 6073-82.

62. Britt, W.J., et al., Antigenic domain 1 is required for oligomerization of human cytomegalovirus glycoprotein B. J Virol, 2005. **79**(7): p. 4066-79.

63. Potzsch, S., et al., B cell repertoire analysis identifies new antigenic domains on glycoprotein B of human cytomegalovirus which are target of neutralizing antibodies. PLoS Pathog, 2011. **7**(8): p. e1002172.

64. Burke, H.G. and E.E. Heldwein, Correction: Crystal Structure of the Human Cytomegalovirus Glycoprotein B. PLoS Pathog, 2015. **11**(11): p. e1005300.

65. Burke, H.G. and E.E. Heldwein, Crystal Structure of the Human Cytomegalovirus Glycoprotein B. PLoS Pathog, 2015. **11**(10): p. e1005227.

66. Compton, T., Receptors and immune sensors: the complex entry path of human cytomegalovirus. Trends Cell Biol, 2004. **14**(1): p. 5-8.

67. Vanarsdall, A.L., et al., Human cytomegalovirus glycoproteins gB and gH/gL mediate epithelial cell-cell fusion when expressed either in cis or in trans. J Virol, 2008. **82**(23): p. 11837-50.

68. Vanarsdall, A.L., M.C. Chase, and D.C. Johnson, Human cytomegalovirus glycoprotein gO complexes with gH/gL, promoting interference with viral entry into human fibroblasts but not entry into epithelial cells. J Virol, 2011. **85**(22): p. 11638-45.

69. Feire, A.L., H. Koss, and T. Compton, Cellular integrins function as entry receptors for human cytomegalovirus via a highly conserved disintegrin-like domain. Proc Natl Acad Sci U S A, 2004. **101**(43): p. 15470-5.

70. Feire, A.L., et al., The glycoprotein B disintegrin-like domain binds beta 1 integrin to mediate cytomegalovirus entry. J Virol, 2010. **84**(19): p. 10026-37.

71. Wang, X., et al., Epidermal growth factor receptor is a cellular receptor for human cytomegalovirus. Nature, 2003. **424**(6947): p. 456-61.

72. Soroceanu, L., A. Akhavan, and C.S. Cobbs, Platelet-derived growth factor-alpha receptor activation is required for human cytomegalovirus infection. Nature, 2008. **455**(7211): p. 391-5.

73. Isaacson, M.K., A.L. Feire, and T. Compton, Epidermal growth factor receptor is not required for human cytomegalovirus entry or signaling. J Virol, 2007. **81**(12): p. 6241-7.

74. Vanarsdall, A.L., et al., PDGF receptor-alpha does not promote HCMV entry into epithelial and endothelial cells but increased quantities stimulate entry by an abnormal pathway. PLoS Pathog, 2012. **8**(9): p. e1002905.

75. Wille, P.T., et al., Human cytomegalovirus (HCMV) glycoprotein gB promotes virus entry in trans acting as the viral fusion protein rather than as a receptor-binding protein. MBio, 2013. **4**(3): p. e00332-13.

76. Lehner, R., H. Meyer, and M. Mach, Identification and characterization of a human cytomegalovirus gene coding for a membrane protein that is conserved among human herpesviruses. J Virol, 1989. **63**(9): p. 3792-800.

77. Mach, M., et al., Complex formation by human cytomegalovirus glycoproteins M (gpUL100) and N (gpUL73). J Virol, 2000. **74**(24): p. 11881-92.

78. Pignatelli, S., et al., Human cytomegalovirus glycoprotein N (gpUL73-gN) genomic variants: identification of a novel subgroup, geographical distribution and evidence of positive selective pressure. J Gen Virol, 2003. **84**(Pt 3): p. 647-55.

79. Krzyzaniak, M., M. Mach, and W.J. Britt, The cytoplasmic tail of glycoprotein M (gpUL100)

expresses trafficking signals required for human cytomegalovirus assembly and replication. J Virol, 2007. **81**(19): p. 10316-28.

80. Mach, M., et al., The carboxy-terminal domain of glycoprotein N of human cytomegalovirus is required for virion morphogenesis. J Virol, 2007. **81**(10): p. 5212-24.

81. Mach, M., et al., Complex formation by glycoproteins M and N of human cytomegalovirus: structural and functional aspects. J Virol, 2005. **79**(4): p. 2160-70.

82. Kari, B. and R. Gehrz, A human cytomegalovirus glycoprotein complex designated gC-II is a major heparin-binding component of the envelope. J Virol, 1992. **66**(3): p. 1761-4.

83. Gretch, D.R., R.C. Gehrz, and M.F. Stinski, Characterization of a human cytomegalovirus glycoprotein complex (gcI). J Gen Virol, 1988. **69** (6): p. 1205-15.

84. Pachl, C., et al., The human cytomegalovirus strain Towne glycoprotein H gene encodes glycoprotein p86. Virology, 1989. **169**(2): p. 418-26.

85. Hutchinson, L., et al., A novel herpes simplex virus glycoprotein, gL, forms a complex with glycoprotein H (gH) and affects normal folding and surface expression of gH. J Virol, 1992. **66**(4): p. 2240-50.

86. Kaye, J.F., U.A. Gompels, and A.C. Minson, Glycoprotein H of human cytomegalovirus (HCMV) forms a stable complex with the HCMV UL115 gene product. J Gen Virol, 1992. **73** (10): p. 2693-8.

87. Spaete, R.R., et al., Coexpression of truncated human cytomegalovirus gH with the UL115 gene product or the truncated human fibroblast growth factor receptor results in transport of gH to the cell surface. Virology, 1993. **193**(2): p. 853-61.

88. Milne, R.S., D.A. Paterson, and J.C. Booth, Human cytomegalovirus glycoprotein H/glycoprotein L complex modulates fusion-from-without. J Gen Virol, 1998. **79**(4): p. 855-65.

89. Huber, M.T. and T. Compton, Intracellular formation and processing of the heterotrimeric gH-gL-gO (gCIII) glycoprotein envelope complex of human cytomegalovirus. J Virol, 1999. **73**(5): p. 3886-92.

90. Stampfer, S.D. and E.E. Heldwein, Stuck in the middle: structural insights into the role of the gH/gL heterodimer in herpesvirus entry. Curr Opin Virol, 2013. **3**(1): p. 13-9.

91. Li, L., J.A. Nelson, and W.J. Britt, Glycoprotein H-related complexes of human cytomegalovirus: identification of a third protein in the gCIII complex. J Virol, 1997. **71**(4): p. 3090-7.

92. Huber, M.T. and T. Compton, The human cytomegalovirus UL74 gene encodes the third component of the glycoprotein H-glycoprotein L-containing envelope complex. J Virol, 1998. **72**(10): p. 8191-7.

93. Wang, D. and T. Shenk, Human cytomegalovirus virion protein complex required for epithelial and endothelial cell tropism. Proc Natl Acad Sci U S A, 2005. **102**(50): p. 18153-8.

94. Adler, B., et al., Role of human cytomegalovirus UL131A in cell type-specific virus entry and release. J Gen Virol, 2006. **87**(Pt 9): p. 2451-60.

95. Paterson, D.A., et al., A role for human cytomegalovirus glycoprotein O (gO) in cell fusion and a new hypervariable locus. Virology, 2002. **293**(2): p. 281-94.

96. Kinzler, E.R. and T. Compton, Characterization of human cytomegalovirus glycoprotein-induced cell-cell fusion. J Virol, 2005. **79**(12): p. 7827-37.

97. Patrone, M., et al., Cytomegalovirus UL131-128 products promote gB conformational transition and gB-gH interaction during entry into endothelial cells. J Virol, 2007. **81**(20): p. 11479-88.

98. Heldwein, E.E., gH/gL supercomplexes at early stages of herpesvirus entry. Curr Opin Virol, 2016. **18**: p. 1-8.

99. Ciferri, C., et al., Structural and biochemical studies of HCMV gH/gL/gO and Pentamer reveal mutually exclusive cell entry complexes. Proc Natl Acad Sci U S A, 2015. **112**(6): p. 1767-72.

100. Chee, M.S., et al., Analysis of the protein-coding content of the sequence of human cytomegalovirus strain AD169. Curr Top Microbiol Immunol, 1990. **154**: p. 125-69.

101. Kinzler, E.R., R.N. Theiler, and T. Compton, Expression and reconstitution of the gH/gL/gO complex of human cytomegalovirus. J Clin Virol, 2002. **25 Suppl 2**: p. S87-95.

102. Zhou, M., et al., Comparative analysis of gO isoforms reveals that strains of human cytomegalovirus differ in the ratio of gH/gL/gO and gH/gL/UL128-131 in the virion envelope. J Virol, 2013. **87**(17): p. 9680-90.

103. Hobom, U., et al., Fast screening procedures for random transposon libraries of cloned herpesvirus genomes: mutational analysis of human cytomegalovirus envelope glycoprotein genes. J Virol, 2000. **74**(17): p. 7720-9.

104. Zhou, M., J.M. Lanchy, and B.J. Ryckman, Human Cytomegalovirus gH/gL/gO Promotes the Fusion Step of Entry into All Cell Types, whereas gH/gL/UL128-131 Broadens Virus Tropism through a Distinct Mechanism. J Virol, 2015. **89**(17): p. 8999-9009.

105. Dunn, W., et al., Functional profiling of a human cytomegalovirus genome. Proc Natl Acad Sci U S A, 2003. **100**(24): p. 14223-8.

106. Jiang, X.J., et al., UL74 of human cytomegalovirus contributes to virus release by promoting secondary envelopment of virions. J Virol, 2008. **82**(6): p. 2802-12.

107. Wille, P.T., et al., A human cytomegalovirus gO-null mutant fails to incorporate gH/gL into the virion envelope and is unable to enter fibroblasts and epithelial and endothelial cells. J Virol, 2010. **84**(5): p. 2585-96.

108. Li, G. and J.P. Kamil, Viral Regulation of Cell Tropism in Human Cytomegalovirus. J Virol, 2015. **90**(2): p. 626-9.

109. Lemmermann, N.A., et al., Non-redundant and redundant roles of cytomegalovirus gH/gL complexes in host organ entry and intra-tissue spread. PLoS Pathog, 2015. **11**(2): p. e1004640.

110. Rasmussen, L., et al., Characterization of two different human cytomegalovirus glycoproteins which are targets for virus neutralizing antibody. Virology, 1988. **163**(2): p. 308-18.

111. Akter, P., et al., Two novel spliced genes in human cytomegalovirus. J Gen Virol, 2003. **84**(5): p. 1117-22.

112. Grazia Revello, M., et al., In vitro selection of human cytomegalovirus variants unable to transfer virus and virus products from infected cells to polymorphonuclear leukocytes and to grow in endothelial cells. J Gen Virol, 2001. **82**(6): p. 1429-38.

113. Gerna, G., et al., Lack of transmission to polymorphonuclear leukocytes and human umbilical vein endothelial cells as a marker of attenuation of human cytomegalovirus. J Med Virol, 2002. **66**(3): p. 335-9.

114. Hahn, G., et al., Human cytomegalovirus UL131-128 genes are indispensable for virus growth in endothelial cells and virus transfer to leukocytes. J Virol, 2004. **78**(18): p. 10023-33.

115. Patrone, M., et al., Human cytomegalovirus UL130 protein promotes endothelial cell infection through a producer cell modification of the virion. J Virol, 2005. **79**(13): p. 8361-73.

116. Ryckman, B.J., et al., Characterization of the human cytomegalovirus gH/gL/UL128-131 complex that mediates entry into epithelial and endothelial cells. J Virol, 2008. **82**(1): p. 60-70.

117. Straschewski, S., et al., Protein pUL128 of human cytomegalovirus is necessary for monocyte infection and blocking of migration. J Virol, 2011. **85**(10): p. 5150-8.

118. Ryckman, B.J., M.C. Chase, and D.C. Johnson, HCMV gH/gL/UL128-131 interferes with virus entry into epithelial cells: evidence for cell type-specific receptors. Proc Natl Acad Sci U S A, 2008. **105**(37): p. 14118-23.

119. Loughney, J.W., et al., Soluble Human Cytomegalovirus gH/gL/pUL128-131 Pentameric Complex, but Not gH/gL, Inhibits Viral Entry to Epithelial Cells and Presents Dominant Native Neutralizing Epitopes. J Biol Chem, 2015. **290**(26): p. 15985-95.

120. Schultz, E.P., et al., Scanning Mutagenesis of Human Cytomegalovirus Glycoprotein gH/gL. J Virol, 2015. **90**(5): p. 2294-305.

121. Baldanti, F., et al., Human cytomegalovirus UL131A, UL130 and UL128 genes are highly conserved among field isolates. Arch Virol, 2006. **151**(6): p. 1225-33.

122. Scrivano, L., et al., HCMV spread and cell tropism are determined by distinct virus populations. PLoS Pathog, 2011. **7**(1): p. e1001256.

123. Li, G., et al., A viral regulator of glycoprotein complexes contributes to human cytomegalovirus cell tropism. Proc Natl Acad Sci U S A, 2015. **112**(14): p. 4471-6.

124. McKeating, J.A., et al., Detection of cytomegalovirus by ELISA in urine samples is inhibited by beta 2 microglobulin. J Med Virol, 1986. **18**(4): p. 341-8.

125. McKeating, J.A., P.D. Griffiths, and J.E. Grundy, Cytomegalovirus in urine specimens has host beta 2 microglobulin bound to the viral envelope: a mechanism of evading the host immune response? J Gen Virol, 1987. **68**(3): p. 785-92.

126. Beersma, M.F., et al., Expression of HLA class I heavy chains and beta 2-microglobulin does not affect human cytomegalovirus infectivity. J Gen Virol, 1991. **72**(11): p. 2757-64.

127. Polic, B., et al., Lack of MHC class I complex expression has no effect on spread and control of cytomegalovirus infection in vivo. J Gen Virol, 1996. **77**(2): p. 217-25.

128. Taylor, H.P. and N.R. Cooper, The human cytomegalovirus receptor on fibroblasts is a 30-kilodalton membrane protein. J Virol, 1990. **64**(6): p. 2484-90.

129. Nowlin, D.M., N.R. Cooper, and T. Compton, Expression of a human cytomegalovirus receptor correlates with infectibility of cells. J Virol, 1991. **65**(6): p. 3114-21.

130. Wright, J.F., et al., Host cellular annexin II is associated with cytomegalovirus particles isolated from cultured human fibroblasts. J Virol, 1995. **69**(8): p. 4784-91.

131. Pietropaolo, R.L. and T. Compton, Direct interaction between human cytomegalovirus glycoprotein B and cellular annexin II. J Virol, 1997. **71**(12): p. 9803-7.

132. Raynor, C.M., et al., Annexin II enhances cytomegalovirus binding and fusion to phospholipid membranes. Biochemistry, 1999. **38**(16): p. 5089-95.

133. Pietropaolo, R. and T. Compton, Interference with annexin II has no effect on entry of human cytomegalovirus into fibroblast cells. J Gen Virol, 1999. **80**(7): p. 1807-16.

134. Soderberg, C., et al., CD13 (human aminopeptidase N) mediates human cytomegalovirus infection. J Virol, 1993. **67**(11): p. 6576-85.

135. Soderberg, C., et al., Definition of a subset of human peripheral blood mononuclear cells that are permissive to human cytomegalovirus infection. J Virol, 1993. **67**(6): p. 3166-75.

136. Larsson, S., C. Soderberg-Naucler, and E. Moller, Productive cytomegalovirus (CMV) infection exclusively in CD13-positive peripheral blood mononuclear cells from CMV-infected individuals: implications for prevention of CMV transmission. Transplantation, 1998. **65**(3): p. 411-5.

137. Giugni, T.D., et al., Neutralization of human cytomegalovirus by human CD13-specific antibodies. J Infect Dis, 1996. **173**(5): p. 1062-71.

138. Li, Q., et al., THY-1 Cell Surface Antigen (CD90) Has an Important Role in the Initial Stage of Human Cytomegalovirus Infection. PLoS Pathog, 2015. **11**(7): p. e1004999.

139. Wang, X., et al., Integrin alphavbeta3 is a coreceptor for human cytomegalovirus. Nat Med, 2005. **11**(5): p. 515-21.

140. Chan, G., M.T. Nogalski, and A.D. Yurochko, Activation of EGFR on monocytes is required for human cytomegalovirus entry and mediates cellular motility. Proc Natl Acad Sci U S A, 2009. **106**(52): p. 22369-74.

141. Miyamoto, S., et al., Integrins can collaborate with growth factors for phosphorylation of receptor tyrosine kinases and MAP kinase activation: roles of integrin aggregation and occupancy of receptors. J Cell Biol, 1996. **135**(6 Pt 1): p. 1633-42.

142. Moro, L., et al., Integrins induce activation of EGF receptor: role in MAP kinase induction and adhesion-dependent cell survival. EMBO J, 1998. **17**(22): p. 6622-32.

143. Fioretti, A., et al., Nonproductive infection of guinea pig cells with human cytomegalovirus. J Virol, 1973. **11**(6): p. 998-1003.

144. Powers, C. and K. Fruh, Rhesus CMV: an emerging animal model for human CMV. Med Microbiol Immunol, 2008. **197**(2): p. 109-15.

145. Rawlinson, W.D., H.E. Farrell, and B.G. Barrell, Analysis of the complete DNA sequence of murine cytomegalovirus. J Virol, 1996. **70**(12): p. 8833-49.

146. Brocchieri, L., et al., Predicting coding potential from genome sequence: application to betaherpesviruses infecting rats and mice. J Virol, 2005. **79**(12): p. 7570-96.

147. Wagner, M., et al., Comparison between human cytomegalovirus pUL97 and murine cytomegalovirus (MCMV) pM97 expressed by MCMV and vaccinia virus: pM97 does not confer ganciclovir sensitivity. J Virol, 2000. **74**(22): p. 10729-36.

148. Schnee, M., et al., Common and specific properties of herpesvirus UL34/UL31 protein family members revealed by protein complementation assay. J Virol, 2006. **80**(23): p. 11658-66.

149. Brune, W., H. Hengel, and U.H. Koszinowski, *A mouse model for cytomegalovirus infection.* Curr Protoc Immunol, 2001. **Chapter 19**: Unit 19.7.

150. Hudson, J.B., The murine cytomegalovirus as a model for the study of viral pathogenesis and persistent infections. Arch Virol, 1979. **62**(1): p. 1-29.

151. Reddehase, M.J., et al., Interstitial murine cytomegalovirus pneumonia after irradiation: characterization of cells that limit viral replication during established infection of the lungs. J Virol, 1985. **55**(2): p. 264-73.

152. Krmpotic, A., et al., Pathogenesis of murine cytomegalovirus infection. Microbes Infect, 2003. **5**(13): p. 1263-77.

153. Mayo, D.R., J.A. Armstrong, and M. Ho, Reactivation of murine cytomegalovirus by cyclophosphamide. Nature, 1977. **267**(5613): p. 721-3.

154. Jordan, M.C., J.D. Shanley, and J.G. Stevens, Immunosuppression reactivates and disseminates latent murine cytomegalovirus. IARC Sci Publ, 1978(24 Pt 2): p. 769-74.

155. Shanley, J.D., et al., Pathogenesis of reactivated latent murine cytomegalovirus infection. Am J Pathol, 1979. **95**(1): p. 67-80.

156. Reddehase, M.J., et al., The conditions of primary infection define the load of latent viral genome in organs and the risk of recurrent cytomegalovirus disease. J Exp Med, 1994. **179**(1): p.

185-93.

157. Hamilton, J.D. and B.J. Seaworth, Transmission of latent cytomegalovirus in a murine kidney tissue transplantation model. Transplantation, 1985. **39**(3): p. 290-6.

158. Scalzo, A.A., et al., The interplay between host and viral factors in shaping the outcome of cytomegalovirus infection. Immunol Cell Biol, 2007. **85**(1): p. 46-54.

159. Kattenhorn, L.M., et al., Identification of proteins associated with murine cytomegalovirus virions. J Virol, 2004. **78**(20): p. 11187-97.

160. Keil, G.M., A. Ebeling-Keil, and U.H. Koszinowski, Sequence and structural organization of murine cytomegalovirus immediate-early gene 1. J Virol, 1987. **61**(6): p. 1901-8.

161. Buhler, B., et al., Characterization of the murine cytomegalovirus early transcription unit e1 that is induced by immediate-early proteins. J Virol, 1990. **64**(5): p. 1907-19.

162. Elliott, R., et al., Transcription analysis and sequence of the putative murine cytomegalovirus DNA polymerase gene. Virology, 1991. **185**(1): p. 169-86.

163. Loh, L.C., N. Balachandran, and L.F. Qualtiere, Characterization of a major virion envelope glycoprotein complex of murine cytomegalovirus and its immunological cross-reactivity with human cytomegalovirus. Virology, 1988. **166**(1): p. 206-16.

164. Rapp, M., et al., Identification of the murine cytomegalovirus glycoprotein B gene and its expression by recombinant vaccinia virus. J Virol, 1992. **66**(7): p. 4399-406.

165. Scrivano, L., et al., The m74 gene product of murine cytomegalovirus (MCMV) is a functional homolog of human CMV gO and determines the entry pathway of MCMV. J Virol, 2010. **84**(9): p. 4469-80.

166. Wagner, F.M., et al., The viral chemokine MCK-2 of murine cytomegalovirus promotes infection as part of a gH/gL/MCK-2 complex. PLoS Pathog, 2013. **9**(7): p. e1003493.

167. Fleming, P., et al., The murine cytomegalovirus chemokine homolog, m131/129, is a determinant of viral pathogenicity. J Virol, 1999. **73**(8): p. 6800-9.

168. MacDonald, M.R., et al., Spliced mRNA encoding the murine cytomegalovirus chemokine homolog predicts a beta chemokine of novel structure. J Virol, 1999. **73**(5): p. 3682-91.

169. Saederup, N., et al., Murine cytomegalovirus CC chemokine homolog MCK-2 (m131-129) is a determinant of dissemination that increases inflammation at initial sites of infection. J Virol, 2001. **75**(20): p. 9966-76.

170. Noda, S., et al., Cytomegalovirus MCK-2 controls mobilization and recruitment of myeloid progenitor cells to facilitate dissemination. Blood, 2006. **107**(1): p. 30-8.

171. Stahl, F.R., et al., Mck2-dependent infection of alveolar macrophages promotes replication of MCMV in nodular inflammatory foci of the neonatal lung. Mucosal Immunol, 2015. **8**(1): p. 57-67.

172. Vogel, F.S., Enhanced susceptibility of proliferating endothelium to salivary gland virus under naturally occurring and experimental conditions. Am J Pathol, 1958. **34**(6): p. 1069-79.

173. Klotman, M.E., et al., Detection of mouse cytomegalovirus nucleic acid in latently infected mice by in vitro enzymatic amplification. J Infect Dis, 1990. **161**(2): p. 220-5.

174. Collins, T., C. Pomeroy, and M.C. Jordan, Detection of latent cytomegalovirus DNA in diverse organs of mice. J Infect Dis, 1993. **168**(3): p. 725-9.

175. Kim, K.S. and R.I. Carp, Growth of murine cytomegalovirus in various cell lines. J Virol, 1971. **7**(6): p. 720-5.

176. Smee, D.F., et al., Evaluation of continuous cell lines in antiviral studies with murine

cytomegalovirus. Arch Virol, 1989. **107**(3-4): p. 253-60.

177. Grant, S.G., et al., Differential plasmid rescue from transgenic mouse DNAs into Escherichia coli methylation-restriction mutants. Proc Natl Acad Sci U S A, 1990. **87**(12): p. 4645-9.

178. Cox, G.W., et al., Heterogeneity of hematopoietic cells immortalized by v-myc/v-raf recombinant retrovirus infection of bone marrow or fetal liver. J Natl Cancer Inst, 1989. **81**(19): p. 1492-6.

179. Plendl, J., F. Sinowatz, and R. Auerbach, A transformed murine myocardial vascular endothelial cell clone: characterization of cells in vitro and of tumours derived from clone in situ. Virchows Arch, 1995. **426**(6): p. 619-28.

180. Venetsanakos, E., et al., Induction of tubulogenesis in telomerase-immortalized human microvascular endothelial cells by glioblastoma cells. Exp Cell Res, 2002. **273**(1): p. 21-33.

181. Sinzger, C., et al., Cloning and sequencing of a highly productive, endotheliotropic virus strain derived from human cytomegalovirus TB40/E. J Gen Virol, 2008. **89**(Pt 2): p. 359-68.

182. Smith, M.G., Propagation of salivary gland virus of the mouse in tissue cultures. Proc Soc Exp Biol Med, 1954. **86**(3): p. 435-40.

183. Messerle, M., et al., Cloning and mutagenesis of a herpesvirus genome as an infectious bacterial artificial chromosome. Proc Natl Acad Sci U S A, 1997. **94**(26): p. 14759-63.

184. Wagner, M., et al., Systematic excision of vector sequences from the BAC-cloned herpesvirus genome during virus reconstitution. J Virol, 1999. **73**(8): p. 7056-60.

185. Jordan, S., et al., Virus progeny of murine cytomegalovirus bacterial artificial chromosome pSM3fr show reduced growth in salivary Glands due to a fixed mutation of MCK-2. J Virol, 2011. **85**(19): p. 10346-53.

186. Reed, L.J.a.M., H., A simple method of estimating fifty per cent endpoints. Am J Epidemiol, 1938. **27**(3): p. 493-497.

187. Huber, M.T. and T. Compton, Characterization of a novel third member of the human cytomegalovirus glycoprotein H-glycoprotein L complex. J Virol, 1997. **71**(7): p. 5391-8.

188. Li, Q., et al., Epstein-Barr virus uses HLA class II as a cofactor for infection of B lymphocytes. J Virol, 1997. **71**(6): p. 4657-62.

189. Negrete, O.A., et al., EphrinB2 is the entry receptor for Nipah virus, an emergent deadly paramyxovirus. Nature, 2005. **436**(7049): p. 401-5.

190. Theiler, R.N. and T. Compton, Characterization of the signal peptide processing and membrane association of human cytomegalovirus glycoprotein O. J Biol Chem, 2001. **276**(42): p. 39226-31.

191. Vanarsdall, A.L., et al., Human Cytomegalovirus gH/gL Forms a Stable Complex with the Fusion Protein gB in Virions. PLoS Pathog, 2016. **12**(4): p. e1005564.

192. Fouts, A.E., et al., Mechanism for neutralizing activity by the anti-CMV gH/gL monoclonal antibody MSL-109. Proc Natl Acad Sci U S A, 2014. **111**(22): p. 8209-14.

193. Li, W., et al., Angiotensin-converting enzyme 2 is a functional receptor for the SARS coronavirus. Nature, 2003. **426**(6965): p. 450-4.

194. Bonaparte, M.I., et al., Ephrin-B2 ligand is a functional receptor for Hendra virus and Nipah virus. Proc Natl Acad Sci U S A, 2005. **102**(30): p. 10652-7.

195. Sprague, E.R., et al., The human cytomegalovirus Fc receptor gp68 binds the Fc CH2-CH3 interface of immunoglobulin G. J Virol, 2008. **82**(7): p. 3490-9.

196. Pandey, J.P., et al., The decoy Fcgamma receptor encoded by the cytomegalovirus UL119-UL118 gene has differential affinity to IgG proteins expressing different GM allotypes. Hum Immunol, 2015. **76**(8): p. 591-4.

197. Atalay, R., et al., Identification and expression of human cytomegalovirus transcription units coding for two distinct Fcgamma receptor homologs. J Virol, 2002. **76**(17): p. 8596-608.

198. Isaacson, M.K. and T. Compton, Human cytomegalovirus glycoprotein B is required for virus entry and cell-to-cell spread but not for virion attachment, assembly, or egress. J Virol, 2009. **83**(8): p. 3891-903.

199. Xu, S., X. Schafer, and J. Munger, Expression of Oncogenic Alleles Induces Multiple Blocks to Human Cytomegalovirus Infection. J Virol, 2016. **90**(9): p. 4346-56.

200. Marx, M., R.A. Perlmutter, and J.A. Madri, Modulation of platelet-derived growth factor receptor expression in microvascular endothelial cells during in vitro angiogenesis. J Clin Invest, 1994. **93**(1): p. 131-9.

201. Osornio-Vargas, A.R., et al., Maximal PDGF-induced lung fibroblast chemotaxis requires PDGF receptor-alpha. Am J Physiol, 1996. **271**(1 Pt 1): p. L93-9.

202. Smith, M.S., et al., HCMV activates PI(3)K in monocytes and promotes monocyte motility and transendothelial migration in a PI(3)K-dependent manner. J Leukoc Biol, 2004. **76**(1): p. 65-76.

203. Bentz, G.L. and A.D. Yurochko, Human CMV infection of endothelial cells induces an angiogenic response through viral binding to EGF receptor and beta1 and beta3 integrins. Proc Natl Acad Sci U S A, 2008. **105**(14): p. 5531-6.

204. Nogalski, M.T., et al., The HCMV gH/gL/UL128-131 complex triggers the specific cellular activation required for efficient viral internalization into target monocytes. PLoS Pathog, 2013. **9**(7): p. e1003463.

205. Nogalski, M.T., et al., Human cytomegalovirus-regulated paxillin in monocytes links cellular pathogenic motility to the process of viral entry. J Virol, 2011. **85**(3): p. 1360-9.

206. Li, W. and J. Schlessinger, Platelet-derived growth factor (PDGF)-induced disulfide-linked dimerization of PDGF receptor in living cells. Mol Cell Biol, 1991. **11**(7): p. 3756-61.

207. Kashishian, A., A. Kazlauskas, and J.A. Cooper, Phosphorylation sites in the PDGF receptor with different specificities for binding GAP and PI3 kinase in vivo. EMBO J, 1992. **11**(4): p. 1373-82.

208. Cobbs, C.S., Cytomegalovirus and brain tumor: epidemiology, biology and therapeutic aspects. Curr Opin Oncol, 2013. **25**(6): p. 682-8.

209. Popovic, M., et al., Human cytomegalovirus infection and atherothrombosis. J Thromb Thrombolysis, 2012. **33**(2): p. 160-72.

210. Stragliotto, G., et al., Effects of valganciclovir as an add-on therapy in patients with cytomegalovirus-positive glioblastoma: a randomized, double-blind, hypothesis-generating study. Int J Cancer, 2013. **133**(5): p. 1204-13.

211. Ullrich, A. and J. Schlessinger, Signal transduction by receptors with tyrosine kinase activity. Cell, 1990. **61**(2): p. 203-12.

212. Mocarski, E.S., Jr. and G.W. Kemble, Recombinant cytomegaloviruses for study of replication and pathogenesis. Intervirology, 1996. **39**(5-6): p. 320-30.

213. Reddehase, M.J., J. Podlech, and N.K. Grzimek, *Mouse models of cytomegalovirus latency: overview.* J Clin Virol, 2002. **25 Suppl 2**: p. S23-36.

6 Appendix

6.1 List of abbreviation

2-ME	2-mercaptoethanol
3D	three dimensional
aa	amino acids
AIDS	acquired immune-deficiency syndrome
APS	ammonium persulfate
BCA	bicinchoninic acid
BSA	bovine serum albumin
CCR	CC chemokine receptor
CD	cluster of differentiation
cDNA	complementary DNA
Co-IP	Co-immunoprecipitation
DMEM	Dulbecco's modified Eagle medium
DMSO	dimethyl sulfoxide
DNA	deoxyribonucleic acid
dNTP	deoxinucleosid-triphosphate
dpi	day(s) post infection
DTT	dithiothreitol
EC	endothelial cells
ECL	enhanced chemiluminescence
EDTA	ethylene diamine tetraacetic acid
e.g.	exempli gratia
EGFR	epidermal growth factor receptor
ELISA	enzyme-linked immunosorbent assay
et al.	et alii/alia
EtBr	ethidium bromide
FACS	fluorescence-activated cell sorter
FBS	fetal bovine serum
FDA	U S Food and Drug Administration
FITC	fluorescein isothiocyanate
gB (H, L, M, N, O)	glycoprotein (H, L, M, N, O)
HA	hemagglutinin
HCMV	human cytomegalovirus
HEPES	N-2-hydroxyethylpiperazine-N'-2 ethanesulfonic acid
HFF	human foreskin fibroblast
HHV	human herpes virus
HIV	human immunodeficiency virus

h p.i.	hour(s) post infection
HRP	horseradish peroxidase
HSPGs	heparan sulfate proteoglycans
HSV	herpes simplex virus
IE	immediate early
IF	immunofluorescence
IFN	interferon
Ig	immunoglobulin
IL	interleukin
mAbs	monoclonal antibodies
MAPK	mitogen-activated protein kinases
MCMV	murine cytomegalovirus
MCP	major capsid protein
MEF	murine embryonic fibroblasts
MOI	multiplicity of infection
OD	optical density
ORF	open reading frame
PAA	polyacrylamide gel electrophoresis
PAGE	polyacrylamide gel electrophoresis
PBS	phosphate buffered saline
PCR	polymerase chain reaction
PFA	paraformaldehyde
PFU	plaque-forming unit
PI3K	phosphatidylinositol 3-kinases
p.i.	post infection
RNA	ribonucleic acid
RT	room temperature
SDS	sodium dodecyl sulfate
SDS-PAGE	SDS-Poly-acrylamid gel electrophoreses
TAE	Tris-Acetate-EDTA
TEMED	N,N,N',N' – Tetramethylethylendiamin
VSV	Vesicular stomatitis virus
VZV	Varicella zoster virus
WT	wildtype
WB	Western Blot
Units	
°C	Degree Celsius
bp	base pair
Da	Dalton
g	gram or gravitational constant

h	hour (s)
L	liter
M	molar (mol/l)
m	meter
min	minute (s)
pH	pondus Hydrogenii
rpm	revolutions per minute
sec	Second
V	volt

Prefixes

k	kilo
m	mini
µ	micro
n	nano

6.2 Publications and posters

This thesis describes work performed at the Max von Pettenkofer-Institute, in Munich between October 2012 and November 2015. Parts of the study were published or presented at conferences.

Publications

1. **Y Wu**, A Prager, S Boos, M Resch, I Brizic, M Mach, S Wildner, L Scrivano, B Adler* *"Human cytomegalovirus glycoprotein complex gH/gL/gO uses PDGFR-α as a key for entry"* PLOS Pathogens, in revision

2. N.A. Lemmermann, A. Krmpotic, J. Podlech, I. Brizic, A. Prager, H. Adler, A. Karbach, **Y Wu**, S. Jonjic, M.J. Reddehase, and B. Adler*. "*Non-redundant and Redundant Roles of Cytomegalovirus gH/gL Complexes in Host Organ Entry and Intra-tissue Spread*" ***PLoS Pathog***. 2015; 11(2): e1004640

Poster presentation

Y Wu, I Brizic, L Scrivano, S Schuller, A Prager and B Adler* (2014) *HCMV glycoprotein complex gH/gL/gO directly promotes virus entry into fibroblasts.* **24th Annual Meeting of the Society for Virology,** 2014, Alpbach, Austria

6.3 Acknowledgements

Accomplishing a Ph.D. study and obtaining a doctor degree in biological science has always been my dream since I entered the university. It is certainly impossible to complete a Ph.D. alone. This thesis marks the end of my four years Ph.D. training. It has been a wonderful experience to study in LMU Munich. Here, I would like to express my cordial thanks to many people for their selfless and countless help during my Ph.D..

Firstly, I would like to express the deepest gratitude to my supervisor PD. Dr. Barbara Adler for offering me the opportunity to work at the Max von Pettenkofer-Institut, for all the guidance, patience and confidence. There is a Chinese proverb saying that "He who teaches me for one day is my father for life". As a superior, you always fully supported me and you were always accessible and willing to answer any of my science questions. Your perpetual enthusiasm to science extremely inspired me in my studies. On that aspect, I regard you as my mother.

Secondly, I would thank China Scholarship Council for the scholarship awarded to me to support my Ph.D. study in Germany.

Thanks to my previous colleague Adrian Prager for his kind tutoring of many techniques in the lab. I would also thank my current colleague Simona Langer for her suggestions of my thesis. Special thanks to Ilija Brizic for providing me with antibodies.

Besides, I would like to thank all the current and former lab members of AG Adler and AG Zsolt Ruzsics, Dr. Laura Scrivano, Dr. Madlen Pogoda, Dr. Felicia Wagner and Simone Boos for their friendly atmosphere throughout the last four years. They have made my time in the lab enjoyable.

In particular, I give my gratitude to my family without reservation for their unconditional love and tremendous supports. It is hard to image how much my parents suffered for raising me and my sister up in such a terrible financial situation.

Above all, I am indebted to my wife, Wei, for her love, understanding and encouragement and for sharing with me the dream of completing our Ph.D. studies. Without her it would have been certainly much more painful to complete Ph.D. study abroad alone.